

Dear Dr. Duncan (co-Editor),

We thank the two anonymous reviewers for helpful comments on the manuscript. We have revised the manuscript to reflect their suggestions. Below we include a **point-by-point response (in bold blue)** to the reviewers, responding to *their comments (in italic)* and explaining the changes made to the manuscript.

Best regards,  
Meiyun Lin  
(on behalf of the authors)

### Response to Anonymous Referee #1

The manuscript on US surface ozone trends and extremes by Lin et al. is clearly one of the best modelling studies I have read in my career. It covers an important scientific topic with political relevance and provides an in-depth analysis of US surface ozone and its drivers to the extent that this can be achieved with a global model. It contains a careful and insightful analysis of observations and model results including a well-designed set of sensitivity experiments to attribute ozone trends and variability to various factors. The text is well structured and very well written. All arguments are clearly presented and justified; there is an adequate recognition of previous work. The figures are also very well designed and clear and readable. This would have almost been the first manuscript which I would recommend to “publish as is”, except that I do have a few very minor comments and suggestions how the text could be even further improved. In short, it was a real pleasure to review this manuscript.

**RE: We truly appreciate the reviewer for carefully reading the manuscript and for favorable comments and insightful suggestions.**

*Introduction: start with at least one general sentence about ozone being an important air pollutant which has been of relevance to the US for a long time.*

**RE: Good suggestion! We now begin with this sentence:**

**“Within the United States, ground-level O<sub>3</sub> has been recognized since the 1940s and 1950s as an air pollutant detrimental to public health.”**

*Page 2, lines 7-10: explicitly mention methane here (part of climate effects?)*

**RE: Done. “There are concerns that rising Asian emissions and global methane ...”**

*Page 2, lines 33/34: this result is based on a previous study with the same model. Don’t state it as undisputed fact. Please write “Previous model simulations indicate . . .” or similar.*

**RE: We now say:**

**“Previous model simulations indicate that import of Asian pollution enhances mean WUS surface O<sub>3</sub> in spring by ~5 ppb (Zhang et al., 2008; Lin et al., 2012b),**

and occasionally contributes 8-15 ppb during springtime pollution episodes observed at rural sites (Lin et al., 2012b).”

*Page 3, line 2: not only precursor trends, but also inter-annual (meteorological) variability make this difficult if not impossible*

**RE: Good point! We now say:**

**“Discerning directly the effect of climate change on air quality from long-term observation records of O<sub>3</sub> would be ideal, but concurrent trends in precursor emissions and large internal climate variability on regional scales impede such an effort.”**

*Page 3, line 14: you may also want to mention that models have difficulties in simulating the seasonal cycle at baseline sites correctly (see recent papers by Parrish et al., Derwent et al.)*

**RE: We did not make change here because the focus of this paper is on long-term trends. Adding discussions on the seasonal cycle somewhat interrupt the overall flow of that paragraph.**

*Section 2: please provide at least one general statement about the GFDL model with a reference to the model description paper before describing the experiments.*

*Page 4, line 22: please provide a reference to the dry deposition climatology*

**RE: Done. We slightly reorganize the first paragraph of Section 2 and include additional information on a sensitivity simulation for 1988 with decreased O<sub>3</sub> dry deposition velocities due to droughts simulated by the GFDL Land Model 3 (see also Section 6, Figures 18 and 19).**

*Page 5, line 22: awkward grammar: “a number of studies (Hiboll).”*

**RE: Changed to “... by a few recent studies (e.g., Hilboll et al., 2013)”**

*Page 6, lines 7-10: statement misleading: there are thousands of long-term monitoring sites from AQS and several hundred “rural” stations. Add “selected”?*

**RE: Add “selected”.**

*Page 6, lines 15-17: Please state if trend was derived from daily MDA8 values or monthly values and how you tested for the appropriateness of a linear trend model.*

**RE: This is clarified in Section 2.3.**

**“The trend is calculated separately for the 5th, 50th and 95th percentiles of daily MDA8 O<sub>3</sub> for each season through ordinary linear least-square regression. Statistics are derived for the slope of the linear regression in units of ppb yr<sup>-1</sup>, the range of the slope with a 95% confidence limit (not adjusted for sample autocorrelation), and the p-value indicating the statistical significance of the trend based on a two-tailed t test.”**

Page 9, line 8 vs. Caption Figure 6: Lee et al. once cited as 2013, and once as 2014.

**RE: Nice catch! Revised.**

Page 10, line 11: Please add a quantitative summary statement how well the Asian trends are captured. Figure 6 indicates within 10-20%, Mt. Happa is within 37%.

**RE: Good suggestion! We now stated “We conclude that GFDL-AM3 captures 65-90% of the observed O<sub>3</sub> increases in Asia, lending confidence in its application to assess the global impacts of rising Asian emissions.”**

Page 11, lines 9-20: I recall from earlier discussions on USNE surface ozone that a large change occurred around 2001 when NO<sub>x</sub> scrubbers in power plants were activated. Is this worth mentioning here? Could this have an impact on the observed trends and/or the relation between spring and summer trends?

**RE: We now mention this in the revised manuscript:**

**“Many northeast states in the late 1990s and early 2000s did not turn on power plant NO<sub>x</sub> emission controls until the O<sub>3</sub> season (May-September), which may also contribute to observed differences between spring and summer O<sub>3</sub> trends.”**

Page 13, line 4 vs. 20 ff: perhaps the rising isoprene discussion could be merged in one place? It is slightly confusing to see this in two places.

**RE: We have moved that sentence down to the next paragraph.**

Page 14, lines 11ff: Figure caption (Figure 13) uses “NAB” as abbreviation for “Background” run. This should be made consistent (also the font of “NAB” in the legend differs from the other legend entries).

**RE: The “NAB” abbreviation is only used in Figure 13 because of limited space. We have used the term “Background” throughout the text in the manuscript.**

Page 15, line 1: Does the statement “can explain 50-65%...” assume linear additivity of the factors controlling surface ozone? Would the impacts be the same if you applied linear regression on the differences between the model simulations (instead of subtracting the linear trend estimates from each other)? Perhaps, Table 2 would be easier to digest if the individual contributions were listed (i.e. the differences) instead of the regression results themselves?

**RE: As suggested by the reviewer, we apply linear regression on the differences between the model simulations and find no significant change from the impacts calculated by subtracting the linear trends in Table 2. Thus, no change is made in the manuscript.**

Page 15, line 38: please add a note how Asian emissions will decrease after 2030 according to RCP8.5. For example, will they reach year 2000 or year 1990 levels?

**RE: Done.**

**“Under the RCP8.5 scenario, Chinese NO<sub>x</sub> emissions are projected to peak in 2020-2030, reflecting an increase of ~50% from 2010 (Fig.1a), followed by a sharp decrease reaching 1990 levels by 2050.”**

*Page 16, lines 33/34: “consistent with the seasonality of pollution transport from Asia.” Isn’t this also the influence of the Asian summer monsoon in July/August which reduces surface ozone over Asia itself?*

**RE: We now say:**

**“The stronger increase measured in June than in July-August is consistent with the influence of the Asian summer monsoon producing surface O<sub>3</sub> minimum in July-August in Asia (e.g., Lin et al., 2009), as well as the seasonality of intercontinental pollution transport.”**

*Page 20, lines 22-27: if possible, the argument about dry deposition influencing the high end of ozone distributions during the 1988 heatwave should be substantiated by an additional (1-year or only summer months) model simulation where dry deposition could be turned off (or reduced).*

**RE: Thanks for the suggestion! We have conducted a sensitivity simulation for 1988 with reduced O<sub>3</sub> deposition velocities as simulated by the GFDL Land Model 3 driven by reanalysis meteorology. This simulation is briefly described in Section 2.1. The results are shown in Figs. 18 and 19 and discussed in Section 6 (please see tracked changes in the revised manuscript).**

*Page 21, lines 1-2: how about “plume chemistry” as another explanation for the overall bias? There are strong NO<sub>x</sub> gradients also in the horizontal, and ozone production efficiency is higher in the medium-NO<sub>x</sub> range than in the high NO<sub>x</sub> range.*

**RE: We don’t think model limitation in resolving plume chemistry is a major explanation for the bias. Travis et al. (2016) used a 0.25°x0.25° model and found 20 ppb biases similar to our 2-degree model before adjustment of NO<sub>x</sub> emissions. No changes are made in the manuscript.**

*Figure 20: why are the observed trends not included in this figure?*

**RE: Because this figure shows decadal mean changes from 1981-1990 to 2003-2013. There are only limited observations available during 1981-1990. We have clarified this in the caption of Fig.20.**

*Conclusions: the conclusions are more a summary than real conclusions. I suggest to shorten this summary of results and instead try to go one step further in assessing the possible consequences of this study. For example: even though methane hasn’t played a major role in the past, will it become more important in the future if, as suggested by the RCPs, Asian NO<sub>x</sub> emissions will decrease again? Or: what do we expect from future NO<sub>x</sub> emissions in the NEUS? In relation to climate change: could there be a greater role of biogenic VOC and would this lead to more or less severe ozone episodes?*



RE: Good suggestion. We have changed the title of Section 7 to “Conclusion and Recommendations”. Now we explicitly discuss the implications of this study: (1) recommendations for future multi-model analysis for the IGAC/Chemistry-Climate Model Initiative (CCMI), (2) the growing importance of rising global methane and NO<sub>x</sub> emissions in the tropical Asian countries, where ozone production is more efficient, in the coming decades, (3) the benefits of future NO<sub>x</sub> emission controls on O<sub>3</sub> reductions in the Southeast US, and (4) uncertainties in the model treatment of land-biosphere couplings and their impacts on pollution extremes in a warming climate. Please see tracked changes in Section 7 of the revised manuscript.

## Response to Anonymous Referee #2

We thank the reviewer for positive comments on the manuscript. Below we include **a point-by-point response (in bold blue)** to the reviewer, responding to *their comments (in italic)* and explaining the changes made to the manuscript.

*This paper uses modeling in conjunction with observations to assess the causes of surface ozone trends in the United States, and applies some novel approaches to this important problem. The analysis is robust and the paper is generally well-written. I have listed some specific comments below to improve the clarity of some parts of the text.*

*Page 1 Line 32: Clarify that this is future springtime O<sub>3</sub>*

**RE: Changed to: “Mean springtime O<sub>3</sub> above the WUS is projected to increase by ~10 ppb from 2010 to 2030 under the RCP8.5 global change scenario.”**

*Page 1 Lines 34-35: Do you mean that the onset of isoprene emissions is earlier in the Southeast than other regions, or that it became earlier over time?*

**RE: We now say “The O<sub>3</sub> decreases driven by NO<sub>x</sub> emission controls were most pronounced in the Southeast, where the seasonal onset of biogenic isoprene emissions and NO<sub>x</sub>-sensitive O<sub>3</sub> production occurs earlier than in the Northeast.”**

*Section 2.1: What time period is the model run for?*

**RE: please see Table 1.**

*P6 Line 18: Why not adjust for sample autocorrelation?*

**RE: We do not adjust the confidence limit for sample autocorrelation to enable a directly comparison with the trends reported in the published literature (e.g., Cooper et al., 2012; Parrish et al., 2014).**

*P6 Line 35: Is it only 1990 that has anomalously low values at some sites, or several of the early years? See, for example, the discussion in Strode et al. [2015].*

**RE: Here we are talking about the cross-site consistency on the anomalies. The other years, such as 1992-1993, also have low-anomalies, but they are consistent across the sites and reflect the influence from the Mount Pinatubo eruption as discussed in Lin et al. (Nature Communications, 2015).**

*P7 Line 27: What is the justification for picking 700 hPa?*

**RE: The level is representative of free tropospheric air since we want to limit the excessive influence from surface pollution in the model.**

*P7 Line 35: Is BASE the same as AM3\_BASE? If so, please use one or the other consistently.*

**RE: Yes, they are the same. We have avoided using AM3\_BASE in the revised manuscript.**

*P11 Line 31: Since a number of studies have examined trends for slightly different time periods (for example, Cooper et al [2012]), it would be helpful to summarize here how your results for trends through 2014 compare with those trends, and what effect the inclusion of recent years has on the trends.*

**RE: Good suggestion!! We now include additional discussions in Section 4.1 regarding the difference in the trends reported in this work compared to prior studies. Copied below:**

**“The north-to-south gradient in springtime O<sub>3</sub> trends over the EUS reflects the earlier seasonal transition from NO<sub>x</sub>-saturated to NO<sub>x</sub>-sensitive O<sub>3</sub> production regimes in the Southeast, where plentiful radiation in spring enhances HO<sub>x</sub> supply and biogenic isoprene emissions are turned on earlier than the Northeast. The different response of springtime O<sub>3</sub> to NO<sub>x</sub> controls in the Southeast vs. Northeast noticed in this work is not present in prior analyses for shorter time periods (1990-2010 in Cooper et al. 2012 and 1998-2013 in Simon et al. 2015). We find 72% of the Southeast sites experiencing significant median O<sub>3</sub> decreases in spring over 1988-2014, while Cooper et al. found only 8%. Sites with significant 95<sup>th</sup> percentile springtime O<sub>3</sub> decreases in the EUS are also more common in our study (85% compared to 43% in Cooper et al.). For the 5<sup>th</sup> percentile, 45% of the Northeast sites in our analysis have significant spring O<sub>3</sub> increases, whereas only 15% in Cooper et al.**

**“Compared to the 1990-2010 trends reported in Cooper et al., the EUS summer O<sub>3</sub> decreases reported here with additional data to 2014 are 33% stronger.”**

*P13 Line 23: How does the GHCNDEX relate to the meteorology used to drive the model? Why not calculate the change in max temperature etc. using the same met fields that drive the model?*

**RE: Note that the model is nudged to NCEP U and V but not temperature (as described in Section 2.1). The simulated change in Tmax is shown in Fig.12b. GHCNDEX represents observations, with input data from the Global Historical Climatology Network (GHCN) Daily station data.**

*P20 Line 16: This is a significant bias, and should be discussed earlier in the paper.*

**RE: We have mentioned the mean model biases in Section 4.2 when referring to Figs. S4 and S5. The high model biases in EUS surface ozone is well known and common across the models. The discussion fits better in Section 6, which focuses on EUS.**

*Fig. 8 caption: What does “colorbar saturates at -0.8” mean?*

**RE: Changed to “The color scale saturates at  $\pm 0.8$ ”. It means that there are values outside of the -0.8 to +0.8 range.**

1 **US surface ozone trends and extremes from 1980-2014: Quantifying the roles of rising**  
2 **Asian emissions, domestic controls, wildfires, and climate**

3  
4 Meiyun Lin<sup>1,2\*</sup>, Larry W. Horowitz<sup>2</sup>, Richard Payton<sup>3</sup>, Arlene M. Fiore<sup>4</sup>, Gail Tonnesen<sup>3</sup>  
5

6 <sup>1</sup>Atmospheric and Oceanic Sciences, Princeton University, Princeton, NJ 08540, USA

7 <sup>2</sup>NOAA Geophysical Fluid Dynamics Laboratory, Princeton, NJ 08540, USA

8 <sup>3</sup>U.S. Environmental Protection Agency, Region 8, Denver, CO 80202, USA

9 <sup>4</sup>Lamont-Doherty Earth-Observatory and Department of Earth and Environmental Sciences,  
10 Columbia University, Palisades, NY 10964, USA

11 **\*Corresponding Author** ([Meiyun.Lin@noaa.gov](mailto:Meiyun.Lin@noaa.gov); Phone: 1-609 452-6551)

12 **Abstract.** US surface O<sub>3</sub> responds to varying global-to-regional precursor emissions, climate,  
13 and extreme weather, with implications for designing effective air quality control policies. We  
14 examine these conjoined processes with observations and global chemistry-climate model  
15 (GFDL-AM3) hindcasts over 1980-2014. The model captures the salient features of observed  
16 trends in daily maximum 8-hour average O<sub>3</sub>: (1) increases over East Asia (up to 2 ppb yr<sup>-1</sup>), (2)  
17 springtime increases at western US (WUS) rural sites (0.2-0.5 ppb yr<sup>-1</sup>) with a baseline sampling  
18 approach, (3) summertime decreases, largest at the 95<sup>th</sup> percentile, and wintertime increases in  
19 the 50<sup>th</sup> to 5<sup>th</sup> percentiles over the eastern US (EUS). Asian NO<sub>x</sub> emissions tripled since 1990,  
20 contributing as much as 65% to modeled springtime background O<sub>3</sub> increases (0.3-0.5 ppb yr<sup>-1</sup>)  
21 over the WUS, outpacing O<sub>3</sub> decreases attained via 50% US NO<sub>x</sub> emission controls. Methane  
22 increases over this period contribute only 15% of the WUS background O<sub>3</sub> increase. Springtime  
23 O<sub>3</sub> observed in Denver has increased at a rate similar to remote rural sites. During summer,  
24 increasing Asian emissions approximately offset the benefits of US emission reductions, leading  
25 to weak or insignificant observed O<sub>3</sub> trends at WUS rural sites. Mean springtime WUS O<sub>3</sub> is  
26 projected to increase by ~10 ppb from 2010 to 2030 under the RCP8.5 global change scenario.  
27 While historical wildfire emissions can enhance summertime monthly mean O<sub>3</sub> at individual  
28 sites by 2-8 ppb, high temperatures and the associated buildup of O<sub>3</sub> produced from regional  
29 anthropogenic emissions contribute most to elevating observed summertime O<sub>3</sub> throughout the  
30 USA. GFDL-AM3 captures the observed interannual variability of summertime EUS O<sub>3</sub> (r=0.8).  
31 However, O<sub>3</sub> deposition sink to vegetation must be reduced by 35% for the model to accurately  
32 simulate observed high-O<sub>3</sub> anomalies during the severe drought of 1988. Regional NO<sub>x</sub>  
33 reductions alleviated the O<sub>3</sub> buildup during the recent heat waves of 2011 and 2012 relative to  
34 earlier heat waves (e.g., 1988; 1999). The O<sub>3</sub> decreases driven by NO<sub>x</sub> controls were most  
35 pronounced in the Southeast US, where the seasonal onset of biogenic isoprene emissions and  
36 NO<sub>x</sub>-sensitive O<sub>3</sub> production occurs earlier than in the Northeast. Without emission controls, the  
37 95<sup>th</sup> percentile summertime O<sub>3</sub> in the EUS would have increased by 0.2-0.4 ppb yr<sup>-1</sup> over  
38 1988-2014 due to more frequent hot extremes and rising biogenic isoprene emissions.

Deleted: S

Deleted: ozone (

Deleted: )

Formatted: Font:Not Bold

Deleted: ;

Deleted: '

Deleted: '

Formatted: Subscript

Deleted: domestic

Deleted: raise

Deleted: by 15%

Deleted: effect

Deleted: Rising Asian emissions and global methane under the RCP8.5 scenario

Deleted: mean springtime WUS O<sub>3</sub>

Deleted:

Deleted: Rising Asian emissions and global methane under the RCP8.5 scenario increase mean springtime O<sub>3</sub> above the WUS by ~10 ppb from 2010 to 2030. Historical EUS O<sub>3</sub> decreases, driven by regional emission controls, were most pronounced in the Southeast with an earlier onset of biogenic isoprene emissions and NO<sub>x</sub>-sensitive O<sub>3</sub> production.

Deleted: also

Formatted: Subscript

Deleted: -

... [1]

## 1. Introduction

Within the United States, ground-level O<sub>3</sub> has been recognized since the 1940s and 1950s as an air pollutant detrimental to public health. Decreases in summertime O<sub>3</sub> were observed in parts of California and throughout the EUS (e.g., Cooper et al., 2012; Simon et al., 2015), following regional NO<sub>x</sub> controls after the lowering of the US National Ambient Air Quality Standard (NAAQS) for O<sub>3</sub> in 1997 to 84 ppb. On the basis of health evidence, the NAAQS level for O<sub>3</sub> has been further lowered to 75 ppb in 2008 and to 70 ppb in 2015 (Federal Register, 2015).

There are concerns that rising Asian emissions and global methane (Jacob et al., 1999; Lin et al., 2015b), more frequent large wildfires in summer (e.g., Jaffe, 2011; Yang et al., 2015; Abatzoglou et al., 2016), and late spring deep stratospheric O<sub>3</sub> intrusions (Lin et al., 2012a; Langford et al., 2014; Lin et al., 2015a) may pose challenges in attaining more stringent O<sub>3</sub> standards at high-elevation WUS regions. A warming climate would also offset some of the air quality improvements gained from regional emission controls (e.g., Fiore et al., 2015). Quantitative understanding on sources of O<sub>3</sub> variability on daily to multi-decadal time scales can provide valuable information to air quality control managers as they develop O<sub>3</sub> abatement strategies under the NAAQS. Here we systemically investigate the response of US surface O<sub>3</sub> means and extremes to changes in Asian and North American anthropogenic emissions, global methane, regional heat waves and wildfires over the course of 35 years from 1980 to 2014, using observations and chemistry-climate model (GFDL-AM3) hindcasts (Lin et al., 2014; 2015a; 2015b).

Rapid economic growth has led to a tripling of O<sub>3</sub> precursor emissions from Asia in the past 25 years (e.g., Granier et al., 2011; Hillboll et al., 2013). Observed 1-hour O<sub>3</sub> mixing ratios can frequently reach 200-400 ppb during regional pollution episodes in eastern China (Wang T. et al., 2006; Li et al., 2016), with a seasonal peak in the late spring to early summer (Wang Y. et al., 2008; Lin et al., 2009). A synthesis of available observations from the mid-1990s to the 2000s indicates increases of 1-2 ppb yr<sup>-1</sup> in spring to summer O<sub>3</sub> in China (Ding et al., 2008; Ma et al., 2015; Sun et al., 2015). Long-range transport of Asian pollution plumes towards western North America has been identified by aircraft and satellite measurements and in chemical transport models (e.g., Jaffe et al., 1999; Fiore et al., 2009; Lin et al., 2012b; Huang et al., 2013; Verstraeten et al., 2015). Systematic comparison of observed and modeled long-term O<sub>3</sub> trends over Asia is lacking in the published literature, but is needed to establish confidence in models used to assess the global impacts of rising Asian emissions.

Model simulations indicate that import of Asian pollution enhances mean WUS surface O<sub>3</sub> in spring by ~5 ppb (Zhang et al., 2008; Lin et al., 2012b), and occasionally contributes 8-15 ppb during springtime pollution episodes observed at rural sites (Lin et al., 2012b) as supported by in situ aerosol composition analysis (VanCuren and Gustin 2015). Stratospheric intrusions can episodically increase daily 8-hour average surface O<sub>3</sub> by 20-40 ppb, contributing to the highest observed O<sub>3</sub> events at high-elevation WUS sites (Lin et al., 2012a; Lin et al., 2015), in addition to pollution transport from California (e.g., Langford et al., 2010). In the densely populated EUS,

Formatted: Subscript

Deleted: increases in

Deleted: anthropogenic

Deleted: see review by

Deleted: a suite of

Deleted: Zhang et al., 2008;

Deleted: ,

Deleted: I

Deleted: ,

1 both changes in regional anthropogenic emissions and air pollution meteorology have the  
2 greatest impacts on summer surface O<sub>3</sub> during pollution episodes (e.g., Jacob and Winner 2009;  
3 Rieder et al., 2015; Porter et al., 2015; Pusede et al., 2015). Discerning directly the effect of  
4 climate change on air quality from long-term observation records of O<sub>3</sub> would be ideal, but  
5 concurrent trends in precursor emissions **and large internal variability in regional climate** impede  
6 such an effort. It is difficult to separate the impacts of changes in global-to-regional precursor  
7 emissions and different meteorological factors on O<sub>3</sub> at given locations without the benefit of  
8 multiple sensitivity experiments afforded by models.

9 On the other hand, process-oriented assessments of the models are needed to build  
10 confidence in their utility for assessing pollution control strategies, estimating tropospheric O<sub>3</sub>  
11 radiative forcing and projecting pollution extremes under future climate scenarios (e.g., Monks et  
12 al., 2015). A number of studies show that global models capture observed decreases in  
13 summertime O<sub>3</sub> over the EUS during 1990-2010, but have difficulty simulating O<sub>3</sub> increases  
14 measured at remote **high-elevation** sites that are believed to represent hemispheric-scale  
15 conditions with little influence from fresh local pollution (hereafter referred to as “baseline”)  
16 (e.g., Lamarque et al., 2010; Koumoutsaris and Bey, 2012; Parrish et al., 2014; Brown-Steiner et  
17 al., 2015; Strobe et al., 2015). Recently, Lin et al. (2015b) examined the representativeness of O<sub>3</sub>  
18 trends derived from sparse measurements in the free troposphere over the WUS, originally  
19 reported by Cooper et al. (2010) and used in **prior** model evaluations. They found that  
20 discrepancies between observed and simulated O<sub>3</sub> trends reflect measurement sampling biases.  
21 Here we seek additional insights into the causes of the model-observation disagreement at the  
22 WUS rural sites with continuous, high-frequency measurements. Notably, we reconcile observed  
23 and simulated O<sub>3</sub> trends at these sites with a baseline sampling approach **in the model**.

24 Our goal in this paper is twofold: first, to systematically evaluate how well our  
25 GFDL-AM3 BASE simulation represents trends and variability of surface O<sub>3</sub> observed at rural  
26 sites across the US; second, to examine changes in US surface O<sub>3</sub> means and extremes in a suite  
27 of multi-decadal hindcast simulations designed to isolate the response of O<sub>3</sub> to increases in Asian  
28 anthropogenic emissions, North American emission controls, rising global methane, wildfires,  
29 and interannual variability in meteorology. We examine trends across the entire probability  
30 distribution of O<sub>3</sub> concentration, which is crucial to assessing the ability of models to simulate  
31 the surface O<sub>3</sub> response under different temperature and chemical regimes depending on seasons,  
32 geographical location, and regional transport patterns. Specifically, we evaluate the trends  
33 separately for the 5<sup>th</sup>, 50<sup>th</sup> and 95<sup>th</sup> percentiles of the O<sub>3</sub> concentration distribution in spring  
34 (MAM), summer (JJA), **autumn (SON)**, and winter (DJF).

35 Section 2 briefly describes the observational records, model experiments, and analysis  
36 approach. As a first step towards assessing our understanding of the impacts of rising Asian  
37 emissions, we briefly review Asian O<sub>3</sub> trends from observations in recent publications and  
38 evaluate modeled trends (Sect. 3). We then focus our analysis on the US, using both observations  
39 and models to assess the response of US surface O<sub>3</sub> to changes in background O<sub>3</sub>, regional

Deleted: altitude

Deleted: 4

Deleted: evious

Deleted: .

Deleted: March-April-May;

Deleted: June-July-August;

Deleted: December-January-February;

anthropogenic emissions and meteorology (Sect. 4). In Section 5, we further separate the influence of background on WUS O<sub>3</sub> into components driven by rising Asian anthropogenic emissions, global methane, and wildfires. We quantify the contribution of these factors to surface O<sub>3</sub> in both rural areas such as national parks (Sect. 5.1 to 5.3) and in densely populated regions such as the Denver Metropolitan area (Sect. 5.4). After evaluating historical trends, we additionally draw upon two simulations following the 21<sup>st</sup> century RCP4.5 versus RCP8.5 global change scenarios to project WUS O<sub>3</sub> through 2050 (Sect. 5.2). Section 6 examines how the EUS summertime O<sub>3</sub> probability distribution and pollution extremes respond to large-scale heat waves, droughts, and regional NO<sub>x</sub> reductions over the past decade, and how well our model simulates the observed features. Finally, we summarize in Section 7 the key drivers of US surface O<sub>3</sub> trends and extremes and discuss the implications of this study.

## 2. Model and Observations

### 2.1 Chemistry-Climate Model Experiments.

(Table 1 about here: Model Experiments)

The GFDL-AM3 model includes interactive stratosphere-troposphere chemistry and aerosols on a cubed sphere grid with a resolution of approximately 200x200 km<sup>2</sup> (Donner et al., 2011). Table 1 summarizes meteorology, radiative forcing agents, and emissions used in each experiment. The hindcast simulations (1979-2014) are nudged to the NCEP/NCAR reanalysis zonal and meridional winds using a height-dependent nudging technique (Lin et al., 2012b). Biogenic isoprene emissions and lightning NO<sub>x</sub> are tied to model meteorology (Guenther et al., 2006; Rasmussen et al., 2012) and thus can respond to changes in climate, whereas soil NO<sub>x</sub> and chemical dry deposition velocities are set to a monthly climatology (Naik et al., 2013), with a diurnal cycle applied for O<sub>3</sub> dry deposition. To investigate the possible influence of drought on O<sub>3</sub> removal (e.g., Emberson et al., 2013), we additionally conduct a sensitivity simulation for 1988 with reduced O<sub>3</sub> deposition velocity (see Sect.6). Our BASE simulation and two additional simulations with modified emissions (FIXEMIS and IAVFIRE) were previously used to interpret the causes of increasing autumnal O<sub>3</sub> measured at Mauna Loa Observatory in Hawaii since 1974 (Lin et al., 2014), interannual variability of springtime O<sub>3</sub> (Lin et al., 2015a) and the representativeness of free tropospheric O<sub>3</sub> measurements over the WUS (Lin et al., 2015b).

With anthropogenic emissions and methane held constant (Table 1), the FIXEMIS and IAVFIRE simulations isolate the influence from meteorology and wildfire emissions, respectively. In IAVASIA, anthropogenic emissions from East Asia (15°N-50°N, 95°E-160°E) and South Asia (5°N-35°N, 50°E-95°E) are allowed to vary from year to year as in BASE, while anthropogenic emissions in the other regions of the world, global methane and wildfire emissions are held constant as in FIXEMIS. In IAVCH<sub>4</sub>, global methane is allowed to vary over time as in BASE, but with anthropogenic and wildfire emissions held constant as in FIXEMIS. The IAVASIA and IAVCH<sub>4</sub> simulations thus isolate the role of rising Asian anthropogenic emissions and global methane, respectively, by contrasting with the FIXEMIS simulation. Both BASE and

Deleted: during heat waves

Deleted: in

Deleted: s

Deleted:

Deleted: model skill and shortcomings

Formatted: Font:Not Bold

Deleted: Table 1 summarizes meteorology, radiative forcing agents and emissions used in each model experiment.

Deleted: All hindcast

Deleted: simulations

Deleted: , with height-dependent nudging

Formatted: Not Highlight

Formatted: Font:Not Italic, Not Highlight

Formatted: Not Highlight

Deleted: Below we describe additional simulations used in this study.

Formatted: Font:Bold

Formatted: Font:Bold

Deleted: the

Deleted: simulation

Deleted: the

Deleted: simulation



1 **IAVCH<sub>4</sub>** simulations apply observed time-varying methane concentrations as a lower boundary  
 2 condition for chemistry (**Fig.S1**). Thus, underestimates in historical methane emissions reported  
 3 recently by Schwietzke et al. (2016) do not affect our results. We quantify the total contributions  
 4 to surface O<sub>3</sub> from meteorological variability, stratosphere-to-troposphere transport, pollution  
 5 from foreign continents and O<sub>3</sub> produced by global methane, lightning NO<sub>x</sub>, wildfires and  
 6 biogenic emissions with the **Background** simulation, in which North American anthropogenic  
 7 emissions are zeroed out relative to **BASE**. We additionally draw upon two simulations with the  
 8 GFDL Coupled Model CM3 following the 21<sup>st</sup> century RCP global change scenarios to project  
 9 changes in WUS O<sub>3</sub> through 2050. Details of these CM3 simulations were described in John et al.  
 10 (2012).

## 11

### 12 **2.2 Anthropogenic and Biomass Burning Emissions**

13 **(Figure 1 about here: Changes in NO<sub>x</sub> emissions)**

14 We first examine how well the emission inventories in AM3 BASE represent changes in  
 15 regional NO<sub>x</sub> emissions over recent decades inferred from satellite measurements of tropospheric  
 16 vertical column density (VCD<sub>trop</sub>) of NO<sub>2</sub>. The combined record of GOME and SCIAMACHY  
 17 shows that VCD<sub>trop</sub> NO<sub>2</sub> over the highly polluted region of eastern China almost tripled during  
 18 1996-2011 (**Fig.1a**). In contrast, VCD<sub>trop</sub> NO<sub>2</sub> over the EUS decreased by ~50% in the 2000s  
 19 (**Fig.1b**) due to NO<sub>x</sub> State Implementation Plans (**commonly known** as the NO<sub>x</sub> SIP Call) and  
 20 many rules that tighten emission standards for mobile sources (McDonald et al., 2012). Similar  
 21 decreases occurred in WUS cities, resulting from the NO<sub>x</sub> control programs to achieve O<sub>3</sub> and  
 22 regional haze planning goals. These trends are consistent with those reported by a **few** recent  
 23 studies (**e.g.**, Hilboll et al., 2013), including those using OMI NO<sub>2</sub> data (Russell et al., 2012;  
 24 Duncan et al., 2016). For comparison with satellite data, we sample the model archived every  
 25 three hours closest to the time of satellite overpass for the SCIAMACHY and GOME products  
 26 we use in Figure 1 (10:00-10:30**am**, local time). Trends in VCD<sub>trop</sub> NO<sub>2</sub> are similar to those in  
 27 NO<sub>x</sub> emissions (orange lines versus red triangles in **Fig.1a-1b**), indicating that any changes in  
 28 NO<sub>x</sub> chemical lifetime **or partitioning** have negligible influence in our model, consistent with NO<sub>2</sub>  
 29 loss against OH being minor during the morning overpasses of GOME and SCIAMACHY. The  
 30 emission inventory used in **BASE**, from Lamarque et al. (2010) with annual interpolation after  
 31 2000 to RCP8.5 (Lamarque et al., 2012), mimics the opposing changes in NO<sub>x</sub> emissions over  
 32 eastern China versus the EUS during 1996-2011, consistent with changes in VCD<sub>trop</sub> NO<sub>2</sub>  
 33 retrieved from the satellite instruments. For comparison, the RCP4.5 interpolation for 2001-2010  
 34 in **CMIP5 historical** simulations analyzed by Parrish et al. (2014) underestimates the increase in  
 35 Chinese NO<sub>x</sub> emissions by a factor of two (**Fig.1a**). **Recent reductions in** Chinese NO<sub>x</sub> emissions  
 36 after 2011 (Duncan et al., 2016) **are** not represented in the **inventories** used in AM3.

37 Our BASE model applies interannually-varying monthly mean emissions from biomass  
 38 burning based on the RETRO inventory (Schultz et al., 2008) for 1970 to 1996 and GFEDv3 (van  
 39 der Werf et al., 2010) for 1997 onwards, distributed vertically as recommend by Dentener et al.

Deleted: Supplementary

Deleted: implemented

Deleted: \_

Deleted: hereafter referred to

Deleted: number of

Deleted: AM

Deleted: AM3\_

Deleted: the historical

Deleted: We note that the levelling-off

Deleted: of

Deleted: is

Deleted: RCP8.5 emission

Deleted: y

1 (2006). **Fig. S2** illustrates the interannual variability of biomass burning CO emissions from the  
 2 main source regions of the Northern Hemisphere over the period 1980-2014. Boreal fire  
 3 emissions in Eurasia almost doubled from 1980-1995 to 1996-2014, with large fires occurring  
 4 more frequently in the recent decade, as found for the WUS (Dennison et al., 2014; Yang et al.,  
 5 2015).

Deleted: Supplementary

Deleted: in

Deleted: in recent studies

## 6 2.3 Ozone Observation Records and Uncertainties

7 Long-term surface O<sub>3</sub> observation records were obtained at 70 selected rural monitoring  
 8 sites with 20 (1995-2014) to 27 (1988-2014) years of continuous hourly measurements from the  
 9 US National Park Services, the US Clean Air Status and Trends Network (CASTNet), and the  
 10 US EPA Air Quality System. Cooper et al. (2012) reported trends in daytime (11am-4pm) O<sub>3</sub>  
 11 over 1990-2010 at 53 rural sites. We investigate trends in daily maximum 8-hour averaged  
 12 (MDA8) O<sub>3</sub> and expand the analysis of Cooper et al. using additional data to 2014 and including  
 13 17 additional sites with measurements begun in 1991-1995. All sites have at least 20 years of  
 14 data. If a site has less than 50% data availability in any season then that particular season is  
 15 discarded. The trend is calculated separately for the 5<sup>th</sup>, 50<sup>th</sup> and 95<sup>th</sup> percentiles of daily MDA8  
 16 O<sub>3</sub> for each season through ordinary linear least-square regression. Statistics are derived for the  
 17 slope of the linear regression in units of ppb yr<sup>-1</sup>, the range of the slope with a 95% confidence  
 18 limit (not adjusted for sample autocorrelation), and the p-value indicating the statistical  
 19 significance of the trend based on a two-tailed t-test.

Deleted: 66

Deleted: (2012)

Deleted: 3

Deleted: O<sub>3</sub>

Deleted:

## 20 (Figure 2 about here: Measurement uncertainties)

21 A cross-site consistency analysis was performed to determine robust changes in the time  
 22 evolution of O<sub>3</sub> over the WUS during 1988-2014 (**Fig.2**). The monitor at Yellowstone National  
 23 Park was moved 1.5 km from the Lake Yellowstone site to the Water Tank site in 1996. While  
 24 the local transport patterns are slightly different for the two sites, using MDA8 data from the  
 25 well-mixed midday period minimizes the differences (Jaffe and Ray, 2007). Observed O<sub>3</sub>  
 26 interannual variations show large-scale similarity across sites over the Intermountain West except  
 27 for the earlier period 1989-1990. During this period, observations at Yellowstone and Rocky  
 28 Mountain National Parks show low-O<sub>3</sub> anomalies that do not appear at other sites but there is no  
 29 change in measurement technique. Jaffe and Ray (2007) suggest this represents large-scale  
 30 variations in background O<sub>3</sub> that are seen in common at these two parks. However, analysis of  
 31 meteorological fields and model diagnostics does not reveal any obvious transport anomaly  
 32 influencing O<sub>3</sub> variations at these sites in 1990 (Lin et al., 2015a). Observations at Pinedale in  
 33 January-February 1990 are also anomalously low relative to Grand Canyon (GRC474),  
 34 Centennial (CNT169), and Gothic (GTH161). These anomalous data at the beginning of  
 35 measurement records can substantially influence trends calculated from short records. For  
 36 example, Cooper et al. (2012) found a summer O<sub>3</sub> increase of 0.42±0.30 ppb yr<sup>-1</sup> at Yellowstone  
 37 over 1990-2010. Removing 1990, we find a weaker increase of 0.28±0.27 ppb yr<sup>-1</sup> (**Fig.2b**).  
 38 Removing 1990 at Rocky Mountain resulted in a weaker springtime O<sub>3</sub> increase of 0.29±0.17

Deleted: at

Deleted: ,

Deleted: time

1 ppb yr<sup>-1</sup> compared to 0.43±0.23 ppb yr<sup>-1</sup> over 1990-2010 (**Fig.2c**). To assess robust O<sub>3</sub> changes,  
2 we thus remove these apparently uncertain measurements in 1990 from the subsequent analysis.

## 2.4 Model Baseline Sampling Approach

(Figure 3 about here: Influence of baseline sampling)

6 Springtime O<sub>3</sub> observations at WUS high-elevation sites (≥ 1.5 km a.s.l.) typically  
7 represent baseline conditions with little influence from fresh local pollution. In a global model  
8 with ~200x200 km<sup>2</sup> horizontal resolution, however, these remote sites can reside in the same grid  
9 cell that contains urban cities where NO<sub>x</sub> emissions decreased over the analysis period. For  
10 example, Rocky Mountain National Park (2.7 km a.s.l.) is less than 100 km from the Denver  
11 Metropolitan area in Colorado. This limitation of large-scale models in resolving urban-to-rural  
12 gradients and sharp topography results in an artificial offset of increased baseline O<sub>3</sub> at remote  
13 sites by decreased urban pollution within the same model grid cell. Thus, coarse-resolution  
14 models are often unable to reproduce observed O<sub>3</sub> increases at the high-elevation sites  
15 representative of remote baseline conditions (**Figs. 3a vs. 3b**), as found in many prior modeling  
16 analyses (e.g., Parrish et al., 2014; Strode et al., 2015 and references therein). This limitation can  
17 be addressed by using a baseline selection procedure to identify conditions for sampling the  
18 model to avoid model artifacts caused by poor spatial resolution, as described below.

19 All measurements presented in this study are unfiltered. We implement a set of regional  
20 CO-like tracers (CO<sub>t</sub>), with a 50-day exponential decay lifetime and surface emissions constant  
21 in time from each of four northern mid-latitude source regions (Lin et al., 2014). We use these  
22 CO<sub>t</sub> tracers to bin modeled O<sub>3</sub> according to the dominant influence of different continental air  
23 regimes. To represent observed baseline conditions at WUS sites, we sample AM3 at 700 hPa  
24 (~3 km a.s.l.) and filter the O<sub>3</sub> data in the BASE simulation to remove the influence from fresh  
25 local pollution. Specifically, our filter excludes days when North American CO<sub>t</sub> (NACOT)  
26 exceeds the 67<sup>th</sup> percentile for each season. This procedure yields higher calculated baseline O<sub>3</sub>  
27 increases (**Fig.3c**), bringing it closer to observations (**Fig.3a**). When sampled at 700 hPa without  
28 filtering (**Fig.3d**), BASE gives statistically significant O<sub>3</sub> increases but the rate of increase is  
29 ~0.1 ppb yr<sup>-1</sup> weaker than with filtering. With North American anthropogenic emissions shut off,  
30 the model simulates significant O<sub>3</sub> increases that are similar at the surface (**Fig.3e**) and at 700  
31 hPa (**Fig.3f**). This finding indicates that the underestimate of O<sub>3</sub> increases in BASE, when  
32 sampled at the surface (**Fig.3b**), reflects an excessive offset from domestic pollution decreases in  
33 the model relative to observed conditions, as opposed to the insufficient mixing of free  
34 tropospheric O<sub>3</sub> to the surface. As individual sites display observed trends falling in between the  
35 filtered model, and those sampled at the surface versus aloft, we can use the model to interpret  
36 which sites are most frequently sampling baseline versus influenced by North American  
37 anthropogenic emissions. For consistency, in the subsequent analysis we apply model baseline  
38 filtering to all WUS sites with elevations greater than 1.5 km altitude. In the EUS, where the  
39 terrain and monitor elevations are much lower than in the west and observed O<sub>3</sub> trends are

Deleted: the

Deleted: -like

Deleted:

Deleted: from

Deleted: intermountain

Deleted: the

Deleted: o

Deleted: tracer

Deleted: trend

Deleted: AM3\_

Deleted: BASE model

Deleted:

Deleted: at altitude

Deleted: the

Deleted: sampling approach

largely controlled by regional emission changes, we always sample the model at the surface without filtering.

Deleted: applying data

### 3. Global Distribution of Lower Tropospheric O<sub>3</sub> Trends

#### 3.1 Global O<sub>3</sub> Burden and Distribution of Trends

(Figure 4 about here: Global distribution)

We begin by examining the global distribution of lower tropospheric O<sub>3</sub> trends over 1988-2014 from the BASE simulation (Fig.4) and focus on the differences between the surface and free troposphere (~700 hPa), with implications for understanding the impact of trends in hemispheric baseline O<sub>3</sub> on surface air quality. The model indicates that surface MDA8 O<sub>3</sub> levels in Asia have increased significantly by 1.5-2.5 ppb yr<sup>-1</sup> in the 95<sup>th</sup> percentile (Fig.4a-b) and by 1-2 ppb yr<sup>-1</sup> in the median values (Fig.4c-d), with the largest increases occurring in South Asia during spring and over Eastern China during summer. In contrast, there is a marked decrease in surface MDA8 O<sub>3</sub> in WUS cities, throughout the EUS and in central Europe, particularly at the high percentiles and during summer. The increase in surface O<sub>3</sub> over Asia and decreases over the US and Europe are consistent with changes in regional emissions of O<sub>3</sub> precursors over this period (Fig.1).

Deleted: center our discussion

Deleted: ern

Over Southeast Asia (south of 30°N) during spring, earlier springtime O<sub>3</sub> photochemical production at lower latitudes coupled with active frontal transport (Liu et al., 2002; Carmichael et al., 2003; Lin et al., 2010) leads to a comparable or even greater increase of O<sub>3</sub> in the free troposphere than at the surface (Figs. 4c vs. 4e). In contrast, over Central East China during summer the simulated trends of O<sub>3</sub> in the free troposphere are at least a factor of three weaker than in surface air (Fig.4d vs. 4f), consistent with the analysis of MOZAIC aircraft data over Beijing in 1995-1999 versus 2003-2005 (Ding et al., 2008). Mean O<sub>3</sub> at 700 hPa above parts of North America and Europe show little change in summer or even increase during spring in the model, similar to the trends at 500 hPa (Fig.S3), despite the significant decreases in surface air. The global tropospheric O<sub>3</sub> burden in the BASE simulation increases by approximately 30 Tg over the past 35 years (Fig.5a), attributed mainly to changes in anthropogenic emissions. Over the 2004-2015 OMI/MLS satellite era, however, meteorological variability contributes approximately half to the total simulated decadal trends of O<sub>3</sub> burden (Fig.5a).

#### 3.2 Comparison of observed and simulated O<sub>3</sub> trends in Asia

(Figures 5 and 6 about here)

Long-term O<sub>3</sub> observations are very sparse in Asia, making it difficult to evaluate modeled O<sub>3</sub> trends. We compile available measurements from the published literature; including ozonesonde profiles at Hong Kong (2000-2014; <http://woudc.org>) and Hanoi (2005-2015; SHADOZ, Thompson et al., 2007), MOZAIC aircraft profiles collected on summer afternoons in the boundary layer (below 1250 m altitude) over Beijing for 1995-2005 (Ding et al., 2008),

1 ground-based measurements at Mt. Tai (1.5 km a.s.l.) in Central Eastern China for July-August  
 2 2003-2015 (Sun et al., 2016), at the GAW stations - Shangdianzi north of Beijing for 2004-2014  
 3 (Ma et al., 2016) and Mt. Waliguan (3.8 km a.s.l.) in the Tibetan Plateau for 1994-2013 (Xu et al.,  
 4 2016), at Taiwan for 1994-2007 (Y-K Lin et al., 2010), South Korea for 1990-2010 (Lee et al.,  
 5 2014), Mt. Happo (1.9 km a.s.l.) in Japan for 1991-2011 (Tanimoto, 2009; Parrish et al., 2014),  
 6 and a coastal site at Hong Kong in Southern China for 1994-2007 (T Wang et al., 2009).

7 We first evaluate the annual trends of O<sub>3</sub> over 900-600 hPa at Hanoi (21°N, 106°E) and  
 8 Hong Kong (22°N, 114°E) ozonesonde sites in Southeast Asia (Fig.5b-5c), where our model  
 9 indicates the greatest O<sub>3</sub> increases (Fig.4e). The ozonesonde frequency is 4 profiles per month at  
 10 Hong Kong and only 1-2 profiles per month at Hanoi. To determine the representativeness of O<sub>3</sub>  
 11 trends derived from these sparse measurements, we compare observations and model results  
 12 co-sampled on sonde launch days with the ‘true average’ determined from O<sub>3</sub> fields archived  
 13 every three hours from the model, as in our prior work for WUS sites (Lin et al., 2015a; Lin et al.,  
 14 2015b). The trends are generally consistent across the sonde data, model co-sampled and ‘true  
 15 average’ results for Hong Kong, with a total increase of ~15% from 2005 to 2014. However,  
 16 sampling deficiencies may influence the trends derived from ozonesondes at Hanoi recently  
 17 reported by Zhang Y. et al. (2016). Observations at Hanoi show an apparently rapid O<sub>3</sub> increase  
 18 of 30% from 2005 to 2014. AM3 BASE sampled sparsely as in the ozonesondes captures the  
 19 observed variability (r<sup>2</sup> = 0.7), whereas the ‘true average’ over this period indicates the trend is  
 20 only half of that inferred from observations. Over the short period 2005-2014, interannual  
 21 variability of O<sub>3</sub> resulting from wildfire emissions and meteorology in IAVFIRE is as large as the  
 22 total O<sub>3</sub> change in BASE. Over the entire 1980-2014 period, the BASE model ‘true average’  
 23 simulates an O<sub>3</sub> increase of ~30%.

24 Expanding the comparison to a suite of sites across East Asia (Fig. 6), we find that AM3  
 25 captures the key features of observed O<sub>3</sub> trends in Asia, including their seasonal to regional  
 26 variations, summertime increases (1-2 ppb yr<sup>-1</sup>) in Central Eastern China where NO<sub>x</sub> emissions  
 27 have approximately tripled since 1990 (Fig.1a), and springtime increases (0.5 ppb yr<sup>-1</sup>) at Taiwan  
 28 and Mt. Happo that are driven by pollution outflow from the Asian continent. Note that to place  
 29 the trends derived from the short observational records into a broader context we show the  
 30 20-year trends over 1995-2014 from the model, except for South Korea (1990-2010) and Happo  
 31 Japan (1991-2011). We match the time period in the model with observations at these two sites  
 32 because AM3 shows weaker O<sub>3</sub> increases when data for the recent years are included, which  
 33 likely reflects the offsetting effects of regional emission reductions in South Korea and Japan.

34 Parrish et al. (2014) show that CMIP5 models underestimate the observed springtime O<sub>3</sub>  
 35 increase at Mt. Happo by a factor of four. This discrepancy may reflect a combination of factors:  
 36 (1) underestimates of Asian emission growth in the RCP4.5 interpolation after 2000 used in  
 37 CMIP5 historical simulations (Fig.1a), (2) trends driven by interannual meteorological  
 38 variability that free-running CMIP5 models are not expected to reproduce exactly, (3) an  
 39 excessive offset from Japanese pollution decreases in the models owing to their coarse resolution

Deleted: observed and simulated

Deleted: free tropospheric

Deleted: ozone

Formatted: Subscript

Deleted: between

Deleted: our analysis indicates that

Deleted: \_

Deleted: ed

Deleted: \_BASE

Deleted: observed

Deleted: from

Deleted: found

Deleted: three chemistry-climate model simulations

Deleted: d

Deleted: at least

Formatted: Font:Bold

Deleted: partly reflects the

1 and limitation in resolving observed baseline conditions at Mt. Hap-  
 2 po. Sampling our BASE  
 3 model at 700 hPa above Hap-  
 4 po, we find an O<sub>3</sub> increase of 0.35±0.13 ppb yr<sup>-1</sup>. When focusing on  
 5 days, strongly influenced by outflow from the East Asian continent (Chinese CO<sub>2</sub> ≥ 67<sup>th</sup>), the  
 6 model O<sub>3</sub> trend increases to 0.48±0.13 ppb yr<sup>-1</sup>, approximating the observed increase of  
 7 0.76±0.35 ppb yr<sup>-1</sup> at Mt. Hap-  
 8 po (Fig.6b). The observed and simulated trends are not statistically  
 9 different given the overlapping confidence limits. The larger confidence limit (uncertainty)  
 10 derived from the Hap-  
 11 po observations reflects the measurement inconsistency before 1998 and  
 12 instrumental problems after 2007 (Tanimoto et al., 2016). We conclude that GFDL-AM3  
 13 captures 65-90% of the observed O<sub>3</sub> increases in Asia, lending confidence in its application to  
 14 assess the global impacts of rising Asian emissions.

#### 12 4. Regional and Seasonal Variability of US Surface O<sub>3</sub> Trends

13 We next focus our analysis on the US where dense, high-frequency, long-term, reliable  
 14 measurements of surface O<sub>3</sub> facilitate process-oriented model evaluation. Comparisons of  
 15 surface O<sub>3</sub> trends over 1988-2014 at 66 rural monitoring sites across the US as observed and  
 16 simulated in AM3 BASE are shown in Figure 7 for spring, Figure 8 for summer, Figure 9 for  
 17 winter, and in Supplementary Fig.S4 for autumn. The trends are calculated separately for the 5<sup>th</sup>,  
 18 50<sup>th</sup> and 95<sup>th</sup> percentiles of the daily MDA8 O<sub>3</sub> concentration distribution, with larger circles on  
 19 the maps indicating sites with statistically significant trends (p<0.05). We first discuss  
 20 observations (Sect. 4.1), followed by model evaluation and trend attribution (Sect. 4.2).

#### 22 4.1 Observations

23 (Figure 7 about here)

24 In spring (Figure 7), observations indicate spatial heterogeneity in O<sub>3</sub> trends across the  
 25 Intermountain West, Northeast (north of 38°N), and Southeast US. At the 95<sup>th</sup> percentile (Fig.7a)  
 26 the pattern of observed trends is homogeneous across the Northeast and Southeast US, with  
 27 approximately 85% of the sites having statistically significant O<sub>3</sub> decreases of 0.4-0.8 ppb yr<sup>-1</sup>  
 28 and no sites showing a significant increase. In contrast, significant increases occur at 25% of the  
 29 sites in the Intermountain West. Only Joshua Tree National Park located downwind of the Los  
 30 Angeles Basin shows a significant decrease at the 95<sup>th</sup> percentile. At the 50<sup>th</sup> percentile (Fig.7b)  
 31 there are significant O<sub>3</sub> decreases of 0.2-0.4 ppb yr<sup>-1</sup> in the Southeast and little overall change in  
 32 the Northeast, while significant increases of 0.2-0.4 ppb yr<sup>-1</sup> occur at 50% of the sites in the  
 33 Intermountain West. Significant springtime O<sub>3</sub> increases occur at all observed percentiles at  
 34 Lassen Volcanic National Park in California, Great Basin National Park in Nevada, Rocky  
 35 Mountain National Park and US Air Force Academy in Colorado. At the 5<sup>th</sup> percentile (Fig.7c)  
 36 significant O<sub>3</sub> increases occur at most sites in the Northeast while little change and some  
 37 negative trends are found in the Southeast. The occurrence of the greatest observed O<sub>3</sub> decreases  
 38 for the highest percentiles are consistent with high-temperature O<sub>3</sub> production being more  
 39 NO<sub>x</sub>-limited (Pusede et al., 2015), and thus more responsive to decreases in NO<sub>x</sub> emissions.

Deleted: of global models

Deleted: , as occurs at WUS sites (Sect. 2.4)

Deleted:

Formatted: Subscript

Deleted: and f

Deleted: ta

Deleted: that are

Deleted: o

Deleted: tracer

Deleted: >

Deleted: percentile

Formatted: Subscript

Deleted: we find an O<sub>3</sub> increase of

Deleted: at Mt. Hap-  
 po (Fig.6b)

Deleted: the ability of

Deleted: to

Deleted: reproduce the marked increases of

Deleted: pollution

Deleted:

Deleted: s

Deleted:

Deleted: 7

Deleted: 0

Deleted: observed

Deleted: the

Deleted: over the past decade



1 The north-to-south gradient in springtime O<sub>3</sub> trends over the EUS reflects the earlier  
 2 seasonal transition from NO<sub>x</sub>-saturated to NO<sub>x</sub>-sensitive O<sub>3</sub> production regimes in the Southeast,  
 3 where plentiful radiation in spring enhances HO<sub>x</sub> supply and biogenic isoprene emissions begin  
 4 earlier than in the Northeast. The different response of springtime O<sub>3</sub> to NO<sub>x</sub> controls in the  
 5 Southeast versus Northeast noticed in this work is not present in prior analyses for shorter time  
 6 periods (1990-2010 in Cooper et al. 2012 and 1998-2013 in Simon et al. 2015). We find 72% of  
 7 the Southeast sites experiencing significant median O<sub>3</sub> decreases in spring over 1988-2014, while  
 8 Cooper et al. found only 8%. Sites with significant 95<sup>th</sup> percentile springtime O<sub>3</sub> decreases in the  
 9 EUS are also much more common in our study (85% versus 43% in Cooper et al.). In the 5<sup>th</sup>  
 10 percentile, 45% of the Northeast sites in our analysis have significant spring O<sub>3</sub> increases,  
 11 whereas only 15% in Cooper et al. Stronger O<sub>3</sub> reductions in the Southeast than the Northeast  
 12 also occur during autumn (Fig.S4), reflecting an extension of biogenic isoprene emissions and  
 13 NO<sub>x</sub>-sensitive O<sub>3</sub> production in the Southeast.

14 (Figure 8 about here)

15 In summer (Figure 8), as radiation intensifies and isoprene emissions peak seasonally,  
 16 the O<sub>3</sub> production becomes more NO<sub>x</sub>-limited across both the Southeast and Northeast US where  
 17 NO<sub>x</sub> emission controls have led to significant O<sub>3</sub> decreases of 0.8-1.8 ppb yr<sup>-1</sup> in the 95<sup>th</sup>  
 18 percentile and 0.4-0.8 ppb yr<sup>-1</sup> in the median value (Fig.8a-8b). In the Southeast, significant  
 19 decreases have also occurred at the lowest percentiles during summer (Fig.8c), in contrast to the  
 20 weak response during spring (Fig.7c). Many northeast states in the late 1990s and early 2000s  
 21 did not turn on power plant NO<sub>x</sub> emission controls until the O<sub>3</sub> season (May-September), which  
 22 may contribute to observed differences between spring and summer O<sub>3</sub> trends. Compared to the  
 23 1990-2010 trends reported in Cooper et al., the EUS summer O<sub>3</sub> decreases reported here with  
 24 additional data to 2014 are 33% stronger. Despite reductions in precursor emissions in the WUS  
 25 cities (Fig.1d), there are no significant summer O<sub>3</sub> decreases at the intermountain sites except in  
 26 Yosemite and Joshua Tree National Parks for the 95<sup>th</sup> percentile. Instead, a significant summer  
 27 increase of ~0.3 ppb yr<sup>-1</sup> occurs across the entire O<sub>3</sub> distribution at Yellowstone. Significant  
 28 summer increases are found in the 5<sup>th</sup> percentile for Lassen, Mesa Verde, and Rocky Mountain  
 29 National Parks.

30 (Figure 9 about here)

31 In winter (Figure 9), observed O<sub>3</sub> increases are more common than in spring and  
 32 summer across the US. The wintertime O<sub>3</sub> increases are strongest in the lowest percentiles over  
 33 the EUS, indicating the influence from weakened NO<sub>x</sub> titration as a result of regional NO<sub>x</sub>  
 34 emission controls (see also Gao et al., 2013; Clifton et al., 2014; Simon et al., 2015). Even during  
 35 winter, some decreasing O<sub>3</sub> trends are found in the highest percentiles over the Southeast  
 36 (Fig.9a), most prominent in Texas (around Dallas and Houston), where tropical climate and  
 37 year-round active photochemistry makes O<sub>3</sub> most responsive to regional NO<sub>x</sub> emission controls.  
 38 Despite the greatest NO<sub>x</sub> emission reductions over the past decade in the central and northeast

Deleted: are turned on

Formatted: Subscript

Formatted: Not Highlight

Formatted: Subscript

Formatted: Superscript

Formatted: Subscript

Formatted: Subscript

Formatted: Subscript

Formatted: Font color: Black

Formatted: Subscript

Formatted: Subscript

Formatted: Subscript

Formatted: Not Highlight

Formatted: Subscript

Formatted: Not Highlight

Deleted: at

Deleted: at

Deleted: National Park

Deleted: Notably,

Deleted: t

Deleted: S

Deleted: over the Southeast even during winter

Deleted: similar to the Los Angeles Basin (not shown)



US regions, observed O<sub>3</sub> reductions have been most pronounced in the Southeast, particularly in spring and winter.

#### 4.2 Model Evaluation and Attribution of Observed O<sub>3</sub> Trends

The BASE simulation with GFDL-AM3 captures the salient features of observed O<sub>3</sub> trends over 1988-2014 at rural sites across the US: (1) the overall springtime increases and the lack of significant trends in summer over the Intermountain West, (2) the north-to-south gradients in O<sub>3</sub> trends during spring and the largest decreases in the 95<sup>th</sup> percentile during summer over the EUS, (3) wintertime increases in the 5<sup>th</sup> and 50<sup>th</sup> percentiles (left vs right panels in **Figs. 7 to 9**). AM3 also simulates a median springtime O<sub>3</sub> increase of  $0.32 \pm 0.11$  ppb yr<sup>-1</sup> over 1988-2014 ( $0.64 \pm 0.50$  ppb yr<sup>-1</sup> over 2004-2014) at Mount Bachelor Observatory in Oregon, consistent with the positive trend ( $0.63 \pm 0.41$  ppb yr<sup>-1</sup>) observed over the shorter 2004-2015 period (Gratz et al., 2014). These analyses imply that GFDL-AM3 represents the underlying chemical and physical processes controlling the response of US surface O<sub>3</sub> means and extremes to changes in global-to-regional precursor emissions and climate, despite mean state biases (**Figs. S5-S6**).

The filtered model shows greater 95<sup>th</sup> percentile O<sub>3</sub> increases than observed at some WUS sites (e.g., Yosemite; Grand Canyon; Canyonlands) for both spring and summer (**Figs. 7a,d and Fig. 8a,d**), reflecting that observations at these sites sometimes can be influenced by transport of photochemically aged plumes from nearby urban areas and from southern California during late spring and summer. When sampled at the surface, AM3 simulates small summertime O<sub>3</sub> decreases in the 95<sup>th</sup> and 50<sup>th</sup> percentiles over the Intermountain West (**Fig. 4b,d**), consistent with observations at Yosemite, Grand Canyon, and Canyonlands (**Fig. 8a,b**). As illustrated in **Fig. 3** for spring and discussed in Sect. 2.4, individual sites in the west display observed trends falling in between the filtered model and those sampled at the surface versus aloft.

(**Figures 10 and 11 about here**)

We examine how US surface O<sub>3</sub> responds to changes in regional anthropogenic emissions, hemispheric background, and meteorology by comparing O<sub>3</sub> trends in the BASE, Background, and FIXEMIS experiments (**Figs. 10-11**). With North American anthropogenic emissions shut off in the Background simulation, little difference is discernable from the BASE simulation for WUS O<sub>3</sub> trends during spring (first vs. second rows in **Fig. 10**), indicating the key role of hemispheric background driving increases in springtime O<sub>3</sub> over the WUS. With anthropogenic emissions held constant in time, FIXEMIS still shows statistically significant spring O<sub>3</sub> increases in the 95<sup>th</sup> percentile (**Fig. 10c**), approximately half of the trends simulated in BASE, for Grand Canyon, Canyonlands, Mesa Verde and Rocky Mountain National Parks. Prior work shows that deep stratospheric intrusions contribute to the highest observed and simulated surface O<sub>3</sub> events at these sites (Langford et al., 2009; Lin et al., 2012a). Strong year-to-year variability of such intrusion events (Lin et al., 2015a) can confound the attribution of springtime O<sub>3</sub> changes over the WUS to anthropogenic emission trends, particularly in the highest percentile and over a short record length. Summer avoids this confounding influence when stratospheric intrusions are at

Deleted: the

Deleted: s

Deleted: 4

Deleted: 5

Deleted: the

Deleted: s

their seasonal minimum, as evidenced by little O<sub>3</sub> change in FIXEMIS over the WUS (Figs. 11c,f). In contrast to spring, the model shows larger differences in WUS O<sub>3</sub> trends between BASE and Background for summer when North American pollution peaks seasonally (Figs.10a,d vs. 10b,e compared to Figs.11a,d vs. 11b,e). There are significant increases of 0.2-0.5 ppb yr<sup>-1</sup> in the 95<sup>th</sup> and 50<sup>th</sup> percentile summer background O<sub>3</sub> at more than 50% of the western sites (Fig.11b,e), offsetting the O<sub>3</sub> decreases resulting from US NO<sub>x</sub> reductions and leading to little overall change in total observed and simulated O<sub>3</sub> at WUS rural sites during summer (Fig.8).

Over the EUS, AM3 also simulates background O<sub>3</sub> increases, occurring in both the 95<sup>th</sup> and 50<sup>th</sup> percentiles, with a rate of 0.1-0.3 ppb yr<sup>-1</sup> during spring (Fig.10b,e) and 0.2-0.5 ppb yr<sup>-1</sup> during summer (Fig.11b,e). Based on prior model estimates that springtime background O<sub>3</sub> is greater in the Northeast than the Southeast (Lin et al., 2012a; Lin et al., 2012b; Fiore et al., 2014), one might assume that the springtime O<sub>3</sub> increases in the 5<sup>th</sup> percentile observed over the Northeast (Fig.7c) have been influenced by a rising background. However, AM3 simulates homogeneous background O<sub>3</sub> trends across the entire EUS (Fig.10b,e), indicating that the observed north-to-south gradient in O<sub>3</sub> trends reflects an earlier seasonal onset of NO<sub>x</sub>-sensitive photochemistry in the Southeast as opposed to the background influence.

(Figure 12 about here).

A warming climate is most likely to worsen the highest O<sub>3</sub> events in polluted regions (e.g., Schnell et al., 2016; Shen et al., 2016). With anthropogenic emissions held constant in time over 1988-2014, FIXEMIS suggests significant increases of 0.2-0.4 ppb yr<sup>-1</sup> in the 95<sup>th</sup> percentile summertime O<sub>3</sub> over the EUS (Fig.11c). Using self-organizing map cluster analysis, Horton et al. (2015) identified robust increases in the occurrence of summer anticyclonic circulations over eastern North America since 1990. We find that biogenic isoprene emissions over this period increased significantly by 1-2% yr<sup>-1</sup> (10 to 20 mg C m<sup>-2</sup> summer<sup>-1</sup>) throughout the EUS in the model, consistent with simulated increases in the 90<sup>th</sup> percentile JJA daily maximum temperature (Fig. 12a-12b). Increases in isoprene emissions contribute to raising EUS background O<sub>3</sub> in summer (Fig.11b,e). Using the Global Land-Based Datasets for Monitoring Climate Extremes (GHCNDEX; Donat et al., 2013), we find increases in the number of warm days above the 90<sup>th</sup> percentile and maximum temperature over the southeast US in August (Fig.12c-12d). The trends in temperature extremes are similar between June and August, but there is no significant trend in July (not shown). While changes in regional temperature extremes on 20 to 30-year time series may reflect internal climate variability (Shepherd, 2015), we suggest that increasing hot extremes and biogenic isoprene emissions over the last two decades may have offset some of the benefits of regional NO<sub>x</sub> reductions in the EUS.

## 5. Impacts of rising Asian emissions, methane and wildfires on western US O<sub>3</sub>

### 5.1 Historical western US O<sub>3</sub> trends in spring

(Figure 13 about here: Time series analysis)

Deleted: during

Deleted: the influence of

Deleted: Rising biogenic isoprene emissions contribute to the EUS background O<sub>3</sub> increase in summer (Fig.12a).

Deleted:

Deleted: and autumn

Deleted: We further analyze

Deleted: and

Deleted: central and

Deleted: merely

Deleted: the increased frequency of

Deleted: rising

Deleted: air quality improvements in the EUS gained from

Deleted: .

Further indications of the factors driving baseline O<sub>3</sub> changes over the WUS can be inferred by examining the time series at several high-elevation sites, which are most frequently sampling baseline O<sub>3</sub> in the free troposphere during spring (Sect. 2.4). **Figure 13** shows the results, both observed and simulated, for six such monitoring sites: Great Basin National Park in Nevada (2.1 km a.s.l.), Rocky Mountain National Park (2.7 km a.s.l.) in Colorado, US Air Force Academy (1.9 km a.s.l.) in Colorado Springs, Yellowstone National Park (2.4 km a.s.l.) and Pinedale (2.4 km a.s.l.) in Wyoming, and Mesa Verde National Park (2.2 km a.s.l.) in the Colorado-New Mexico-Arizona-Utah four corner region. The observed median values of springtime MDA8 O<sub>3</sub> have increased significantly at a rate of 0.2-0.5 ppb yr<sup>-1</sup> over the past 20-27 years at these sites, except Pinedale, where the increase in background O<sub>3</sub> is likely offset by the O<sub>3</sub> decrease due to recent emission control for the large oil and gas production fields in this area (<http://deq.wyoming.gov/aqd/winter-ozone/resources/technical-documents/>). When filtered to remove the influence from fresh local pollution (Sect.2.4), AM3 BASE captures the long-term trends of O<sub>3</sub> observed at these sites.

Correlating AM3 Background with observed O<sub>3</sub> indicates that most of the observed variability reflects changes in the background, with fluctuations in stratospheric influence contributing to anomalies on interannual time scales (e.g., the 1999 anomaly, Lin et al., 2015a), whereas Asian influence dominates the decadal trends as discussed below. The O<sub>3</sub> reduction resulting from US anthropogenic emission controls is less than 0.1 ppb yr<sup>-1</sup> (BASE minus Background) at these baseline sites. We show model results for the entire 1980-2014 period for Great Basin, Rocky Mountain, and US Air Force Academy to provide context for observed trends in the two most recent decades (**Fig.13a**). In the 1980s when Chinese NO<sub>x</sub> emissions (~4 Tg/yr NO) were much lower than US NO<sub>x</sub> emissions (~15 Tg/yr NO) (Granier et al., 2011), there was little overall O<sub>3</sub> change over the WUS in the model. From the mid-1990s onwards, with NO<sub>x</sub> emissions in China rising steeply (**Fig.1a**) and surpassing US emissions in the 2000s, the O<sub>3</sub> trends at remote WUS sites appear to be dominated by trends of background, reflecting rising emissions outside the US. The largest spring O<sub>3</sub> increases from 1981-1990 to 2003-2012 at 700 hPa extend from Southeast Asia to the subtropical North Pacific Ocean to the southwestern US (**Fig.S7a**), consistent with the influence of rising Asian precursor emissions.

#### (Table 2 about here: Trend attribution)

**Table 2** contains a summary of the drivers of O<sub>3</sub> trends in the model at seven CASTNet sites that exhibit a significant spring O<sub>3</sub> increase observed over 1988-2012. Here we focus our attribution analysis on the period 1988-2012 (instead of 1988-2014) because the IAVASIA and IAVCH<sub>4</sub> simulations only extend to 2012. Meteorology varies from year to year in all experiments. Thus, we quantify the contributions of rising Asian emissions in IAVASIA, global methane in IAVCH<sub>4</sub>, and wildfire emissions in IAVFIRE by subtracting out the slope of the linear regression of seasonal O<sub>3</sub> means in FIXEMIS. Simulated O<sub>3</sub> with anthropogenic emissions varying in both South and East Asia, but held constant elsewhere shows statistically significant increases of 0.1-0.2 ppb yr<sup>-1</sup> (p<0.01; IAVASIA minus FIXEMIS in **Table 2**), consistent with

Deleted: directly

Deleted: the

Deleted: ations

Formatted: Subscript

Deleted: we find that

Deleted: Supporting the Asian influence, the regions experiencing

Deleted: t

Deleted: time

Deleted: 6

Deleted: .

Deleted:

Deleted: with

Deleted: time

Deleted: the period

Deleted: from

Deleted: (red boxes in Fig.1c)

Deleted: give

trends of 0.2 ppb yr<sup>-1</sup> estimated by scaling results from HTAP phase 1 multi-model sensitivity experiments with Asian emissions reduced by 20% (Riedmiller et al., 2009). This Asian influence can explain 50-65% of the modeled background O<sub>3</sub> increase in spring (Table 2).

Deleted: from ...TAP phase 1 multi-model sensitivity ... [2]

With only methane varying, the model trends are less than 0.1 ppb yr<sup>-1</sup> (IAVCH<sub>4</sub> minus FIXEMIS), accounting for an average of 15% of the background increase. The contribution from wildfire emissions during spring is of minor importance (IAVFIRE minus FIXEMIS, Table 2). A stratospheric O<sub>3</sub> tracer (O<sub>3</sub>Strat) in AM3 (Lin et al., 2012a; Lin et al., 2015a) demonstrates a positive but insignificant trend in stratospheric O<sub>3</sub> transport to the sites. We examine the trends of lower tropospheric O<sub>3</sub> at these sites when transport conditions favor the import of Asian pollution into western North America, as diagnosed by East Asian CO tracer (EACOT) exceeding the 67<sup>th</sup> percentile for each spring. Similar to the conclusion of Lin et al., (2015b), we find that the rate of O<sub>3</sub> increase in the Background simulation is greater by 0.05-0.1 ppb yr<sup>-1</sup> under strong transport from Asia than without filtering. Filtering the IAVASIA simulation for Asian influence also results in greater O<sub>3</sub> increases than filtering for baseline conditions (Table 2).

Deleted: total ...ackground increases... The contributi... [3]

Rising Asian emissions even influence trends of O<sub>3</sub> downwind of the Los Angeles Basin during spring. O<sub>3</sub> measured in Joshua Tree National Park shows an increase of 0.31±0.25 ppb yr<sup>-1</sup> in spring over 1990-2010 (Cooper et al., 2012), despite significant improvements in O<sub>3</sub> air quality in the Los Angeles Basin (Warneke et al., 2012). The O<sub>3</sub> record extended to 2014 shows a decline in the 95<sup>th</sup> percentile O<sub>3</sub> in Joshua Tree National Park for both spring and summer (Figs. 7-8), whereas the 5<sup>th</sup> percentile continues to increase in spring and there is no significant trend in the median. Sampling the AM3 Background simulation at this site indicates rising background (0.31±0.14 ppb yr<sup>-1</sup>). Aircraft measurements in May-June 2010 indicate the presence of Asian pollution layers 2 km above southern California with distinct sulfate enhancements coincident with low organic mass (Lin et al., 2012b), supporting the conclusion that rising Asian emissions can contribute to trends of O<sub>3</sub> observed in this region. Yosemite National Park (1.6 km a.s.l.) and Chiricahua National Monument (1.5 km a.s.l.) are also influenced by increases in Asian emissions and concurrent decreases in local pollution in California. O<sub>3</sub> observed at Yosemite shows an increase from 1995 to around 2012 (0.37±0.32 ppb yr<sup>-1</sup>; Fig.S8), which the model attributes primarily to rising Asian emissions (Table 2), but observations have remained constant since then, reflecting an offset by O<sub>3</sub> decreases in California (Fig.4).

Deleted: ... Increasing O<sub>3</sub> from ...r...sing A... [4]

Formatted: Subscript

Deleted: zone...observed at Yosemite shows an increa... [5]

## 5.2 Projecting western US springtime O<sub>3</sub> for the 21<sup>st</sup> Century

(Figure 14 about here: Future Projections).

Under the RCP8.5 scenario, Chinese NO<sub>x</sub> emissions are projected to peak in 2020-2030, reflecting an increase of ~50% from 2010 (Fig.1a), followed by a sharp decrease reaching 1990 levels by 2050. Global methane increases by ~60% from 2010 to 2050 under RCP8.5 (Fig.S1). Under the RCP4.5 scenario, in contrast, NO<sub>x</sub> emissions in China change little over 2010-2030 and global methane remains almost constant from 2010 to 2050. NO<sub>x</sub> emissions in the US decrease through 2050 under both scenarios, by ~40% from 2010. A number of studies have

Deleted: year ...010 by ~50% ... [6]

Formatted: Font:Not Bold

Deleted: and ...g...obal methane increases by ~60% fr... [7]

examined future US O<sub>3</sub> changes under the RCPs (e.g., Gao et al., 2013; Clifton et al., 2014; Pfister et al., 2014; Fiore et al., 2015; Barnes et al., 2016). However, as discussed earlier, the trends of O<sub>3</sub> in the model when sampled near the surface are overwhelmingly dominated by US anthropogenic emission trends. Thus, the future O<sub>3</sub> changes estimated by these prior studies do not represent baseline conditions, particularly the response to rising Asian emissions. In Fig. 14 we show changes of WUS free tropospheric (700 hPa) O<sub>3</sub> relative to 2010 in the CM3 future simulations under RCP8.5 versus RCP4.5. Historical hindcasts and observations are also shown for context. Under RCP4.5, springtime O<sub>3</sub> over the WUS shows little overall change over 2010-2050. Under RCP8.5, in contrast, springtime WUS O<sub>3</sub> increases by ~10 ppb from 2010 to 2030 and remains almost constant from 2030 to 2050, consistent with the projected trends in Asian emissions and global methane.

### 5.3 Trends and variability of western US O<sub>3</sub> in summer (Figure 15 about here: Yellowstone)

Yellowstone National Park is the only site with statistically significant summer O<sub>3</sub> increases observed across all percentiles (Fig. 8a-8c). The 1988-2012 trends for the median observed and simulated O<sub>3</sub> are summarized in Figure 15a. Observations show an increase of 0.32±0.18 ppb yr<sup>-1</sup> for JJA, with a greater rate of increase in June (0.38±0.25 ppb yr<sup>-1</sup>) than in July-August (0.26±0.18 ppb yr<sup>-1</sup>). AM3 BASE sampled at 700 hPa and filtered for baseline conditions (hatched pink bar in Fig. 15a) captures the observed increase. Without baseline filtering (solid pink bar), North American emission reductions offset almost 50% of the simulated O<sub>3</sub> increase at Yellowstone, causing the model to underestimate the observed O<sub>3</sub> trend. The model attributes much of the observed summer O<sub>3</sub> increase at Yellowstone to rising Asian emissions, with IAVASIA simulating an O<sub>3</sub> increase of 0.31±0.19 ppb yr<sup>-1</sup> under baseline conditions, increasing to 0.42±0.23 ppb yr<sup>-1</sup> under conditions of Asian influence (EACOt ≥ 67<sup>th</sup> percentile). The stronger increase measured in June than in July-August is consistent with the influence of the Asian summer monsoon producing a surface O<sub>3</sub> minimum in July-August in East Asia (e.g., Lin et al., 2009), as well as the seasonality of intercontinental pollution transport. Changes in methane, wildfires, and meteorology over this period are of minor importance for the JJA O<sub>3</sub> trends at Yellowstone.

Enhanced wildfire activity in hot and dry weather is thought to be a key driver of interannual variability of surface O<sub>3</sub> in the Intermountain West in summer (Jaffe et al., 2008; Jaffe, 2011). However, hot and dry conditions also facilitate the buildup of O<sub>3</sub> produced from regional anthropogenic emissions, which can complicate the unambiguous attribution of observed O<sub>3</sub> enhancements. Using August data at Yellowstone as an example, we isolate the relative contribution of these two processes to observed O<sub>3</sub> with the IAVFIRE versus FIXEMIS experiments (Fig. 15b). Here we sample AM3 at the surface to account for any influence of varying boundary layer mixing depths. Even without interannual variations of wildfire emissions, FIXEMIS captures much of the observed year-to-year variability of August mean O<sub>3</sub> at

Deleted: in this study

Deleted: the trends of

Deleted: s

Deleted: over the WUS

Deleted: averaged from Lassen, Great Basin, and Rocky Mountain

Deleted: over the WUS

Deleted: anthropogenic

Deleted: from

Deleted: ations

Deleted: model

Formatted: Subscript

Deleted: ions

Deleted: \_

Deleted: in the model

Deleted: time

Deleted: when

Deleted: from Asia

Deleted: . In contrast,

Deleted: c

Deleted: decadal

Deleted: from

Deleted: into fall

Deleted: Pfister et al., 2008;

Deleted: ;

Deleted: note that h

Deleted: from

Deleted: )

Deleted: held constant in time

Yellowstone ( $r=0.67$ ). IAVFIRE with interannually-varying fire emissions only moderately improves the correlations ( $r = 0.75$ ). FIXEMIS also captures the observed  $O_3$  increase from the early 1990s to around 2002, likely reflecting warmer temperatures and deeper mixing depths allowing more baseline  $O_3$  to mix down to the surface. Over the entire 1988-2014 (or 1980-2014) period, IAVFIRE gives  $\sim 0.1$  ppb  $yr^{-1}$  greater  $O_3$  increases in August than FIXEMIS, consistent with an overall increase in boreal wildfire activity (Fig.S2 and Fig.S7b).

(Figure 16 about here: Wildfires)

Figure 16 shows year-to-year variability in surface MDA8  $O_3$  enhancements from wildfires during summer, as diagnosed by the differences between IAVFIRE and FIXEMIS. The results are shown for individual months since fires are highly episodic. During the summers of 1998, 2002, and 2003, biomass fires burned a large area of Siberia and parts of the North American boreal forests, raising carbon monoxide burden across the Northern Hemisphere as detected from space (van der Werf et al., 2010; Yurganov et al., 2005). Long-range transport of Siberian fire plumes resulted in 2-6 ppb enhancements in surface MDA8  $O_3$  at the US west coast and in parts of the Intermountain West in AM3. The model calculates enhancements in monthly mean MDA8  $O_3$  of up to 8 ppb from the intense wildfire events in Northern California during July 2008 (Huang et al., 2013; Pfister et al., 2013), over Texas-Mexico during June 2011 (Y Wang et al., 2015), and in Wyoming-Utah during August 2012 (Jaffe et al., 2013). The AM3 estimates are roughly consistent with a previous analysis of boundary layer aircraft data with and without fire influences (as diagnosed by  $CH_3CN$ ) during June 2008 over California (Pfister et al., 2013).

While fires during hot and dry summers clearly result in enhanced  $O_3$  at individual sites for some summers, the ability of AM3 with constant fire emissions to simulate variability of  $O_3$  ( $\pm 8$  ppb) for a high (e.g., 1988; 2002; 2006) versus low (e.g., 1997; 2009) fire year (Fig.15b) indicates that biomass burning is not the primary driver of observed  $O_3$  interannual variability. Year-to-year variability of JJA mean MDA8  $O_3$  observed at Yellowstone is strongly correlated ( $r > 0.6$ ) with observed large-scale variations in JJA mean daily maximum temperature across the Intermountain West (Fig.15c). Correlations for other ground stations show a similar large-scale feature. Similar to the conclusion from Zhang L. et al. (2014), our analysis indicates that the correlation between  $O_3$  and biomass burning reported by Jaffe et al. (2008, 2011) at rural sites reflects common underlying correlations with temperature rather than a causal relationship of fire on  $O_3$ . At remote mountain sites (e.g., Yellowstone), warmer surface temperatures lead to deeper mixed layers that facilitate mixing of free tropospheric  $O_3$ -rich air down to the surface (Brown-Steiner and Hess, 2011). At sites near sources of air pollution, hot conditions enhance regional  $O_3$  production and orographic lifting of urban pollution to mountain-top sites during daytime, as occurs at Rocky Mountain National Park located downwind of the Denver Metropolitan area during summer (Sect. 5.4). Reactive volatile organic compound (VOC) emissions from fires may enhance  $O_3$  production in  $NO_x$ -rich urban areas (Baker et al., 2016), although evaluating these impacts needs high-resolution models and better treatment of sub-grid scale fire plumes.

Deleted: time

Deleted: pulling down

Deleted: trend

Deleted: 6

Deleted: ,

Deleted: (Jaffe et al., 2004;

Deleted: the

Deleted: according to

Deleted: activity

Deleted: summer

Deleted: and the Great Plains

Deleted: cd

Formatted: Not Superscript/ Subscript

Deleted: with higher  $O_3$  concentrations

Deleted: by

Deleted: Baker et al. (2016) found that

Deleted: r

Deleted: can

Deleted: .

Deleted: E

Deleted: s



1

2 **5.4 Ozone Trends in the Denver Metropolitan Area**

3 **(Figure 17 about here: Denver)**

4 Efforts to improve air quality have led to a marked decrease in high-O<sub>3</sub> events in the Los  
5 Angeles Basin as illustrated by the annual 4<sup>th</sup> highest MDA8 O<sub>3</sub> at Crestline – a regionally  
6 representative monitor operated continuously from 1980 to present (Fig.17a). In striking contrast,  
7 the 4<sup>th</sup> highest MDA8 O<sub>3</sub> in the Denver Metropolitan area shows little change over the past  
8 decades, despite significant reductions in NO<sub>x</sub> (Fig.1) and CO emissions (~80% from 1990-2010;  
9 Cooper et al., 2012). Recent field measurements indicate that increased VOC emissions from oil  
10 and natural gas operations are an important source of O<sub>3</sub> precursors in the Denver-Julesberg  
11 Basin (Gilman et al., 2013; Halliday et al., 2016; McDuffie et al., 2016). However, total VOC  
12 emissions in Denver may not be increasing over time due to the marked reductions in VOC  
13 emissions from vehicles (Bishop and Stedman, 2008; 2015). We seek insights into the causes of  
14 the lack of significant O<sub>3</sub> responses to emission controls in Denver by separately analyzing  
15 trends in spring and summer (Fig.17b-17c).

16 The ~200x200 km<sup>2</sup> AM3 model is not expected to resolve the urban-to-rural differences  
17 between Rocky Mountain National Park and the Denver Metropolitan area. However, if observed  
18 O<sub>3</sub> variability in Denver correlates with that at remote sites in the Intermountain West, then  
19 model attribution for the remote sites can be used to infer sources of observed O<sub>3</sub> in Denver. This  
20 is demonstrated in Fig.17b for spring using data at three representative sites in Denver: Rocky  
21 Flats North, National Renewable Energy Lab (NREL), and Welby with continuous  
22 measurements since the early 1990s. Year-to-year variability of median MDA8 O<sub>3</sub> at these sites  
23 during spring correlates strongly with that in Great Basin National Park (r = 0.7), a fairly remote  
24 site in Nevada not influenced by urban emissions from Denver. Median spring O<sub>3</sub> observations in  
25 Denver increased significantly by ~0.3 ppb yr<sup>-1</sup> similar to the rate of increase in Great Basin  
26 National Park which the model attributes to rising background (Fig.13a), implying that the  
27 tripling of Asian emissions since 1990 also raised mean springtime O<sub>3</sub> in the Denver  
28 Metropolitan area. Trends in the 95<sup>th</sup> percentile are statistically insignificant.

29 During summer, changes in regional emissions and temperature have the greatest impacts  
30 on the highest observed O<sub>3</sub> concentrations in polluted environments. Fig.17c shows times series  
31 of July-August 95<sup>th</sup> percentile MDA8 O<sub>3</sub> in Denver, together with the distribution of daily  
32 maximum temperature. In every year since 1993, the highest summer MDA8 O<sub>3</sub> observed at  
33 these sites exceeds the 70 ppb NAAQS level. There is a small negative trend that is swamped by  
34 large interannual variability. The summers with the highest observed O<sub>3</sub> coincide with those with  
35 the highest observed temperatures, such as 1998, 2003, 2007, 2011 and 2012. During these  
36 summers, enhancements of MDA8 O<sub>3</sub> were also recorded in Rocky Mountain National Park,  
37 reflecting enhanced lifting of pollution from Denver under warmer conditions (Brodin et al.,  
38 2010). Applying quantile regression (e.g., Porter et al., 2015) to daily observations at Rocky Flats  
39 North over 1993-2015, we find a 2 ppb °C<sup>-1</sup> sensitivity of 95<sup>th</sup> percentile July-August O<sub>3</sub> to

Deleted: with

Deleted: s

Deleted: increasing

Deleted: simulations

Deleted: are

Deleted: -

Deleted: in

Deleted: at



changes in maximum daily temperature. We suggest that the substantial increases in extreme heat occurrence over central North America over the last two decades, as found by Horton et al. (2015), contribute to raising summer O<sub>3</sub> in Denver, which offsets O<sub>3</sub> reductions that otherwise would have occurred due to emission controls in Denver. Potential shifts in the O<sub>3</sub> photochemistry regime can also contribute to trends of summer O<sub>3</sub> in Denver, although advancing this knowledge would require a high-resolution air quality model.

## 6. Impacts of heat waves and droughts on eastern US summer O<sub>3</sub>

(Figure 18 about here: Interannual Variability)

We discuss in this section interannual variability and long-term changes in summer O<sub>3</sub> over the EUS, where air stagnation and high temperatures typically yield the highest O<sub>3</sub> observed in surface air (e.g., Jacob and Winner 2009). Evaluating the ability of models to simulate the high-O<sub>3</sub> anomalies during historical heat waves and droughts is crucial to establishing confidence in the model projection of pollution extremes under a warming climate. Figure 18a shows comparisons of July mean MDA8 O<sub>3</sub> at one regionally representative site, the Pennsylvania State University (PSU) CASTNet site, from observations and model simulations. With time-varying emissions, the BASE model simulates an O<sub>3</sub> decrease ( $-0.45 \pm 0.32$  ppb yr<sup>-1</sup>) consistent with observations ( $-0.67 \pm 0.33$  ppb yr<sup>-1</sup>), and captures the observed July mean O<sub>3</sub> interannual variability ( $r = 0.82$ ) that is correlated with large-scale variations in daily maximum temperature ( $r = 0.57$ ). In particular, O<sub>3</sub> pollution extremes are successfully simulated during the EUS summer heat waves of 1988, 1995, 1999, 2002, 2011 and 2012 (Leibensperger et al., 2008; Fiore et al., 2015; Jia et al., 2016). Year-to-year variations in air stagnation events can explain 30% of the total observed O<sub>3</sub> variability ( $r = 0.55$ ), as inferred by FIXEMIS with constant anthropogenic emissions. If US anthropogenic emissions remained at 1990s levels (as in FIXEMIS), then anomalies in July mean MDA8 O<sub>3</sub> would have been 10 ppb greater during the 2011 and 2012 heat waves. Loughner et al. (2014) found that half of the days in July 2011 would have been classified as O<sub>3</sub> exceedance days for much of the mid-Atlantic region if emissions had not declined.

(Figure 19 about here: Changes in O<sub>3</sub> distribution)

Figure 19a compares the probability density functions of MDA8 O<sub>3</sub> at 40 EUS surface sites for JJA in the pre-NO<sub>x</sub> SIP Call (1988-2002) versus post-NO<sub>x</sub> SIP Call (2003-2014) periods and during the extreme heat waves of 1988 versus 2012. Following the NO<sub>x</sub> SIP Call, the probability distribution of observed JJA MDA8 O<sub>3</sub> over the EUS shifted downward (solid black vs. dotted gray lines in Fig. 19a), with the median value declining by 9 ppb and the largest decreases occurring in the upper tails, leading to weaker day-to-day O<sub>3</sub> variability and a narrower O<sub>3</sub> range (standard deviation  $\sigma$  decreased from 16.4 to 12.9 ppb). These observed O<sub>3</sub> changes driven by regional NO<sub>x</sub> reductions are even more prominent when comparing the heat waves of 1988 versus 2012 (solid purple vs. dotted brown lines in Fig. 19a):  $\sigma = 22.3$  vs. 13.4 ppb and median value  $\mu = 68.6$  vs. 52.2 ppb.

Deleted: S

Deleted: pollution extremes over the eastern US

Deleted: large-scale

Deleted: -

Deleted: -

Deleted: as

Deleted: ed

Deleted: simulated by the

Deleted: the

Deleted: such

Deleted: manifested a

Deleted: shift in the probability distribution

Deleted: Using fewer data in 1995-1998 vs. 2002-2005, Rieder et al. (2015) also noted a shift in the O<sub>3</sub> distribution.

Deleted: red

Deleted: Regional emission reductions significantly alleviated the O<sub>3</sub> buildup during the 2012 heat wave relative to earlier heat waves.

1 **Fig.19b** shows the corresponding comparisons using the results from AM3 BASE. Despite  
2 the high mean model bias ( $\sim 20$  ppb), AM3 captures the overall structure of the changes in the  
3 surface  $O_3$  distributions and thus the response of surface  $O_3$  to the  $NO_x$  SIP Call, including the  
4 reductions of high- $O_3$  events during the heat wave of 2012 compared to 1988. Nevertheless,  
5 there is a noticeable difference between the observations and simulations in the shape of MDA8  
6  $O_3$  probability distributions for summer 1988, particularly in the upper tail of the distribution  
7 above 110 ppb (purple lines in **Figs.19a vs. 19b**). The BASE model also underestimates the  
8 magnitude of observed July mean  $O_3$  anomaly in 1988 at PSU by  $\sim 10$  ppb (purple vs. black dots  
9 in **Fig.18a**). One possible explanation for these biases is that drought stress can effectively  
10 reduce the  $O_3$  deposition sink to vegetation, leading to an increase in surface  $O_3$  concentrations  
11 as found during the 2003 European heat wave (Solberg et al., 2008), whereas AM3 does not  
12 include interannually varying dry deposition velocities.

13 The North American drought of 1988 ranks among the worst episodes of drought in the US  
14 (e.g., Seager and Hoerling, 2014), with JJA soil moisture deficits occurring over the northern  
15 Great Plains – Midwest region with magnitudes of 1-2.5 mm standardized departures from the  
16 1979-2010 climatology (Fig.19c). Huang et al. (2016) found that monthly mean  $O_3$  dry  
17 deposition velocities ( $V_{d,O_3}$ ) for forests decreased by 33% over Texas during the dry summer of  
18 2011. Based on this estimate, we conduct a sensitivity simulation for 1988 using BASE  
19 emissions but decreasing monthly mean  $V_{d,O_3}$  from May to August by 35% in the areas over  
20 North America ( $20^\circ N$ - $60^\circ N$ ) where soil moisture deficits in 1988 exceed  $-1.0\sigma$  mm (Fig.19c).  
21 This experiment (hereafter referred to as IAVDEP) simulates  $\sim 10$  ppb higher July mean MDA8  
22  $O_3$  at PSU CASTNet site than the BASE model and matches the observed  $O_3$  anomaly in 1988  
23 relative to the record mean (green symbol in Fig.18a). The impact is largest (up to 15 ppb) on  
24 days when observed MDA8  $O_3$  exceeds 100 ppb (Fig.18b;  $T_{max} \geq 30^\circ C$ ). Simulated JJA MDA8  
25  $O_3$  at EUS sites in IAVDEP shows an upward shift in the probability distribution, particularly in  
26 the upper tail above 110 ppb (green vs. purple lines in Fig.19b), bringing it closer to observations  
27 in 1988 (Fig.19a). The  $O_3$  standard deviation in IAVDEP ( $\sigma = 18$  ppb) shifts towards that in  
28 observations ( $\sigma = 22$  ppb) relative to the BASE model ( $\sigma = 16$  ppb).

29 Quantile mapping can be applied to correct systematic distributional biases in surface  $O_3$   
30 compared to observations (Rieder et al., 2015), but this approach has limitations if there are  
31 structural biases in the  $O_3$  distribution due to missing physical processes in the model (e.g.,  
32 variations of  $V_{d,O_3}$  with droughts). Travis et al. (2016) suggest that the National Emission  
33 Inventory (NEI) for  $NO_x$  from the US EPA is too high nationally by 50% and that decreasing US  
34  $NO_x$  emissions by this amount corrects their model bias for boundary layer  $O_3$  by 12 ppb in the  
35 Southeast for summer 2013, while surface MDA8  $O_3$  in their model is still biased high by  $6 \pm 14$   
36 ppb, which the authors attribute to excessive boundary layer mixing. US  $NO_x$  emissions in the  
37 emission inventory used in AM3 (Sect. 2.2) are approximately 15% lower than those from the  
38 NEI. The 35% decrease in  $NO_x$  emissions from the pre- $NO_x$  SIP Call to the post- $NO_x$  SIP Call in  
39 the model reduces mean  $O_3$  by 8 ppb in the EUS, implying that the  $NO_x$  emission bias could

Deleted: red
Formatted: Subscript
Deleted: is
Deleted: the 1988 heat wave coincided with severe
Deleted: conditions (Seager and Hoerling, 2014), which can
Formatted: Font:Bold
Deleted: "turn off"
Deleted: substantial
Deleted: as found during the 2003 European heat wave
Deleted: ; Emberson et al., 2013
Deleted: ,
Deleted: whereas AM3 does not include interannually varying dry deposition velocities for $O_3$ .
Formatted: Font:Bold
Formatted: Subscript
Formatted: Not Superscript/ Subscript
Formatted: Not Superscript/ Subscript
Formatted: Font:Bold
Formatted: Subscript
Formatted: Subscript
Formatted: Font:Bold
Formatted: Subscript
Formatted: Font:Bold
Formatted: Subscript
Formatted: Font:Bold
Formatted: Font:Bold
Formatted: Subscript
Formatted: Subscript
Deleted: +
Formatted: Font:Not Bold, Font color: Black
Formatted: Font color: Auto
Deleted: 8
Formatted: Not Highlight
Deleted: 3
Formatted: Not Highlight

correct 40% of our model mean bias of ~20 ppb. These estimates support the idea that the common model biases in simulating surface O<sub>3</sub> over the Southeast US (e.g., Fiore et al., 2009) may partly reflect excessive NO<sub>x</sub> emissions. Some of the positive O<sub>3</sub> biases could be also due to the averaging over a deep vertical box in the model surface layer (~60 m in AM3) that can't resolve near-surface gradients (Travis et al., 2016).

## 7. Conclusions and Recommendations

Through an observational and modeling analysis of interannual variability and long-term trends in sources of O<sub>3</sub> over the past 35 years, we have identified the key drivers of O<sub>3</sub> pollution over the US. We initially evaluated the trends of O<sub>3</sub> in Asia resulting from rising Asian precursor emissions. Our synthesis of available observations and simulations indicates that surface and free tropospheric O<sub>3</sub> over East Asia has increased by 1-2 ppb yr<sup>-1</sup> since 1990 (i.e., 25-50 ppb over 25 years), with significant implications for regional air quality and global tropospheric O<sub>3</sub> burden (Figs.4-6). Shifting next to the US, we find 0.2-0.5 ppb yr<sup>-1</sup> increases in median springtime MDA8 O<sub>3</sub> measured at 50% of sixteen WUS rural sites, with 25% of the sites showing increases across the entire O<sub>3</sub> concentration distribution, despite stringent US domestic emission controls (Fig. 7). While many prior studies show that global models have difficulty simulating O<sub>3</sub> increases observed at rural baseline sites (e.g., Koumoutsaris and Bey, 2012; Parrish et al., 2014), we reconcile observed and simulated O<sub>3</sub> trends in GFDL-AM3 with a novel baseline sampling approach (Figs.3 and 13). We suggest that the common model-observation disagreement in baseline O<sub>3</sub> trends reflects limitations of coarse-resolution global models in resolving observed baseline conditions. This representativeness problem can be addressed by filtering model O<sub>3</sub> for hemispheric-scale baseline conditions using the easy-to-implement, low-cost regional CO-like tracers. This approach allows trends of O<sub>3</sub> measured at baseline sites to be compared directly with multi-decadal global model hindcasts, such as those being conducted for the Chemistry-Climate Model Initiative (CCMI; Morgenstern et al., 2016).

The ability of the GFDL-AM3 model to reproduce observed US surface O<sub>3</sub> trends lends confidence in its application to attribute these observed trends to specific processes (Figs.7 to 11). We summarize the overall statistics in Fig.20, drawing upon the decadal mean O<sub>3</sub> changes from 1981-1990 to 2003-2012 in the BASE and sensitivity simulations. The changes in BASE are: over the WUS 4.3±1.8 ppb for spring and 1.6±1.2 ppb for summer; over the Northeast -1.8±1.7 ppb for spring and -6.0±2.0 ppb for summer; over the Southeast -3.9±1.4 ppb for spring and -7.5±1.6 ppb for summer. Increasing O<sub>3</sub> in the WUS under BASE coincides with an increase of background O<sub>3</sub> by 6.3±1.9 ppb for spring and 4.2±2.0 ppb for summer. Under conditions of strong transport from Asia (East Asian COt ≥ 67<sup>th</sup>), the background trend rose to 7.6±2.2 ppb for spring and 6.0±2.1 ppb for summer (green dots in Fig.20). The WUS background O<sub>3</sub> increase reflects contributions from: increases in Asian anthropogenic emissions (accounting for 50% of background increase in spring; 52% in summer), rising global methane (13% in spring; 23% in summer), and variability in biomass burning (6% in spring; 12% in summer; excluding the

Formatted: Font:10.5 pt, Check spelling and grammar

Deleted: .

Field Code Changed

Deleted: (Figure 20 about here: 2003-2012 minus 1981-1990)

Deleted: a comprehensive

Deleted: discussed

Deleted: factors controlling US

Formatted: Subscript

Formatted: Subscript

Formatted: Subscript

Formatted: Font:12 pt

Formatted: Font:Not Bold, Font color: Auto

Formatted: Font:Not Bold

Formatted: Font:Not Bold

Formatted: Font:Not Bold

Deleted: In Fig.20,

Deleted: w

Deleted: MDA8

Deleted: AM3

Deleted: for the WUS

Formatted: Superscript

Deleted: in the WUS

Deleted: the

Deleted: with

1 meteorological influence).

2 We conclude that ~~the increase in~~ Asian anthropogenic emissions ~~is~~ the major driver of

3 ~~rising~~ background O<sub>3</sub> over the WUS for both spring and summer ~~in the past decades, with a~~

4 ~~lesser contribution from~~ methane increases ~~over this period~~. The tripling of Asian NO<sub>x</sub> emissions

5 since 1990 contributes ~~up to~~ 65% of modeled springtime background O<sub>3</sub> increases (0.3-0.5 ppb

6 yr<sup>-1</sup>) over the WUS, outpacing O<sub>3</sub> decreases resulting from ~~50% US NO<sub>x</sub> emission controls~~ (~~≤ 0.1~~

7 ~~ppb yr<sup>-1</sup>~~; ~~Table 2 and Fig.10~~). Springtime O<sub>3</sub> observed in the Denver metropolitan area, has

8 increased at a rate similar to remote rural sites (~~Fig. 17b~~). ~~Mean springtime O<sub>3</sub> above the WUS is~~

9 ~~projected to~~ increase by ~10 ppb from 2010 to 2030 under the RCP8.5 global change scenario

10 but ~~to~~ remain constant throughout 2010 to 2050 under the RCP4.5 scenario (~~Fig.14~~). As NO<sub>x</sub>

11 ~~emissions in China continue to decline in response to efforts to improve air quality~~ (Krotkov et

12 ~~al., 2016; Liu et al., 2016), rising global methane and NO<sub>x</sub> emissions in South Asian countries~~

13 ~~(e.g., India) in the tropics, where O<sub>3</sub> production is more efficient, may become more important in~~

14 ~~the coming decades. A global perspective is necessary when designing a strategy to meet US O<sub>3</sub>~~

15 ~~air quality objectives.~~

16 During summer, ~~a tripling of~~ Asian anthropogenic emissions ~~from 1988 to 2014~~

17 approximately offsets the ~~benefits of 50% reductions in~~ US domestic emissions, leading to weak

18 or insignificant O<sub>3</sub> trends observed at most WUS rural sites (~~Figs.8 and 11~~). Rising Asian

19 emissions contribute to observed ~~summertime O<sub>3</sub> increases~~ (0.3 ppb yr<sup>-1</sup>) at Yellowstone National

20 Park. ~~Our findings confirm the earliest projection of Jacob et al. (1999) with a tripling of Asian~~

21 ~~emissions~~. While wildfire emissions can result in 2-8 ppb enhancements to monthly mean O<sub>3</sub> at

22 individual sites in some summers, they are not the primary driver of observed O<sub>3</sub> interannual

23 variability over the Intermountain West (~~Figs.15 and 16~~). Instead, boundary layer depth, high

24 temperatures and the associated buildup of O<sub>3</sub> produced from regional anthropogenic emissions

25 contribute most to observed ~~interannual~~ variability of O<sub>3</sub> in summer. ~~Summertime O<sub>3</sub> measured~~

26 ~~in Denver during pollution episodes frequently exceeds the 70 ppb NAAQS level, with little~~

27 ~~overall trend despite stringent precursor emission controls~~ (~~Fig.17c~~), ~~likely due to the effects of~~

28 ~~more frequent occurrences of hot extremes in the last decade.~~

29 In the eastern US, ~~if emissions had not declined~~, the 95<sup>th</sup> percentile summertime O<sub>3</sub>

30 ~~would have increased by 0.2-0.4 ppb yr<sup>-1</sup> over 1988-2014~~ (~~Fig.11c~~), due to more frequent hot

31 summer extremes and increases in biogenic isoprene emissions over this period (~~Fig.12~~).

32 ~~Regional NO<sub>x</sub> reductions alleviated the O<sub>3</sub> buildup during the recent heat waves of 2011 and~~

33 ~~2012 relative to earlier heat waves (e.g., 1988; 1995; 1999). GFDL-AM3 captures year-to-year~~

34 ~~variability in monthly mean O<sub>3</sub> enhancements associated with large-scale variations in~~

35 ~~temperatures~~ (~~Figs. 18 and 19~~). However, there is a need to improve the model representation of

36 O<sub>3</sub> deposition sink to vegetation, in particular its reduced efficiency under drought stress, as we

37 demonstrated for the severe North American drought of 1988. Such land-biosphere couplings are

38 poorly represented in current models and further work is needed to examine their impacts on O<sub>3</sub>

39 pollution extremes in a warming climate.

Deleted: subtracted out

Deleted: rising ...sian anthropogenic emissions is are ... [10]

Deleted: domestic ...mission controls (≤ 0.1 ppb yr<sup>-1</sup>, Table 2 and Fig.10) [11]

Formatted: Subscript

Formatted ... [12]

Deleted: rising ...sian anthropogenic emissions from ... [13]

Deleted: rRegional NO<sub>x</sub> controls also alleviated the O<sub>3</sub> buildup during the recent heat waves of 2011 and 2012 relative to earlier heat waves (Figs. 18 and 19). Despite high mean state biases, the model captures the salient features of observed O<sub>3</sub> trends over the EUS, including the largest summertime decreases in the 95<sup>th</sup> percentile, the north-to-south gradient in springtime O<sub>3</sub> trends, as well as wintertime increases in the 5<sup>th</sup> and 50<sup>th</sup> percentiles. The model also captures enhancements in monthly mean O<sub>3</sub> due to large-scale heat ... [14]

Formatted ... [15]

1 Following the NO<sub>x</sub> SIP Call, surface O<sub>3</sub> in the eastern US declined throughout its  
 2 probability distribution, with the largest decreases occurring in the highest percentiles during  
 3 summer (-0.8 to -1.8 ppb yr<sup>-1</sup>; Fig.8). Spatially, historical O<sub>3</sub> decreases during non-summer  
 4 seasons were more pronounced in the Southeast, where the seasonal onset of biogenic isoprene  
 5 emissions and NO<sub>x</sub>-sensitive O<sub>3</sub> production occurs earlier than in the Northeast (Figs.7, 9 and  
 6 S4). The 95<sup>th</sup> percentile O<sub>3</sub> concentration in the Southeast even decreased significantly during  
 7 winter. Despite high mean-state biases, GFDL-AM3 captures the key features of observed O<sub>3</sub>  
 8 trends over the EUS, including wintertime increases in the 5<sup>th</sup> and 50<sup>th</sup> percentiles in the  
 9 Northeast, greater springtime decreases in the Southeast than the Northeast, and summertime  
 10 decreases throughout the O<sub>3</sub> probability distribution. These results suggest that NO<sub>x</sub> emission  
 11 controls will continue to provide long-term O<sub>3</sub> air quality benefits in the Southeast during all  
 12 seasons.

13  
 14 **Acknowledgments.** This work was supported by funding from the NASA grants  
 15 NNH13ZDA001N-AURAST and NNX14AR47G to M.Y. Lin. We thank O. Cooper, S. Fan and  
 16 J. Schnell for helpful comments on the manuscript. We acknowledge the free use of ozonesonde  
 17 data at Hong Kong available on [woude.org](http://woude.org) and GOME-SCIAMACHY tropospheric NO<sub>2</sub> column  
 18 data available on [www.temis.nl](http://www.temis.nl). AMF acknowledges support under EPA Assistance Agreement  
 19 No. 83587801. The views expressed in this document are solely those of the authors and do not  
 20 necessarily reflect those of the Agency. M.Y. Lin devotes this article to her father Tianci Lin  
 21 who is the motivation of her life and research career.

**Deleted:** In contrast to the WUS, the observed trends of surface O<sub>3</sub> in the EUS are overwhelmingly dominated by decreases in regional anthropogenic emissions.

**Deleted:** F

**Deleted:** over the EUS

**Deleted:** manifested a downward shift in the

**Deleted:** are

**Deleted:** most

**Deleted:**

**Deleted:** with an earlier

**Deleted:** and

**Formatted:** Font:Not Bold

**Formatted:** Superscript

**Formatted:** Subscript

**Formatted:** Subscript

**Formatted:** Subscript

## References:

- Abatzoglou, J.T. and A.P. Williams (2016), Impact of anthropogenic climate change on wildfire across western US forests, *Proc. Natl. Acad. Sci. U.S.A.*, 11770–11775, doi: 10.1073/pnas.1607171113
- Baker, K. R., M. C. Woody, G. S. Tonnesen, et al. (2016), Contribution of regional-scale fire events to ozone and PM<sub>2.5</sub> air quality estimated by photochemical modeling approaches, *Atmos. Environ.*, 140, 539-554, doi: 10.1016/j.atmosenv.2016.06.032.
- Barnes, E. A., A. M. Fiore, and L. W. Horowitz (2016), Detection of trends in surface ozone in the presence of climate variability, *J. Geophys. Res.*, 121(10), 6112-6129, doi: 10.1002/2015jd024397.
- Bishop, G. A., and D. H. Stedman (2008), A decade of on-road emissions measurements, *Environ. Sci. Technol.*, 42(5), 1651-1656, doi: 10.1021/es702413b.
- Bishop, G. A., and D. H. Stedman (2015), Reactive Nitrogen Species Emission Trends in Three Light-/Medium-Duty United States Fleets, *Environ. Sci. Technol.*, 49(18), 11234-11240, doi: 10.1021/acs.est.5b02392.
- Boersma, K. F., H. J. Eskes, and E. J. Brinksma (2004), Error analysis for tropospheric NO<sub>2</sub> retrieval from space, *J. Geophys. Res.*, 109(D4), doi: 10.1029/2003jd003962.
- Brodin, M., D. Helmig, and S. Oltmans (2010), Seasonal ozone behavior along an elevation gradient in the Colorado Front Range Mountains, *Atmos. Environ.*, 44(39), 5305-5315, doi: 10.1016/j.atmosenv.2010.06.033.
- Brown-Steiner, B., and P. Hess (2011), Asian influence on surface ozone in the United States: A comparison of chemistry, seasonality, and transport mechanisms, *J. Geophys. Res.*, 116, doi: 10.1029/2011jd015846.
- Brown-Steiner, B., P. G. Hess, and M. Y. Lin (2015), On the capabilities and limitations of GCM simulations of summertime regional air quality: A diagnostic analysis of ozone and temperature simulations in the US using CESM CAM-Chem, *Atmos. Environ.*, 101, 134-148, doi: 10.1016/j.atmosenv.2014.11.001.
- Carmichael, G. R., et al. (2003), Regional-scale chemical transport modeling in support of the analysis of observations obtained during the TRACE-P experiment, *J. Geophys. Res.*, 108(D21), doi: 10.1029/2002jd003117.
- Clifton, O. E., A. M. Fiore, G. Correa, L. W. Horowitz, and V. Naik (2014), Twenty-first century reversal of the surface ozone seasonal cycle over the northeastern United States, *Geophys. Res. Lett.*, 41(20), 7343-7350, doi: 10.1002/2014gl061378.

1 Cooper, O. R., R.-S. Gao, D. Tarasick, T. Leblanc, and C. Sweeney (2012), Long-term ozone trends at rural  
2 ozone monitoring sites across the United States, 1990–2010, *J. Geophys. Res.*, 117, doi:  
3 10.1029/2012JD018261.

4 Cooper, O. R., et al. (2010), Increasing springtime ozone mixing ratios in the free troposphere over western  
5 North America, *Nature*, 463(7279), 344-348, doi: 10.1038/nature08708.

6 Dennison, P. E., S. C. Brewer, J. D. Arnold, and M. A. Moritz (2014), Large wildfire trends in the western  
7 United States, 1984-2011, *Geophys. Res. Lett.*, 41(8), 2928-2933, doi: 10.1002/2014gl059576.

8 Dentener, F., et al. (2006), Emissions of primary aerosol and precursor gases in the years 2000 and 1750  
9 prescribed data-sets for AeroCom, *Atmos. Chem. Phys.*, 6, 4321-4344, 10.5194/acp-6-4321-2006

10 Ding, A. J., T. Wang, V. Thouret, J. P. Cammas, and P. Nedelec (2008), Tropospheric ozone climatology over  
11 Beijing: analysis of aircraft data from the MOZAIC program, *Atmos. Chem. Phys.*, 8(1), 1-13,  
12 doi:10.5194/acp-8-1-2008

13 Donat, M. G., L. V. Alexander, H. Yang, I. Durre, R. Vose, and J. Caesar (2013), Global land-based datasets for  
14 monitoring climatic extremes. *Bull. Amer. Meteor. Soc.*, 94, 997–1006, doi:10.1175/BAMS-D-12-00109.1.

15 Donner, L. J., et al. (2011), The Dynamical Core, Physical Parameterizations, and Basic Simulation  
16 Characteristics of the Atmospheric Component AM3 of the GFDL Global Coupled Model CM3, *J. Clim.*,  
17 24(13), 3484-3519, doi: 10.1175/2011jcli3955.1.

18 Duncan, B. N., L. N. Lamsal, A. M. Thompson et al. (2016), A space-based, high-resolution view of notable  
19 changes in urban NO<sub>x</sub> pollution around the world (2005-2014), *J. Geophys. Res.*, 121(2), 976-996, doi:  
20 10.1002/2015jd024121.

21 Emberson, L. D., N. Kitwiroon, S. Beevers, P. Buker, and S. Cinderby (2013), Scorched Earth: how will  
22 changes in the strength of the vegetation sink to ozone deposition affect human health and ecosystems?, *Atmos.*  
23 *Chem. Phys.*, 13(14), 6741-6755, doi: 10.5194/acp-13-6741-2013.

24 Federal Register (2015). US Environmental Protection Agency, National Ambient Air Quality Standards for  
25 Ozone – Final Rule, Federal Register 80 (206), 65292-65468, available at  
26 <http://www.gpo.gov/fdsys/pkg/FR-2015-10-26/pdf/2015-26594.pdf>.

27 Fiore, A. M., V. Naik, and E. M. Leibensperger (2015), Air Quality and Climate Connections, *J. Air Waste*  
28 *Manage. Assoc.*, 65(6), 645-685, doi: 10.1080/10962247.2015.1040526.

Deleted: .

Deleted: ,

Deleted: a



1 Fiore, A. M., J. T. Oberman, M. Y. Lin, ~~et al.~~ (2014), Estimating North American background ozone in U.S.  
2 surface air with two independent global models: Variability, uncertainties, and recommendations Atmos.  
3 Environ., 96, 284-300, doi: doi:10.1016/j.atmosenv.2014.07.045.

4 Fiore, A. M., et al. (2009), Multimodel estimates of intercontinental source-receptor relationships for ozone  
5 pollution, J. Geophys. Res., 114, doi: 10.1029/2008jd010816.

6 Gao, Y., J. S. Fu, J. B. Drake, J. F. Lamarque, and Y. Liu (2013), The impact of emission and climate change on  
7 ozone in the United States under representative concentration pathways (RCPs), Atmos. Chem. Phys., 13(18),  
8 9607-9621, doi: 10.5194/acp-13-9607-2013.

9 Gilman, J. B., B. M. Lerner, W. C. Kuster, and J. A. de Gouw (2013), Source Signature of Volatile Organic  
10 Compounds from Oil and Natural Gas Operations in Northeastern Colorado, Environ. Sci. Technol., 47(3),  
11 1297-1305, doi: 10.1021/es304119a.

12 Granier, C., et al. (2011), Evolution of anthropogenic and biomass burning emissions of air pollutants at global  
13 and regional scales during the 1980-2010 period, Climatic Change, 109(1-2), 163-190, doi:  
14 10.1007/s10584-011-0154-1.

15 Gratz, L. E., D. A. Jaffe, and J. R. Hee (2014), Causes of increasing ozone and decreasing carbon monoxide in  
16 springtime at the Mt. Bachelor Observatory from 2004 to 2013, Atmos. Environ., 109, 323-330, doi:  
17 10.1016/j.atmosenv.2014.05.076.

18 Guenther, A., T. Karl, P. Harley, C. Wiedinmyer, P. I. Palmer, and C. Geron (2006), Estimates of global  
19 terrestrial isoprene emissions using MEGAN (Model of Emissions of Gases and Aerosols from Nature), Atmos.  
20 Chem. Phys., 6, 3181-3210.

21 Halliday, H. S., A. M. Thompson, and A. Wisthaler, et al. (2016), Atmospheric benzene observations from oil  
22 and gas production in the Denver Julesburg basin in July and August 2014, J. Geophys. Res. Atmos., 121,  
23 doi:10.1002/2016JD025327, 2016., 121, doi: 10.1002/2016JD025327.

24 Harris, I., P. D. Jones, T. J. Osborn, and D. H. Lister (2014), Updated high-resolution grids of monthly climatic  
25 observations - the CRU TS3.10 Dataset, Journal of Climatology, 34(3), 623-642, doi: 10.1002/joc.3711.

26 Hilboll, A., A. Richter, and J. P. Burrows (2013), Long-term changes of tropospheric NO<sub>2</sub> over megacities  
27 derived from multiple satellite instruments, Atmos. Chem. Phys., 13, 4145-4169, doi:  
28 10.5194/acp-13-4145-2013.

**Deleted:** , L. Zhang, O. E. Clifton, D. J. Jacob, V. Naik, L. W.  
Horowitz, and J. P. Pinto

- 1 Horton, D. E., N. C. Johnson, D. Singh, D. L. Swain, B. Rajaratnam, and N. S. Diffenbaugh (2015),  
2 Contribution of changes in atmospheric circulation patterns to extreme temperature trends, *Nature*, 522(7557),  
3 465-469, doi: 10.1038/nature14550.
- 4 [Huang, L., E. C. McDonald-Buller, G. McGaughey, Y. Kimura, and D. T. Allen \(2016\), The impact of drought  
5 on ozone dry deposition over eastern Texas, \*Atmospheric Environment\*, 127, 176-186, doi:  
6 10.1016/j.atmosenv.2015.12.022.](#)
- 7
- 8 Huang, M., et al. (2013), Impacts of transported background pollutants on summertime western US air quality:  
9 model evaluation, sensitivity analysis and data assimilation, *Atmos. Chem. Phys.*, 13(1), 359-391, doi:  
10 10.5194/acp-13-359-2013.
- 11 [Jacob, D. J., Logan, J. A., Murti, P. P. Effect of rising Asian emissions on surface ozone in the United States.  
12 \*Geophys. Res. Lett.\* 26, 2175-2178 \(1999\).](#)
- 13 Jacob, D. J., and D. A. Winner (2009), Effect of climate change on air quality, *Atmos Environ*, 43(1), 51-63,  
14 doi: 10.1016/j.atmosenv.2008.09.051.
- 15 Jaffe, D. A., et al. (1999), Transport of Asian air pollution to North America, *Geophys. Res. Lett.*, 26, 711-714,  
16 doi:10.1029/1999GL900100
- 17 Jaffe, D. (2011), Relationship between Surface and Free Tropospheric Ozone in the Western U.S, *Environ. Sci.*  
18 *Technol*, 45(2), 432-438, doi: 10.1021/es1028102.
- 19 Jaffe, D., D. Chand, W. Hafner, A. Westerling, and D. Spracklen (2008), Influence of fires on O<sub>3</sub>  
20 concentrations in the western US, *Environ. Sci. Technol.*, 42(16), 5885-5891, doi: 10.1021/es800084k.
- 21 [Jaffe, D., and J. Ray \(2007\), Increase in surface ozone at rural sites in the western US, \*Atmos. Environ.\*, 41\(26\),  
22 5452-5463, doi: 10.1016/j.atmosenv.2007.02.34.](#)
- 23
- 24 Jaffe, D., N. Wigder, N. Downey, G. Pfister, A. Boynard, and S. B. Reid (2013), Impact of Wildfires on Ozone  
25 Exceptional Events in the Western US, *Environ. Sci. Technol.*, 47(19), 11065-11072, doi: 10.1021/es402164f.
- 26 [Jia, L. W., G. A. Vecchi, X. S. Yang, et al. \(2016\), The Roles of Radiative Forcing, Sea Surface Temperatures,  
27 and Atmospheric and Land Initial Conditions in US Summer Warming Episodes, \*J. Climate\*, 29\(11\),  
28 4121-4135, doi: 10.1175/Jcli-D-15-0471.1.](#)
- 29 John, J. G., A. M. Fiore, V. Naik, L. W. Horowitz, and J. P. Dunne (2012), Climate versus emission drivers of

Deleted: -

Formatted: Normal, Space After: 0 pt

Deleted: Jaffe, D., I. Bertsch, L. Jaegle, P. Novelli, J. S. Reid, H. Tanimoto, R. Vingarzan, and D. L. Westphal (2004), Long-range transport of Siberian biomass burning emissions and impact on surface ozone in western North America, *Geophys. Res. Lett.*, 31(16), doi: 10.1029/2004gl020093. .

Deleted: R. G. Gudgel, T. L. Delworth, W. F. Stern, K. Paffendorf, S. D. Underwood, and F. R. Zeng

1 methane lifetime against loss by tropospheric OH from 1860-2100, Atmos. Chem. Phys., 12(24), 12021-12036,  
2 doi: 10.5194/acp-12-12021-2012.

3 Koumoutsaris, S., and I. Bey (2012), Can a global model reproduce observed trends in summertime surface  
4 ozone levels?, Atmos. Chem. Phys., 12(15), 6983-6998, doi: 10.5194/acp-12-6983-2012.

5 Lamarque, J. F., G. P. Kyle, M. Meinshausen, et al. (2012), Global and regional evolution of short-lived  
6 radiatively-active gases and aerosols in the Representative Concentration Pathways, Climatic Change 109(1-2),  
7 191-212, doi: 10.1007/s10584-011-0155-0.

8 Lamarque, J. F., et al. (2010), Historical (1850-2000) gridded anthropogenic and biomass burning emissions of  
9 reactive gases and aerosols: methodology and application, Atmos. Chem. Phys., 10(15), 7017-7039, doi:  
10 10.5194/acp-10-7017-2010.

11 Langford, A. O., K. C. Aikin, C. S. Eubank, and E. J. Williams (2009), Stratospheric contribution to high  
12 surface ozone in Colorado during springtime, Geophys. Res. Lett., 36, doi: 10.1029/2009gl038367.

13 Langford, A. O., C. J. Senff, R. J. Alvarez, II, R. M. Banta, and R. M. Hardesty (2010), Long-range transport  
14 of ozone from the Los Angeles Basin: A case study, Geophys. Res. Lett., 37, doi: 10.1029/2010gl042507.

15 Langford, A. O., et al. (2014), An overview of the 2013 Las Vegas Ozone Study (LVOS): Impact of  
16 stratospheric intrusions and long-range transport on surface air quality, Atmos. Environ., 109, 305-322, doi:  
17 10.1016/j.atmosenv.2014.08.040.

18 Lee, H.-J., S.-W. Kim, J. Brioude, et al. (2014), Transport of NO<sub>x</sub> in East Asia identified by satellite and in situ  
19 measurements and Lagrangian particle dispersion model simulations, J. Geophys. Res. Atmos., 119, 2574-2596,  
20 doi:10.1002/2013JD021185.

21 Leibensperger, E. M., L. J. Mickley, and D. J. Jacob (2008), Sensitivity of US air quality to mid-latitude  
22 cyclone frequency and implications of 1980-2006 climate change, Atmos. Chem. Phys., 8(23), 7075-7086.

23 Li, G., Bei, N., Cao, J., Wu, J., Long, X., Feng, T., Dai, W., Liu, S., Zhang, Q., and Tie, X.: Widespread and  
24 Persistent Ozone Pollution in Eastern China, Atmos. Chem. Phys. Discuss., doi:10.5194/acp-2016-864, in  
25 review, 2016.

26 Lin, M., T. Holloway, G. R. Carmichael, and A. M. Fiore (2010), Quantifying pollution inflow and outflow  
27 over East Asia in spring with regional and global models, Atmos. Chem. Phys., 10(9), 4221-4239, doi:  
28 10.5194/acp-10-4221-2010.

**Deleted:** K. Riahi, S. J. Smith, D. P. van Vuuren, A. J. Conley, and F. Vitt

**Deleted:** O. R. Cooper, G. J. Frost, C.-H. Kim, R. J. Park, M. Trainer, and J.-H. Woo

**Formatted:** Font:Times, 10.5 pt, Subscript

**Deleted:** ,

**Deleted:** doi:

- 1 Lin, M., T. Holloway, T. Oki, D. G. Streets, and A. Richter (2009), Multi-scale model analysis of boundary
- 2 layer ozone over East Asia, *Atmos. Chem. Phys.*, 9(10), 3277-3301, doi: 10.5194/acp-9-3277-2009.
- 3 Lin, M., A. M. Fiore, O. R. Cooper, [et al.](#) (2012a), Springtime high surface ozone events over the western
- 4 United States: Quantifying the role of stratospheric intrusions, *J. Geophys. Res.*, 117, D00V22, doi:
- 5 10.1029/2012jd018151.
- 6 Lin, M., A.M. Fiore, L.W. Horowitz, et al. (2012b), Transport of Asian ozone pollution into surface air over the
- 7 western United States in spring, *J. Geophys. Res.*, 117, D00V07, doi: 10.1029/2011jd016961.
- 8 Lin, M., A. M. Fiore, L. W. Horowitz, [et al.](#) (2015a), Climate variability modulates western U.S. ozone air
- 9 quality in spring via deep stratospheric intrusions, *Nature Communications*, 6(7105), doi:
- 10 10.1038/ncomms8105.
- 11 Lin, M., L. W. Horowitz, O. R. Cooper, [et al.](#) (2015b), Revisiting the evidence of increasing springtime ozone
- 12 mixing ratios in the free troposphere over western North America, *Geophys. Res. Lett.*, 42(20), 8719-8728, doi:
- 13 10.1002/2015GL065311.
- 14 Lin, M., L. W. Horowitz, S. J. Oltmans, A. M. Fiore, and S. Fan (2014), Tropospheric ozone trends at Mauna
- 15 Loa Observatory tied to decadal climate variability, *Nature Geoscience*, 7, 136–143, doi: 10.1038/ngeo2066.
- 16 Lin, Y.-K., T.-H. Lin, and S.-C. Chang (2010), The changes in different ozone metrics and their implications
- 17 following precursor reductions over northern Taiwan from 1994 to 2007, *Environ. Monit. Assess.*, 169(1-4),
- 18 143-157, doi: 10.1007/s10661-009-1158-4.
- 19 [Liu, F., Q. Zhang, J. V. Ronald, B. Zheng, D. Tong, L. Yan, Y. X. Zheng, and K. B. He \(2016\), Recent](#)
- 20 [reduction in NO<sub>x</sub> emissions over China: synthesis of satellite observations and emission inventories, \*Environ\*](#)
- 21 [Res Lett](#), 11(11), doi: 10.1088/1748-9326/11/11/114002.
- 22 Liu, H. Y., D. J. Jacob, L. Y. Chan, [et al.](#) (2002), Sources of tropospheric ozone along the Asian Pacific Rim:
- 23 An analysis of ozonesonde observations, *J. Geophys. Res.*, 107(D21), doi: 4573 10.1029/2001jd002005.
- 24 Loughner, C. P., B. N. Duncan, and J. Hains (2014), The benefit of historical air pollution emissions reductions
- 25 during extreme heat, *Environmental Manager* (September), 34-38.
- 26 Ma, Z., J. Xu, W. Quan, Z. Zhang, W. Lin, and X. Xu (2016), Significant increase of surface ozone at a rural
- 27 site, north of eastern China, *Atmos. Chem. Phys.*, 16, 3969-3977, doi: doi:10.5194/acp-16-3969-2016.

**Deleted:** L. W. Horowitz, A. O. Langford, H. Levy, B. J. Johnson, V. Naik, S. J. Oltmans, and C. J. Senff

**Deleted:** A. O. Langford, S. J. Oltmans, D. Tarasick, and H. E. Rieder

**Deleted:** D. Tarasick, S. Conley, L. T. Iraci, B. Johnson, T. Leblanc, I. Petropavlovskikh, and E. L. Yates

**Formatted:** Font:Times, 10.5 pt

**Formatted:** Font:Times, 10.5 pt, Subscript

**Formatted:** Font:Times, 10.5 pt

**Deleted:** S. J. Oltmans, I. Bey, R. M. Yantosca, J. M. Harris, B. N. Duncan, and R. V. Martin

1 McDonald, B. C., T. R. Dallmann, E. W. Martin, and R. A. Harley (2012), Long-term trends in nitrogen oxide  
 2 emissions from motor vehicles at national, state, and air basin scales, *J. Geophys. Res.*, 117, D00V18, doi:  
 3 10.1029/2012jd018304.

4 McDuffie, E. E., et al. (2016), Influence of oil and gas emissions on summertime ozone in the Colorado  
 5 Northern Front Range, *J. Geophys. Res. Atmos.*, 121, doi: 10.1002/2016JD025265.

6 Monks, P. S., Archibald, A. T., Colette, A., et al. (2015): Tropospheric ozone and its precursors from the urban  
 7 to the global scale from air quality to short-lived climate forcer, *Atmos. Chem. Phys.*, 15, 8889-8973,  
 8 doi:10.5194/acp-15-8889-2015.

9 Morgenstern, O., Hegglin, M. I., Rozanov, E., et al. (2016): Review of the global models used within the  
 10 Chemistry-Climate Model Initiative (CCMI), *Geosci. Model Dev. Discuss.*, doi:10.5194/gmd-2016-199, in  
 11 review, 2016.

12 Naik, V., L. W. Horowitz, A. M. Fiore, P. Ginoux, J. Q. Mao, A. M. Aghedo, and H. Levy (2013), Impact of  
 13 preindustrial to present-day changes in short-lived pollutant emissions on atmospheric composition and climate  
 14 forcing, *J. Geophys. Res.*, 118(14), 8086-8110, doi: 10.1002/jgrd.50608.

15

16 Krotkov, N. A., McLinden, C. A., Li, C., et al: Aura OMI observations of regional SO<sub>2</sub> and NO<sub>2</sub> pollution  
 17 changes from 2005 to 2015, *Atmos. Chem. Phys.*, 16, 4605-4629, doi:10.5194/acp-16-4605-2016, 2016.

18 Parrish, D. D., et al. (2014), Long-term changes in lower tropospheric baseline ozone concentrations:  
 19 Comparing chemistry-climate models and observations at northern midlatitudes, *J. Geophys. Res.*, 119(9),  
 20 5719-5736, doi: 10.1002/2013JD021435.

21 ~~Pfister, G. G., S. Walters, L. K. Emmons, D. P. Edwards, and J. Avise (2013), Quantifying the contribution of~~  
 22 ~~inflow on surface ozone over California during summer 2008, *J. Geophys. Res.*, 118(21), 12282-12299, doi:~~  
 23 ~~10.1002/2013jd020336.~~

24 Pfister, G. G., S. Walters, J. F. Lamarque, J. Fast, M. C. Barth, J. Wong, J. Done, G. Holland, and C. L. Bruyere  
 25 (2014), Projections of future summertime ozone over the US, *J. Geophys. Res.*, 119(9), 5559-5582, doi:  
 26 10.1002/2013jd020932.

27 Porter, W. C., C. L. Heald, D. Cooley, and B. Russell (2015), Investigating the observed sensitivities of  
 28 air-quality extremes to meteorological drivers via quantile regression, *Atmos. Chem. Phys.*, 15(18),  
 29 10349-10366, doi: 10.5194/acp-15-10349-2015.

Formatted: Font:Times, 10.5 pt

Formatted: Normal, Space After: 0 pt

Deleted: Pfister, G. G., C. Wiedinmyer, and L. K. Emmons  
 (2008), Impacts of the fall 2007 California wildfires on  
 surface ozone: Integrating local observations with global  
 model simulations, *Geophys. Res. Lett.*, 35(19), doi:  
 10.1029/2008gl034747.

1 Pusede, S. E., A. L. Steiner, and R. C. Cohen (2015), Temperature and Recent Trends in the Chemistry of  
2 Continental Surface Ozone, *Chem. Rev.*, 115(10), 3898-3918, doi: 10.1021/cr5006815.

3 Rasmussen, D. J., A. M. Fiore, V. Naik, L. W. Horowitz, S. J. McGinnis, and M. G. Schultz (2012), Surface  
4 ozone-temperature relationships in the eastern US: A monthly climatology for evaluating chemistry-climate  
5 models, *Atmos. Environ.*, 47, 142-153, doi: 10.1016/j.atmosenv.2011.11.021.

6 Reidmiller, D. R., et al. (2009), The influence of foreign vs. North American emissions on surface ozone in the  
7 US, *Atmos. Chem. Phys.*, 9(14), 5027-5042, doi:10.5194/acp-9-5027-2009

8 Rieder, H. E., A. M. Fiore, L. W. Horowitz, and V. Naik (2015), Projecting policy-relevant metrics for high  
9 summertime ozone pollution events over the eastern United States due to climate and emission changes during  
10 the 21st century, *J. Geophys. Res.*, 120(2), 784-800, doi: 10.1002/2014jd022303.

11 Russell, A. R., L. C. Valin, and R. C. Cohen (2012), Trends in OMI NO<sub>2</sub> observations over the United States:  
12 effects of emission control technology and the economic recession, *Atmos. Chem. Phys.*, 12(24), 12197-12209,  
13 doi: 10.5194/acp-12-12197-2012.

14 Schnell, J. L., M. J. Prather, B. Josse, et al. (2016), Effect of climate change on surface ozone over North  
15 America, Europe, and East Asia, *Geophys. Res. Lett.*, 43, 3509-3518, doi: 10.1002/2016GL068060.

16 Schultz, M. G., A. Heil, J. J. Hoelzemann, et al. (2008), Global wildland fire emissions from 1960 to 2000,  
17 *Global Biogeochem. Cycles*, 22(2), doi: 10.1029/2007gb003031.

18 Schwietzke, S., et al. (2016), Upward revision of global fossil fuel methane emissions based on isotope  
19 database, *Nature*, 538(7623), 88-91, doi: 10.1038/nature19797.

20 Seager, R., and M. Hoerling (2014), Atmosphere and Ocean Origins of North American Droughts, *J. Climate*,  
21 27(12), 4581-4606, doi: 10.1175/Jcli-D-13-00329.1.

22 Shen, L., L. J. Mickley, and E. Gilleland (2016), Impact of increasing heat waves on US ozone episodes in the  
23 2050s: Results from a multimodel analysis using extreme value theory, *Geophys. Res. Lett.*, 43(8), 4017-4025,  
24 doi: 10.1002/2016gl068432.

25  
26 Shepherd, T. G. (2015), CLIMATE SCIENCE: The dynamics of temperature extremes, *Nature*, 522(7557),  
27 422-424.

28 Simon, H., A. Reff, B. Wells, J. Xing, and N. Frank (2015), Ozone Trends Across the United States over a

**Deleted:** V. Naik, L. W. Horowitz, G. Zeng, D. T. Shindell,  
and G. Faluvegi

**Deleted:** A. Spessa, K. Thonicke, J. G. Goldammer, A. C.  
Held, J. M. C. Pereira, and M. van het Bolscher

**Formatted:** Normal, Space After: 0 pt

**Deleted:** .

**Formatted:** Font:Times, 10.5 pt

1 Period of Decreasing NO<sub>x</sub> and VOC Emissions, *Environ. Sci. Technol.*, 49(1), 186-195, doi:  
2 10.1021/es504514z.

3 Solberg, S., O. Hov, A. Sovde, [et al.](#) (2008), European surface ozone in the extreme summer 2003, *J. Geophys.*  
4 *Res.*, 113(D7), doi:10.1029/2007jd009098.

5 Strode, S. A., J. M. Rodriguez, J. A. Logan, et al. (2015), Trends and variability in surface ozone over the  
6 United States, *J. Geophys. Res.*, 120, 9020-9042, doi: 10.1002/2014JD022784.

7 Sun, L., L. Xue, T. Wang, J. Guo, A. Ding, O. R. Cooper and M. Y. Lin, et al. (2016), Significant increase of  
8 summertime ozone at Mount Tai in Central Eastern China, *Atmos. Chem. Phys.*, 16, 10637-10650, doi:  
9 10.5194/acp-16-10637-2016.

10 Tanimoto, H. (2009), Increase in springtime tropospheric ozone at a mountainous site in Japan for the period  
11 1998-2006, *Atmos. Environ.*, 43(6), 1358-1363, doi: 10.1016/j.atmosenv.2008.12.006.

12 Tanimoto, H., R. M. Zbinden, V. Thouret, and P. Nédélec (2016), Consistency of tropospheric ozone  
13 observations made by different platforms and techniques in the global databases, *Tellus Series B-Chemical*  
14 *and Physical Meteorology*, 67, 27073, doi: 10.3402/tellusb.v67.27073.

15 Thompson, A. M., J. C. Witte, H. G. J. Smit, [et al.](#) (2007), Southern Hemisphere Additional Ozonesondes  
16 (SHADOZ) 1998-2004 tropical ozone climatology: 3. Instrumentation, station-to-station variability, and  
17 evaluation with simulated flight profiles, *J. Geophys. Res.*, 112, D03304, doi:10.1029/2005JD007042.

18 Travis, K. R., et al. (2016), Why do models overestimate surface ozone in the Southeast United States?, *Atmos.*  
19 *Chem. Phys.*, 16, 13561-13577, doi: 10.5194/acp-16-13561-2016.

20

21 van der Werf, G. R., J. T. Randerson, L. Giglio, [et al.](#) (2010), Global fire emissions and the contribution of  
22 deforestation, savanna, forest, agricultural, and peat fires (1997-2009), *Atmos. Chem. Phys.*, 10(23),  
23 11707-11735, doi: 10.5194/acp-10-11707-2010.

24 [VanCuren, R., and M. S. Gustin \(2015\), Identification of sources contributing to PM<sub>2.5</sub> and ozone at elevated](#)  
25 [sites in the western US by receptor analysis: Lassen Volcanic National Park, California, and Great Basin](#)  
26 [National Park, Nevada, \*Sci. Total Environ.\*, 530, 505-518, doi: 10.1016/j.scitotenv.2015.03.091.](#)

27

28 Wang, T., A. Ding, J. Gao, and W. S. Wu (2006), Strong ozone production in urban plumes from Beijing, China,  
29 *Geophys. Res. Lett.*, 33, L21806, doi:10.1029/2006GL027689.

**Deleted:** I. S. A. Isaksen, P. Coddeville, H. De Backer, C. Forster, Y. Orsolini, and K. Uhse

**Deleted:** S. J. Oltmans, B. J. Johnson, V. W. J. H. Kirchhoff, and F. J. Schmidlin

**Deleted:** G. J. Collatz, M. Mu, P. S. Kasibhatla, D. C. Morton, R. S. DeFries, Y. Jin, and T. T. van Leeuwen

**Formatted:** Normal, Space After: 0 pt



- 1 Wang, T., X. L. Wei, A. J. Ding, C. N. Poon, K. S. Lam, Y. S. Li, L. Y. Chan, and M. Anson (2009), Increasing  
2 surface ozone concentrations in the background atmosphere of Southern China, 1994-2007, *Atmos. Chem.*  
3 *Phys.*, 9, 6217-6227, doi: doi:10.5194/acp-9-6217-2009.
- 4 Wang, Y., Y. Xie, L. Cai, W. Dong, Q. Zhang, and L. Zhang (2015), Impact of the 2011 Southern US Drought  
5 on Ground-Level Fine Aerosol Concentration in Summertime, *J. Atmos. Sci.*, 72(3), 1075-1093, doi:  
6 10.1175/jas-d-14-0197.1.
- 7 Wang, Y., McElroy, M. B., Munger, J. W., Hao, J., Ma, H., Nielsen, C. P., and Chen, Y. (2008): Variations of O<sub>3</sub>  
8 and CO in summertime at a rural site near Beijing, *Atmos. Chem. Phys.*, 8(21), 6355–6363.
- 9 Warneke, C., J. A. de Gouw, J. S. Holloway, et al., (2012), Multiyear trends in volatile organic compounds in  
10 Los Angeles, California: Five decades of decreasing emissions, *J. Geophys. Res.*, 117, doi:  
11 10.1029/2012jd017899.
- 12 Xu, W., W. Lin, X. Xu, J. Tang, J. Huang, H. Wu, and X. Zhang (2016), Long-term trends of surface ozone and  
13 its influencing factors at the Mt Waliguan GAW station, China - Part 1: Overall trends and characteristics,  
14 *Atmos. Chem. Phys.*, 16, 6191-6205, doi: doi:10.5194/acp-16-6191-2016.
- 15 Yang, J., H. Q. Tian, B. Tao, W. Ren, S. F. Pan, Y. Q. Liu, and Y. H. Wang (2015), A growing importance of  
16 large fires in conterminous United States during 1984-2012, *J Geophys Res-Bioge*, 120(12), 2625-2640, doi:  
17 10.1002/2015jg002965.
- 18 Yurganov, L. N., et al. (2005), Increased Northern Hemispheric carbon monoxide burden in the troposphere in  
19 2002 and 2003 detected from the ground and from space, *Atmos. Chem. Phys.*, 5, 563-573.
- 20 Zhang, L., et al. (2008), Transpacific transport of ozone pollution and the effect of recent Asian emission  
21 increases on air quality in North America: an integrated analysis using satellite, aircraft, ozonesonde, and  
22 surface observations, *Atmos. Chem. Phys.*, 8(20), 6117-6136, doi: 10.5194/acp-8-6117-2008.
- 23  
24 Zhang, L., D. J. Jacob, X. Yue, N. V. Downey, D. A. Wood, and D. Blewitt (2014), Sources contributing to  
25 background surface ozone in the US Intermountain West, *Atmos. Chem. Phys.*, 14(11), 5295-5309, doi:  
26 10.5194/acp-14-5295-2014.
- 27 Zhang, Y., O. R. Cooper, A. Gaudel, A. M. Thompson, Philippe Nédélec, S.-Y. Ogino, and J. J. West (2016),  
28 Tropospheric ozone change from 1980 to 2010 dominated by equatorward redistribution of emissions, *Nature*  
29 *Geoscience*, doi:10.1038/ngeo2827.

Deleted: J. Peischl, T. B. Ryerson, E. Atlas, D. Blake, M. Trainer, and D. D. Parrish

Deleted: , 2016

## Figure captions

**Figure 1. Changes in NO<sub>x</sub> emissions.** (a-b) Mean annual vertical column densities of tropospheric (VCD<sub>trop</sub>) NO<sub>2</sub> normalized to year 2000 for the Eastern China and Eastern US domains (black boxes on map) from GOME (1996-2002, open circles) and SCIAMACHY (2003-2011, closed circles) measurements and AM3 BASE simulations (orange lines). Triangles indicate trends in NO<sub>x</sub> emissions (normalized to 2000) from Lamarque et al. (2010) with annual interpolation after 2000 to RCP8.5 (red) versus RCP4.5 (blue). (c-d) Differences in annual mean SCIAMACHY VCD<sub>trop</sub> NO<sub>2</sub> from 2003-2005 to 2009-2011. The red boxes denote the regions where emissions vary over time in the IAVASIA simulation (Table 1). Satellite NO<sub>2</sub> data are from www.temis.nl, with retrieval technique described in Boersma et al. (2004).

**Figure 2. Measurement uncertainties.** (a) Comparison of observed monthly mean MDA8 O<sub>3</sub> at WUS CASTNet sites. All sites have more than 90% data availability in every month shown. The grey shading denotes the period when data at Yellowstone (red) and Rocky Mountain (black) were inconsistent with the other sites. (b-c) The 1990-2010 trends of median JJA MDA8 O<sub>3</sub> at Yellowstone and median MAM MDA8 O<sub>3</sub> at Rocky Mountain with and without data in 1990.

**Figure 3. Influence of baseline sampling.** Median spring MDA8 O<sub>3</sub> trends over 1988-2014 at WUS sites from: (a) Observations; (b) BASE model sampled at the surface; (c) BASE sampled at 700 hPa and filtered to remove the influence from fresh local pollution (see Sect. 2.4); (d) BASE sampled at 700 hPa without filtering; and (e-f) Background (with North American anthropogenic emissions shut off) sampled at the surface versus at 700 hPa. Note that three low-elevation (<1.5 km) sites Joshua Tree, Big Bend and Glacier National Parks are always sampled at the surface. Larger circles indicate sites with statistically significant trends ( $p < 0.05$ ).

**Figure 4.** Global distribution of MDA8 O<sub>3</sub> trends from AM3 BASE over 1988-2014 for boreal spring (left) and summer (right) for the 95th percentile at the surface (a-b), median at the surface (c-d), and median in the free troposphere (700 hPa; e-f). Stippling indicates areas where the trend

is statistically significant ( $p < 0.05$ ). The color scale is designed to resolve regional features rather than extreme values and saturates. The range of trends is  $-1$  to  $+2.5$  ppb  $\text{yr}^{-1}$ .

**Figure 5.** (a) Time series of changes in global tropospheric  $\text{O}_3$  burden relative to the 1981-1990 mean from BASE and FIXEMIS simulations (Table 1). (b) Time series of 12-month running mean anomalies (in percent relative to the 2005-2014 mean) of  $\text{O}_3$  averaged over 900-600 hPa at Hong Kong from: the averages of ozonesonde samples (black circles) and BASE model co-sampled on sonde launch days (orange circles) versus the true average from BASE and IAVFIRE with continuous daily sampling (solid lines). (c) Same as (b) but for Hanoi.

**Figure 6. Surface  $\text{O}_3$  trends in Asia.** (a) Observation sites superimposed on a map of the 95th percentile summer MDA8  $\text{O}_3$  trends over 1995-2014 from AM3 BASE. (b) Comparison of median  $\text{O}_3$  trends from AM3 (1995-2014) with observations (see text for periods): in Central Eastern China at Mt. Tai (July-August, Sun et al. 2016), Beijing (May-June-July, Ding et al. 2008) and Shangdianzi (SDZ) (JJA, Ma et al. 2016); in South China at Hong Kong (HK) (annual average, Wang et al. 2009) and Taiwan (MAM, Lin YK et al. 2010); at Mt. Waliguan (WLG) in western China (MAM, Xu et al. 2016); at South Korea (JJA, Lee et al. 2014) and Mt. Happono Japan (MAM, Tanimoto 2009). For Mt. Happono (triangle on map) AM3 is sampled at 700 hPa and filtered for the influence from Asian continental air - more representative of observed baseline conditions in spring.

**Figure 7.** Linear trends in spring (MAM) MDA8  $\text{O}_3$  over 1988-2014 at US rural sites for the 95<sup>th</sup>, 50<sup>th</sup>, and 5<sup>th</sup> percentiles as observed (left) and simulated (right) in AM3 BASE. Larger circles indicate sites with statistically significant trends ( $p < 0.05$ ). For WUS high-elevation sites, the model is sampled at 700 hPa and filtered to remove local influence (see text in Sect. 2.4).

**Figure 8.** As in Figure 7, but for summer (JJA). Note that the color scale saturates at  $\pm 0.8$ .

**Figure 9.** As in Figure 7, but for winter (DJF). Large squares in (a) denote AQS sites with significant  $\text{O}_3$  decreases.

**Figure 10.** Linear trends in the 95<sup>th</sup> (left) and 50<sup>th</sup> (right) percentile springtime MDA8  $\text{O}_3$  over

Formatted: Subscript

1 1988-2014 at US rural sites from BASE (top), Background (middle) and FIXEMIS simulations  
2 (bottom). Larger circles indicate sites with statistically significant trends ( $p < 0.05$ ). Top panels are  
3 repeated from Fig. 7d,e. Note that the 95<sup>th</sup> (50<sup>th</sup>) percentile is sampled separately from the  
4 Background and FIXEMIS simulations without depending on the times when the BASE  
5 simulation is experiencing the 95<sup>th</sup> (50<sup>th</sup>) percentile days.

6  
7 **Figure 11.** As in Figure 10, but for summer. Top panels are repeated from Fig. 8d,e.

8  
9 **Figure 12.** The 1990-2012 trends in: (a) model JJA total biogenic isoprene emissions; (b) model 90th  
10 percentile JJA daily maximum temperature; (c) the warmest daily maximum temperature and (d)  
11 the frequency of warm days (i.e., those above the 90th percentile for  
12 the base period 1961-90) for August obtained from GHCNDEX dataset (Donat et al., 2013;  
13 available at [http://www.climdex.org/view\\_download.html](http://www.climdex.org/view_download.html)). Stippling denotes areas where the  
14 change is statistically significant ( $p < 0.05$ ). Note that the trends are calculated for the 1990-2012  
15 period, instead of 1988-2014, to avoid the influence from hot extremes in 1988 and cold  
16 conditions in 2014 (Sect. 6). When these years are included, the trends in (c) and (d) are  
17 swamped by the anomalies. The trends in (a) and (b) are similar between 1990-2012 and  
18 1988-2014.

19  
20  
21 **Figure 13a.** Time series of median spring MDA8 O<sub>3</sub> anomalies (relative to the 1995-2014 mean)  
22 at Great Basin, Rocky Mountain, and US Air Force Academy as observed (black) and simulated  
23 in AM3 BASE filtered for baseline conditions (red, see Sect. 2.4) and in Background with North  
24 American anthropogenic emissions zeroed out (NAB; green). Presented on the top of the graph  
25 are statistics from the linear fit and correlations between observations and simulations. Numbers  
26 on the bottom of the graph denote the sample size of observations for each year. Grey dots  
27 indicate uncertain observations that are removed from the linear fit (see Sect. 2.3).

28  
29  
30 **Figure 13b.** Same as Figure 13a, but for Yellowstone, Pinedale, and Mesa Verde over the period  
31 1988-2012.

32  
33  
34 **Figure 14. Future projections.** Time series of median springtime O<sub>3</sub> changes relative to 2010 in

GFDL AM3 hindcast (orange circles) and CM3 future simulations for RCP8.5 (red) versus RCP4.5 (blue; shading represents the range of three ensemble members), sampled at 700 hPa over the WUS (35-45N,120-105W). Black circles indicate observed changes averaged from Lassen, Great Basin, and Rocky Mountain National Parks.

**Figure 15. Summertime O<sub>3</sub> in Yellowstone National Park.** (a) Median JJA MDA8 O<sub>3</sub> trends over 1988-2012 at Yellowstone from observations (black) and simulations sampled at 700 hPa for BASE without filtering (pink), BASE filtered for baseline conditions (hatched pink), IAVASIA (solid purple, baseline), IAVASIA filtered for Asian influence (EACOT<sub>≥</sub>67th, hatched purple), IAVCH4 (cyan), IAVFIRE (orange) and FIXEMIS (red). (b) Time series of anomalies in August median MDA8 O<sub>3</sub> at Yellowstone as observed (black) and simulated by the model sampled at the surface, with constant (red) and time-varying wildfire emissions (orange). Trends over 1988-2014 are reported. (c) Interannual correlations of JJA mean MDA8 O<sub>3</sub> observed at Yellowstone with JJA mean daily maximum temperature from observations (Harris et al., 2014).

**Figure 16.** Surface MDA8 O<sub>3</sub> enhancements from wildfire emissions for individual months in the years with large biomass burning in boreal regions (1998, 2002, 2003) and over the WUS (2008, 2011, 2012), as diagnosed by the differences between IAVFIRE and FIXEMIS. The black circle denotes the location of Yellowstone National Park.

**Figure 17. Surface O<sub>3</sub> trends in Denver.** (a) Comparison of observed trends in annual 4th highest MDA8 O<sub>3</sub> at Crestline Los Angeles (brown) and in Denver (blue, computed from all monitors available in Denver non-attainment counties). (b) Time series of observed median MAM MDA8 O<sub>3</sub> at Great Basin National Park (red), in comparison with three monitors in Denver. (c) Time series of observed 95th percentile July-August MDA8 O<sub>3</sub> in Denver, together with statistics (25th, 50th, 75th, 95th) of observed July-August daily maximum temperature at Rocky Flats (red, right axis).

**Figure 18.** (a) Time series of July mean MDA8 O<sub>3</sub> anomalies (relative to 1988-2014) at the Pennsylvania State University (PSU) CASTNET site as observed (black) and simulated by the GFDL-AM3 model with time-varying (purple) and constant anthropogenic emissions (red), along with observed anomalies in July mean daily max temperature (gray lines; right axis). The

green triangle denotes the 1988 O<sub>3</sub> anomaly from a sensitivity simulation using BASE emissions but with 35% decreases in V<sub>d,O3</sub> (IAVDEP). (b) Time series of daily MDA8 O<sub>3</sub> at PSU from June 1 to July 16 in 1988 from observations (black), BASE (purple), and IAVDEP simulations (green).

**Figure 19.** (a) Comparisons of probability distributions of summertime MDA8 O<sub>3</sub> from 40 EUS CASTNet sites for the pre-NO<sub>x</sub> SIP Call (1988-2002; solid black) versus post-NO<sub>x</sub> SIP Call (2003-2014; dashed gray) periods and during the extreme heat waves of 1988 (solid purple) versus 2012 (dashed brown). The median ( $\mu$ ) and standard deviation ( $\sigma$ ) are shown (ppb). (b) Same as (a) but from AM3 BASE. Also shown is the O<sub>3</sub> distribution in 1988 from a sensitivity simulation with 35% decreases in V<sub>d,O3</sub> in drought areas (green). (c) Standardized soil moisture departures for JJA 1988 (calculated by dividing anomalies by the 1979-2010 climatological standard deviation, using data from NOAA Climate Prediction Center).

**Figure 20. Summary of US surface O<sub>3</sub> trends and drivers.** Changes in decadal mean MDA8 O<sub>3</sub> from 1981-1990 to 2003-2012 simulated in a suite of GFDL-AM3 experiments for spring and summer for the western (32N-46N and 123W-102W), Northeast (37N-45N and 90W-65W) and Southeast (30N-36N and 95W-77W) US domains. Observations are not shown because limited data are available during 1981-1990. Experiments are color-coded with the error bars indicating the range of the mean change at the 95% confidence level. Filled circles represent the changes under Background (green) and IAVASIA (purple) when filtered for Asian influence (EACOt  $\geq$  67<sup>th</sup>), while other results are from the unfiltered models. The text near the bottom of the plot provides the change in NO<sub>x</sub> emissions over the same period for each region.





Page 15: [4] Deleted	Meiyun Lin	1/20/17 4:24:00 PM
----------------------	------------	--------------------

Page 15: [4] Deleted	Meiyun Lin	1/20/17 4:24:00 PM
----------------------	------------	--------------------

Page 15: [4] Deleted	Meiyun Lin	1/20/17 4:24:00 PM
----------------------	------------	--------------------

Page 15: [5] Deleted	Meiyun Lin	12/21/16 5:35:00 PM
----------------------	------------	---------------------

zone

Page 15: [5] Deleted	Meiyun Lin	12/21/16 5:35:00 PM
----------------------	------------	---------------------

zone

Page 15: [5] Deleted	Meiyun Lin	12/21/16 5:35:00 PM
----------------------	------------	---------------------

zone

Page 15: [5] Deleted	Meiyun Lin	12/21/16 5:35:00 PM
----------------------	------------	---------------------

zone

Page 15: [6] Deleted	Meiyun Lin	1/7/17 6:45:00 PM
----------------------	------------	-------------------

year

Page 15: [6] Deleted	Meiyun Lin	1/7/17 6:45:00 PM
----------------------	------------	-------------------

year

Page 15: [7] Deleted	Meiyun Lin	12/12/16 3:11:00 PM
----------------------	------------	---------------------

and

Page 15: [7] Deleted	Meiyun Lin	12/12/16 3:11:00 PM
----------------------	------------	---------------------

and

Page 15: [7] Deleted	Meiyun Lin	12/12/16 3:11:00 PM
----------------------	------------	---------------------

and

Page 15: [7] Deleted	Meiyun Lin	12/12/16 3:11:00 PM
----------------------	------------	---------------------

and

Page 15: [7] Deleted	Meiyun Lin	12/12/16 3:11:00 PM
----------------------	------------	---------------------

and

Page 20: [8] Deleted	Meiyun Lin	12/20/16 12:44:00 PM
----------------------	------------	----------------------

Page 21: [9] Deleted	Meiyun Lin	12/22/16 12:54:00 PM
----------------------	------------	----------------------

(Figure 20 about here: 2003-2012 minus 1981-1990)

Page 22: [10] Deleted	Meiyun Lin	1/6/17 3:19:00 PM
-----------------------	------------	-------------------

rising

[illegible]



rRegional NO<sub>x</sub> controls also alleviated the O<sub>3</sub> buildup during the recent heat waves of 2011 and 2012 relative to earlier heat waves (**Figs. 18 and 19**). Despite high mean state biases, the model captures the salient features of observed O<sub>3</sub> trends over the EUS, including the largest summertime decreases in the 95<sup>th</sup> percentile, the north-to-south gradient in springtime O<sub>3</sub> trends, as well as wintertime increases in the 5<sup>th</sup> and 50<sup>th</sup> percentiles. The model also captures enhancements in monthly mean O<sub>3</sub> due to large-scale heat waves.

rRegional NO<sub>x</sub> controls also alleviated the O<sub>3</sub> buildup during the recent heat waves of 2011 and 2012 relative to earlier heat waves (**Figs. 18 and 19**). Despite high mean state biases, the model captures the salient features of observed O<sub>3</sub> trends over the EUS, including the largest summertime decreases in the 95<sup>th</sup> percentile, the north-to-south gradient in springtime O<sub>3</sub> trends, as well as wintertime increases in the 5<sup>th</sup> and 50<sup>th</sup> percentiles. The model also captures enhancements in monthly mean O<sub>3</sub> due to large-scale heat waves.

rRegional NO<sub>x</sub> controls also alleviated the O<sub>3</sub> buildup during the recent heat waves of 2011 and 2012 relative to earlier heat waves (**Figs. 18 and 19**). Despite high mean state biases, the model captures the salient features of observed O<sub>3</sub> trends over the EUS, including the largest summertime decreases in the 95<sup>th</sup> percentile, the north-to-south gradient in springtime O<sub>3</sub> trends, as well as wintertime increases in the 5<sup>th</sup> and 50<sup>th</sup> percentiles. The model also captures enhancements in monthly mean O<sub>3</sub> due to large-scale heat waves.

rRegional NO<sub>x</sub> controls also alleviated the O<sub>3</sub> buildup during the recent heat waves of 2011 and 2012 relative to earlier heat waves (**Figs. 18 and 19**). Despite high mean state biases, the model captures the salient features of observed O<sub>3</sub> trends over the EUS, including the largest summertime decreases in the 95<sup>th</sup> percentile, the north-to-south gradient in springtime O<sub>3</sub> trends, as well as wintertime increases in the 5<sup>th</sup> and 50<sup>th</sup> percentiles. The model also captures enhancements in monthly mean O<sub>3</sub> due to large-scale heat waves.

rRegional NO<sub>x</sub> controls also alleviated the O<sub>3</sub> buildup during the recent heat waves of 2011 and 2012 relative to earlier heat waves (**Figs. 18 and 19**). Despite high mean state biases, the model captures the salient features of observed O<sub>3</sub> trends over the EUS, including the largest summertime decreases in the 95<sup>th</sup> percentile, the north-to-south gradient in springtime O<sub>3</sub> trends, as well as wintertime increases in the 5<sup>th</sup> and 50<sup>th</sup> percentiles. The model also captures enhancements in monthly mean O<sub>3</sub> due to large-scale heat waves.

rRegional NO<sub>x</sub> controls also alleviated the O<sub>3</sub> buildup during the recent heat waves of 2011 and 2012 relative to earlier heat waves (**Figs. 18 and 19**). Despite high mean state biases, the model captures the salient features of observed O<sub>3</sub> trends over the EUS, including the largest summertime decreases in the 95<sup>th</sup> percentile, the north-to-south gradient in springtime O<sub>3</sub> trends, as well as wintertime increases in the 5<sup>th</sup> and 50<sup>th</sup> percentiles. The model also captures enhancements in monthly mean O<sub>3</sub> due to large-scale heat waves.

Font:Not Bold

**Page 22: [15] Formatted**

**Meiyun Lin**

**12/9/16 9:47:00 AM**

Font:Not Bold

**Table 1** Summary of forcings and emissions used in AM3 hindcasts and CM3 projections

Experiment	Time Periods	Meteorology	Radiative forcings	CH <sub>4</sub> (chemistry)	Anthropogenic emissions	Fire Emissions
BASE	1979-2014	Nudged to NCEP	Historical	Historical	Historical	Historical
Background	1979-2014	as BASE	Historical	Historical	Zeroed out in N. America; As BASE elsewhere	Historical
FIXEMIS	1979-2014	as BASE	Historical	2000	Constant*	Constant*
IAVFIRE	1979-2014	as BASE	Historical	2000	Constant*	Historical
IAVASIA	1979-2012 <sup>+</sup>	as BASE	Historical	2000	Varying in Asia as BASE; as in FIXEMIS elsewhere	Constant*
IAVCH <sub>4</sub>	1979-2012 <sup>+</sup>	as BASE	Historical	Historical	Constant*	Constant*
CM3_RCP4.5	2005-2050	Free running	RCP4.5	RCP4.5	RCP4.5	RCP4.5
CM3_RCP8.5	2005-2050	Free running	RCP8.5	RCP8.5	RCP8.5	RCP8.5

\*Averaged over the whole 1970-2010 period.

+Note that the IAVASIA and IAVCH<sub>4</sub> simulations only extend to 2012.

**Table 2.** Summary of linear trends in spring MDA8 O<sub>3</sub> for 1988 to 2012 (ppb yr<sup>-1</sup>) observed at seven western U.S. sites and as simulated in the AM3 experiments. Trends with the 95% confidence intervals and levels of significance (**bold**: <1%; *italic*, 1-5%;  , ≥5%) were estimated by the two-tailed *t*-test.

Experiment <sup>a</sup>	Lassen	Great Basin	Rocky Mountain	Mesa Verde	Yellowstone	Yosemite	Chiricahua
<b>Spring (MAM)</b>							
Observed	<b>0.38±0.14</b>	<b>0.38±0.26</b>	<b>0.37±0.18</b>	<b>0.30±0.18</b>	<i>0.21±0.19</i>	<i>0.37±0.32</i>	<b>0.17±0.10</b>
BASE*	<b>0.33±0.11</b>	<b>0.34±0.12</b>	<b>0.32±0.13</b>	<b>0.37±0.14</b>	<b>0.21±0.11</b>	<b>0.35±0.17</b>	<i>0.25±0.19</i>
Background	<b>0.31±0.12</b>	<b>0.40±0.13</b>	<b>0.45±0.13</b>	<b>0.43±0.17</b>	<b>0.30±0.11</b>	<b>0.41±0.16</b>	<b>0.32±0.21</b>
Background <sub>EA</sub>	<b>0.41±0.12</b>	<b>0.39±0.18</b>	<b>0.50±0.15</b>	<b>0.52±0.20</b>	<b>0.40±0.16</b>	<b>0.47±0.17</b>	<b>0.47±0.21</b>
IAVASIA*	<b>0.29±0.13</b>	<b>0.31±0.11</b>	<b>0.25±0.11</b>	<b>0.27±0.11</b>	<b>0.19±0.11</b>	<b>0.24±0.14</b>	<span style="background-color: #cccccc;">0.15±0.15</span>
IAVASIA <sub>EA</sub>	<b>0.26±0.16</b>	<b>0.26±0.16</b>	<b>0.35±0.13</b>	<b>0.32±0.13</b>	<b>0.27±0.16</b>	<b>0.31±0.18</b>	<b>0.25±0.15</b>
IAVCH <sub>4</sub> *	<i>0.18±0.12</i>	<b>0.20±0.11</b>	<i>0.12±0.09</i>	<i>0.16±0.12</i>	<span style="background-color: #cccccc;">0.09±0.12</span>	<span style="background-color: #cccccc;">0.15±0.16</span>	<span style="background-color: #cccccc;">0.04±0.15</span>
IAVFIRE	<span style="background-color: #cccccc;">0.10±0.12</span>	<i>0.14±0.12</i>	<i>0.17±0.14</i>	<i>0.16±0.14</i>	<span style="background-color: #cccccc;">0.11±0.13</span>	<span style="background-color: #cccccc;">0.15±0.16</span>	<span style="background-color: #cccccc;">0.08±0.17</span>
FIXEMIS	<span style="background-color: #cccccc;">0.08±0.12</span>	<i>0.12±0.12</i>	<i>0.16±0.12</i>	<i>0.13±0.12</i>	<span style="background-color: #cccccc;">0.09±0.13</span>	<span style="background-color: #cccccc;">0.12±0.16</span>	<span style="background-color: #cccccc;">0.04±0.16</span>
O <sub>3</sub> Strat	<span style="background-color: #cccccc;">0.18±0.18</span>	<span style="background-color: #cccccc;">0.20±0.25</span>	<span style="background-color: #cccccc;">0.18±0.18</span>	<i>0.25±0.23</i>	<span style="background-color: #cccccc;">0.15±0.18</span>	<span style="background-color: #cccccc;">0.27±0.30</span>	<span style="background-color: #cccccc;">0.07±0.24</span>

a. The \* mask indicates data filtered to represent baseline conditions (NACOt ≤ 67<sup>th</sup>). The EA subscript indicates that data were filtered to represent transport conditions favoring the import of Asian pollution (EACOt ≥ 67<sup>th</sup>).



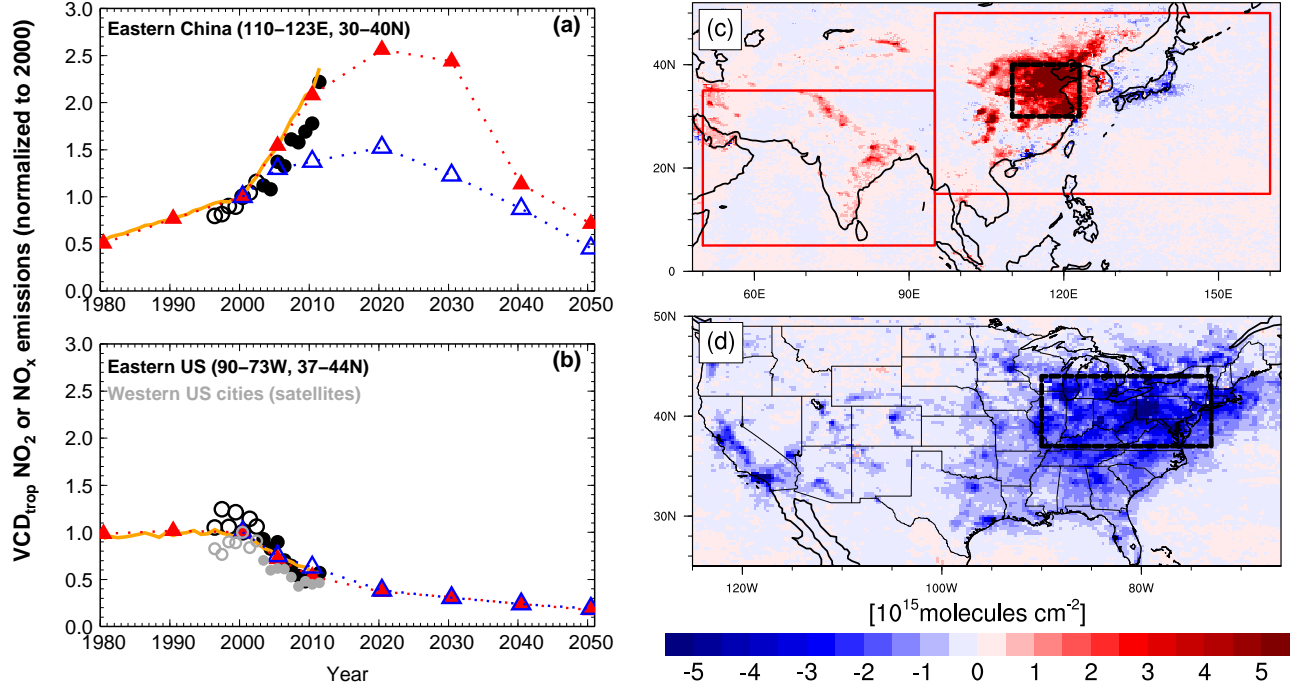


Figure 1. **Changes in  $\text{NO}_x$  emissions.** (a-b) Mean annual vertical column densities of tropospheric ( $\text{VCD}_{\text{trop}}$ )  $\text{NO}_2$  normalized to year 2000 for the Eastern China and Eastern US domains (black boxes on map) from GOME (1996–2002, open circles) and SCIAMACHY (2003–2011, closed circles) measurements and AM3 BASE simulations (orange lines). Triangles indicate trends in  $\text{NO}_x$  emissions (normalized to 2000) from Lamarque et al. (2010) with annual interpolation after 2000 to RCP8.5 (red) versus RCP4.5 (blue). (c-d) Differences in annual mean SCIAMACHY  $\text{VCD}_{\text{trop}}$   $\text{NO}_2$  from 2003–2005 to 2009–2011. The red boxes denote the regions where emissions vary over time in the IAVASIA simulation (Table 1). Satellite  $\text{NO}_2$  data are from [www.temis.nl](http://www.temis.nl), with retrieval technique described in Boersma et al. (2004).

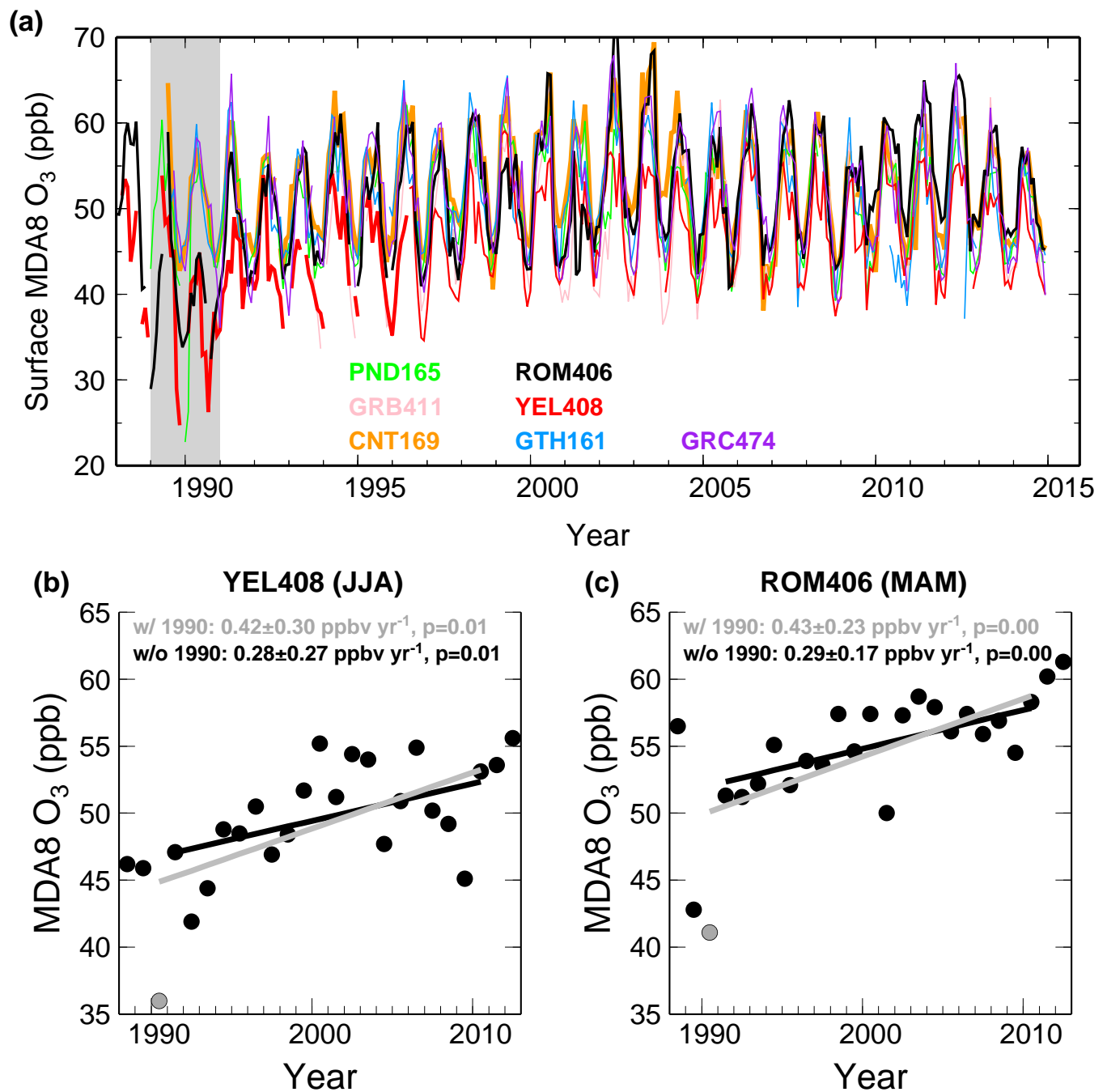


Figure 2. **Measurement uncertainties.** (a) Comparison of observed monthly mean MDA8 O<sub>3</sub> at WUS CASTNet sites. All sites have more than 90% data availability in every month shown. The grey shading denotes the period when data at Yellowstone (red) and Rocky Mountain (black) were inconsistent with the other sites. (b-c) The 1990-2010 trends of median JJA MDA8 O<sub>3</sub> at Yellowstone and median MAM MDA8 O<sub>3</sub> at Rocky Mountain with and without data in 1990.

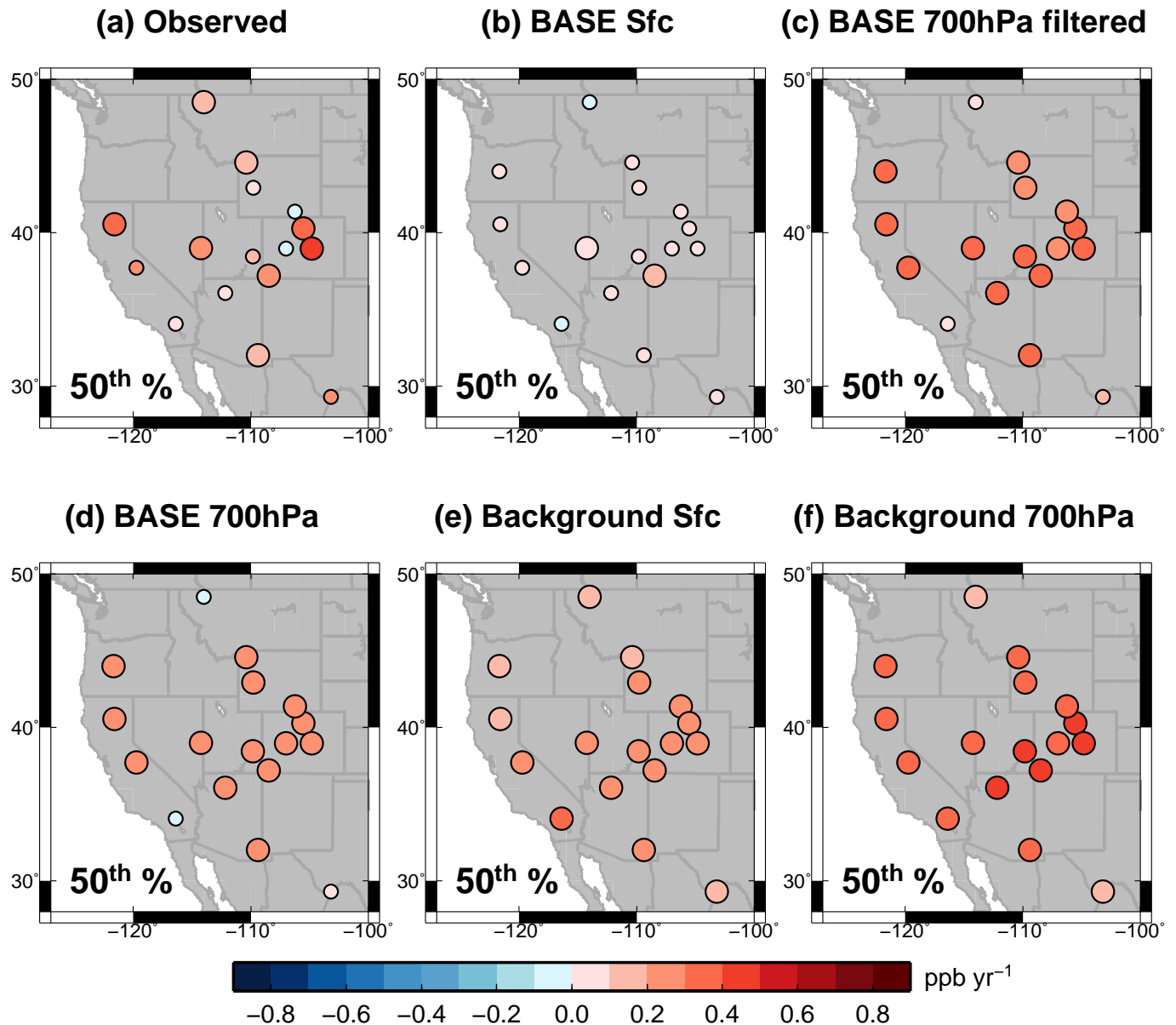


Figure 3. **Influence of baseline sampling.** Median spring MDA8 O<sub>3</sub> trends over 1988-2014 at WUS sites from: (a) Observations; (b) BASE model sampled at the surface; (c) BASE sampled at 700 hPa and filtered to remove the influence from fresh local pollution (see Sect. 2.4); (d) BASE sampled at 700 hPa without filtering; and (e-f) Background (with North American anthropogenic emissions shut off) sampled at the surface versus at 700 hPa. Note that three low-elevation (<1.5 km) sites Joshua Tree, Big Bend and Glacier National Parks are always sampled at the surface. Larger circles indicate sites with statistically significant trends (p < 0.05).

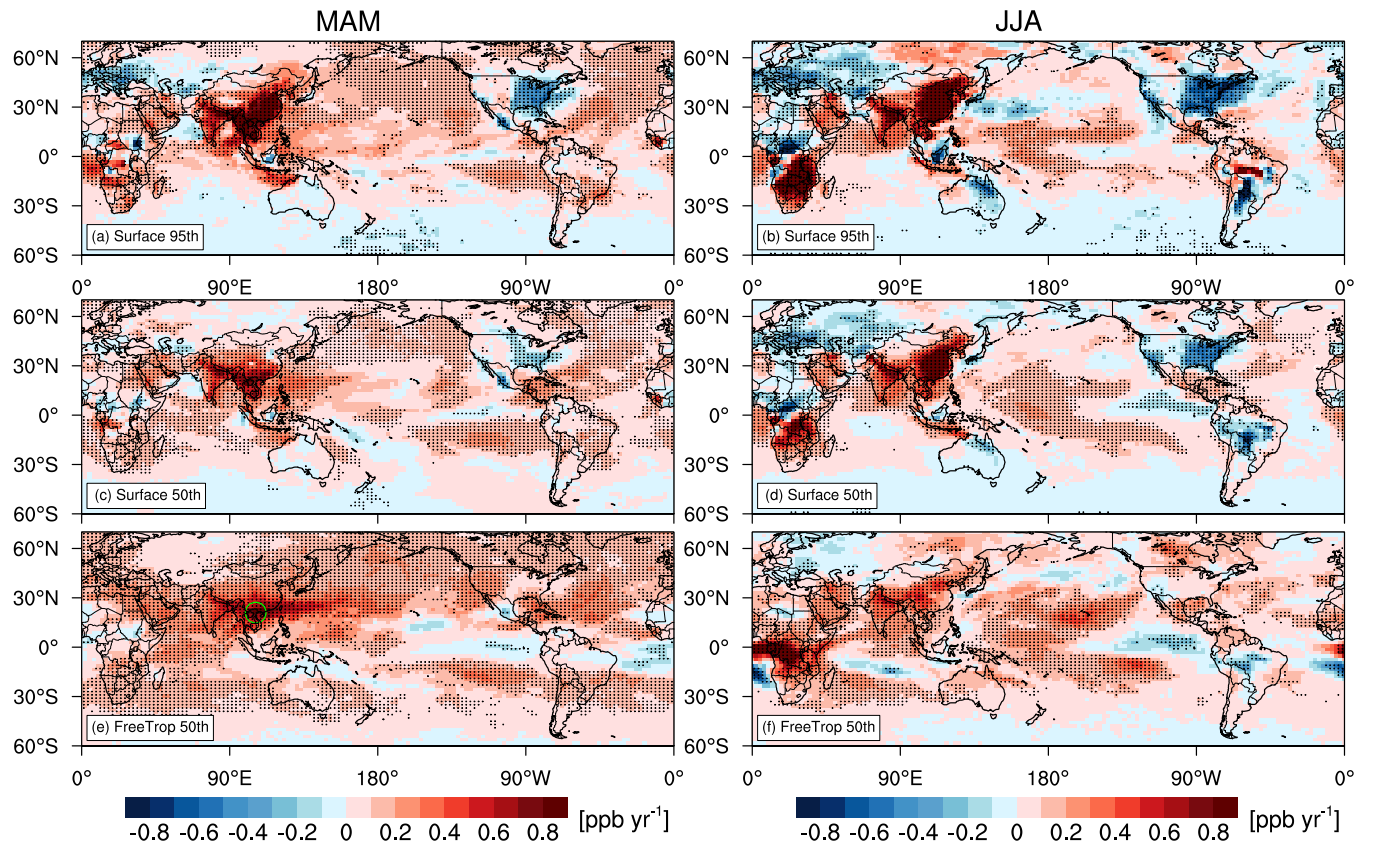


Figure 4. Global distribution of MDA8 O<sub>3</sub> trends from AM3 BASE over 1988-2014 for boreal spring (left) and summer (right) for the 95th percentile at the surface (a-b), median at the surface (c-d), and median in the free troposphere (700 hPa; e-f). Stippling indicates areas where the trend is statistically significant ( $p < 0.05$ ). The color scale is designed to resolve regional features rather than extreme values and saturates. The range of trends is -1 to +2.5 ppb yr<sup>-1</sup>.

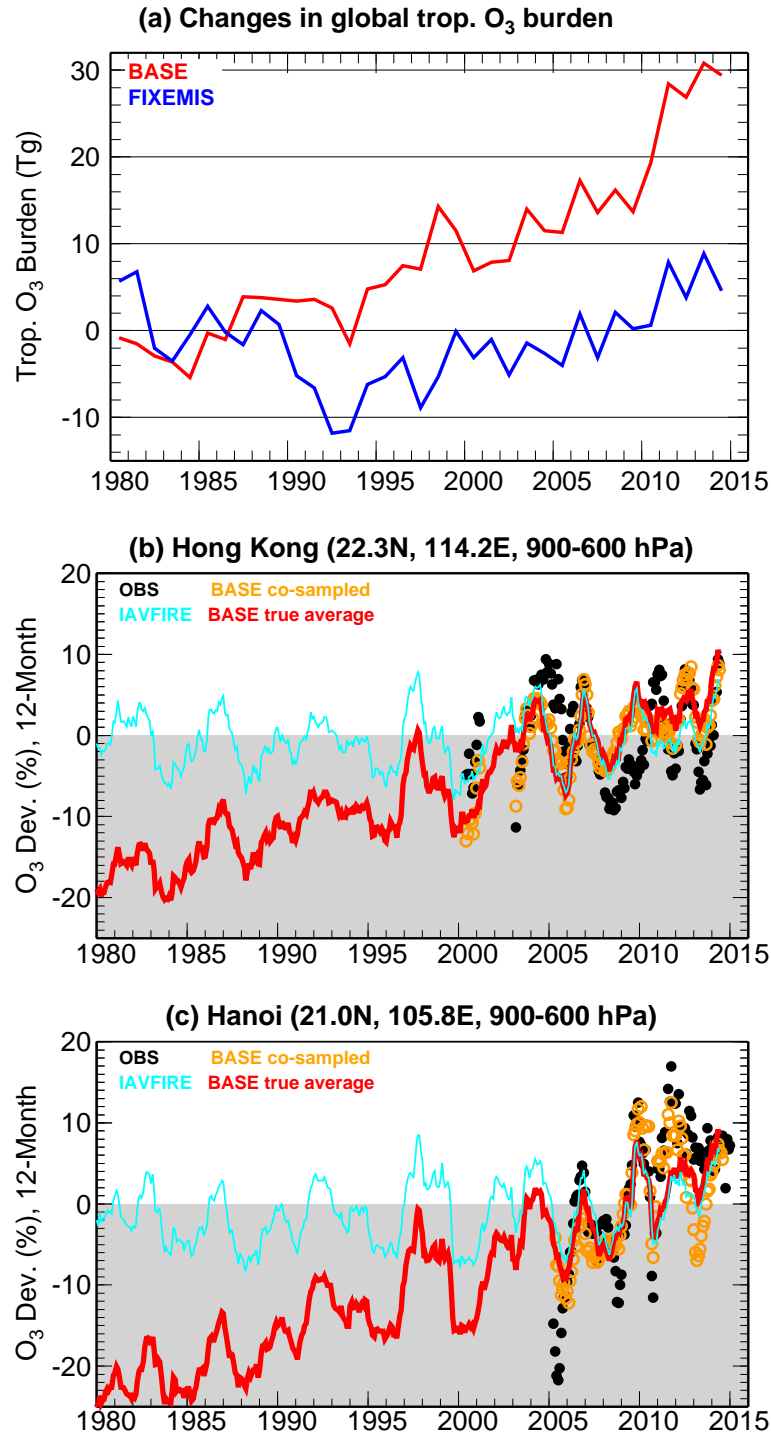


Figure 5. **(a)** Time series of changes in global tropospheric O<sub>3</sub> burden relative to the 1981-1990 mean from BASE and FIXEMIS simulations (Table 1). **(b)** Time series of 12-month running mean anomalies (in percent relative to the 2005-2014 mean) of O<sub>3</sub> averaged over 900-600 hPa at Hong Kong from: the averages of ozonesonde samples (black circles) and BASE model co-sampled on sonde launch days (orange circles) versus the true average from BASE and IAVFIRE with continuous daily sampling (solid lines). **(c)** Same as **(b)** but for Hanoi.

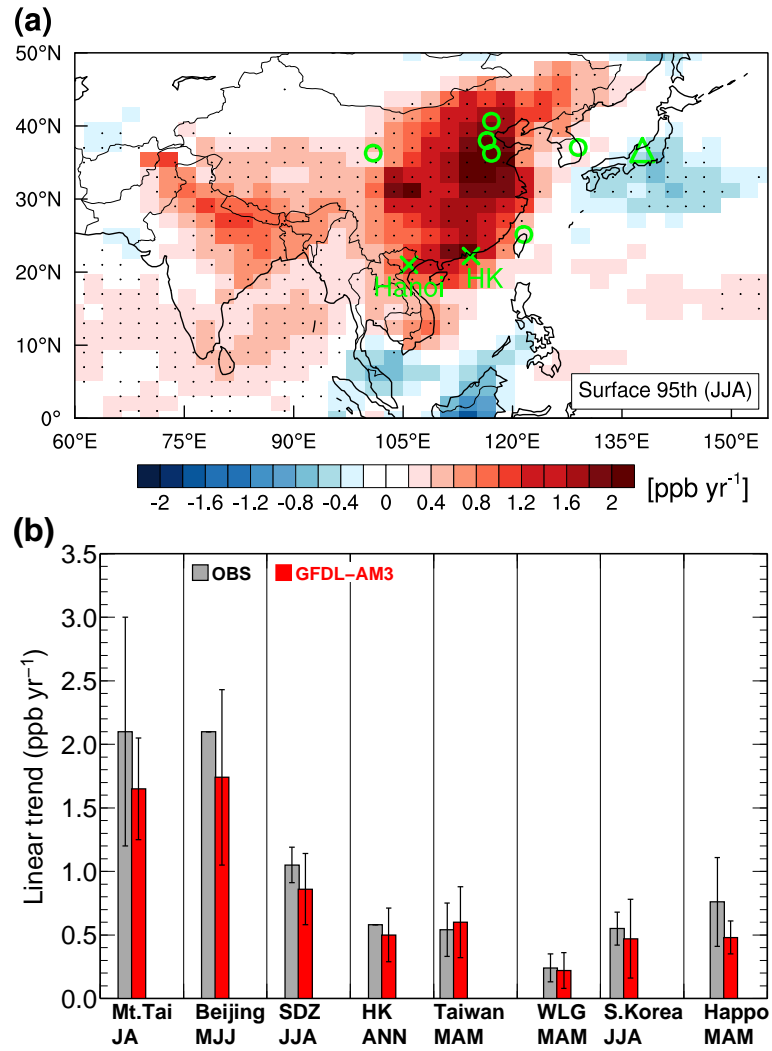


Figure 6. **Surface O<sub>3</sub> trends in Asia.** (a) Observation sites superimposed on a map of the 95<sup>th</sup> percentile summer MDA8 O<sub>3</sub> trends over 1995-2014 from AM3 BASE. (b) Comparison of median O<sub>3</sub> trends from AM3 (1995-2014) with observations (see text for periods): in Central Eastern China at Mt. Tai (July-August, Sun et al. 2016), Beijing (May-June-July, Ding et al. 2008) and Shangdianzi (SDZ) (JJA, Ma et al. 2016); in South China at Hong Kong (HK) (annual average, Wang et al. 2009) and Taiwan (MAM, Lin YK et al. 2010); at Mt. Waliguan (WLG) in western China (MAM, Xu et al. 2016); at South Korea (JJA, Lee et al. 2014) and Mt. Haplo Japan (MAM, Tanimoto 2009). For Mt. Haplo (triangle on map) AM3 is sampled at 700 hPa and filtered for the influence from Asian continental air - more representative of observed baseline conditions in spring.

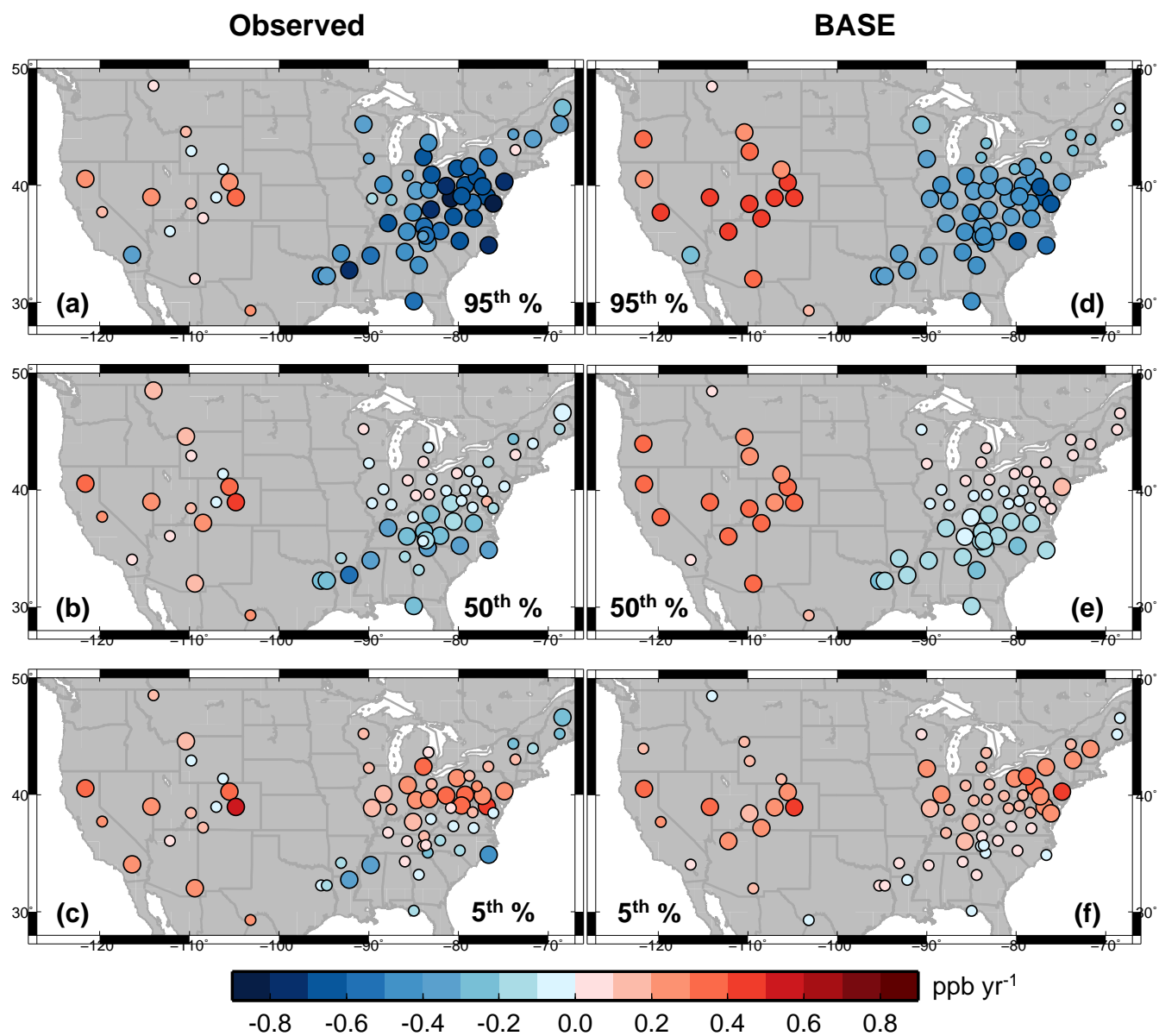


Figure 7. Linear trends in spring (MAM) MDA8 O<sub>3</sub> over 1988-2014 at US rural sites for the 95th, 50th, and 5th percentiles as observed (left) and simulated (right) in AM3 BASE. Larger circles indicate sites with statistically significant trends ( $p < 0.05$ ). For WUS high-elevation sites, the model is sampled at 700 hPa and filtered to remove local influence (see text in Sect. 2.4).



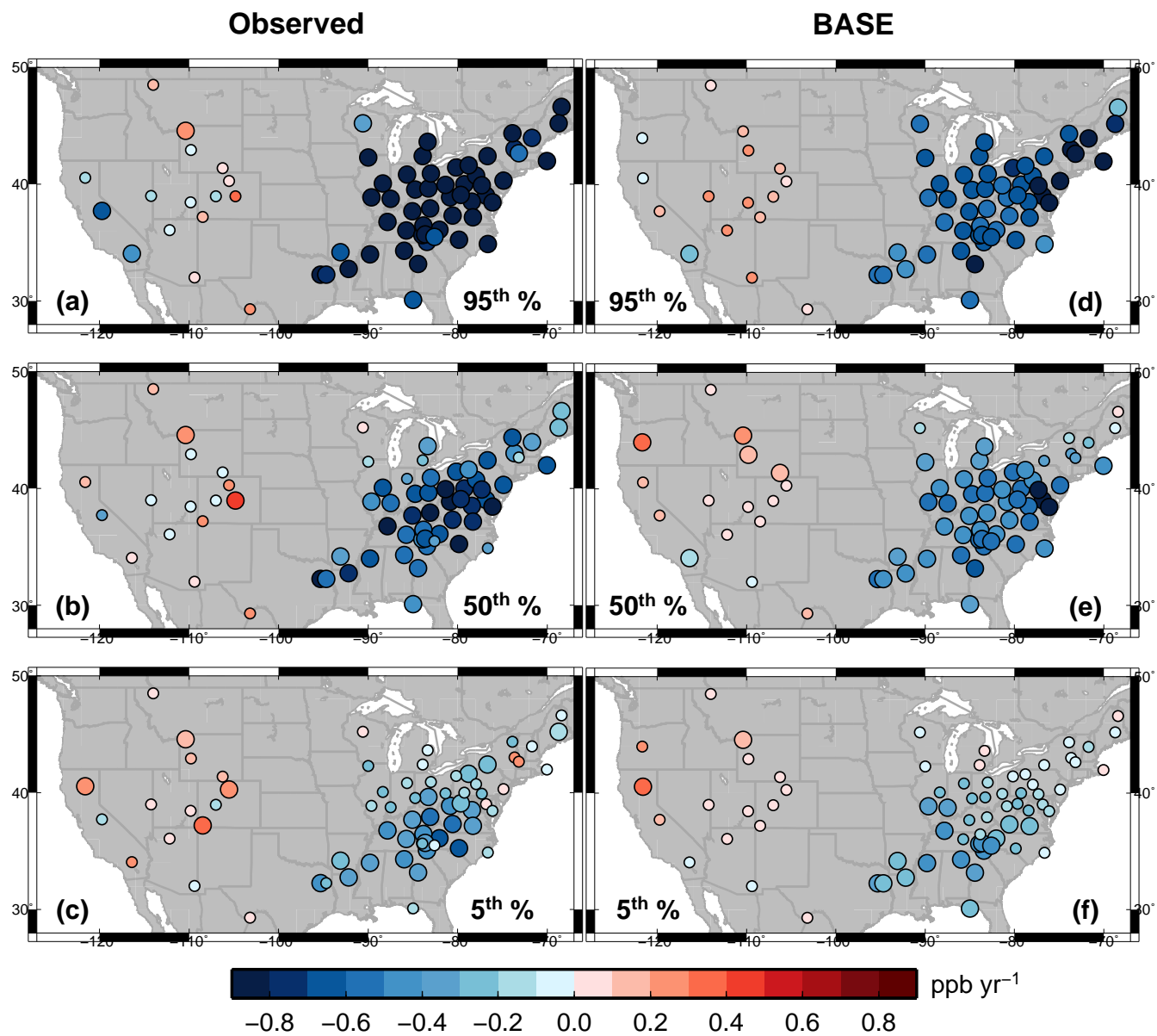


Figure 8. As in Figure 7, but for summer (JJA). Note that the color scale saturates at  $\pm 0.8$ .

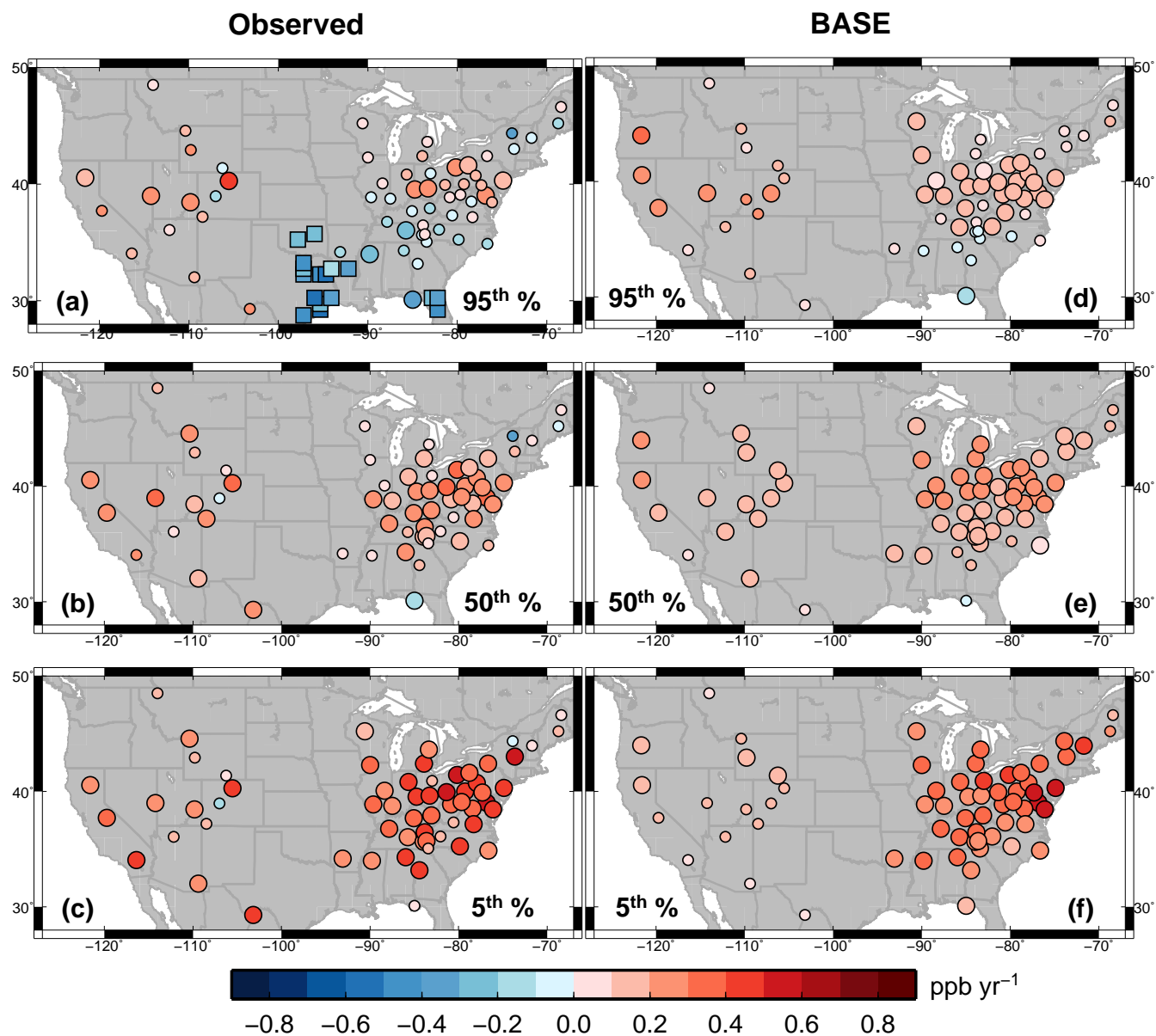


Figure 9. As in Figure 7, but for winter (DJF). Large squares in (a) denote AQS sites with significant O<sub>3</sub> decreases.

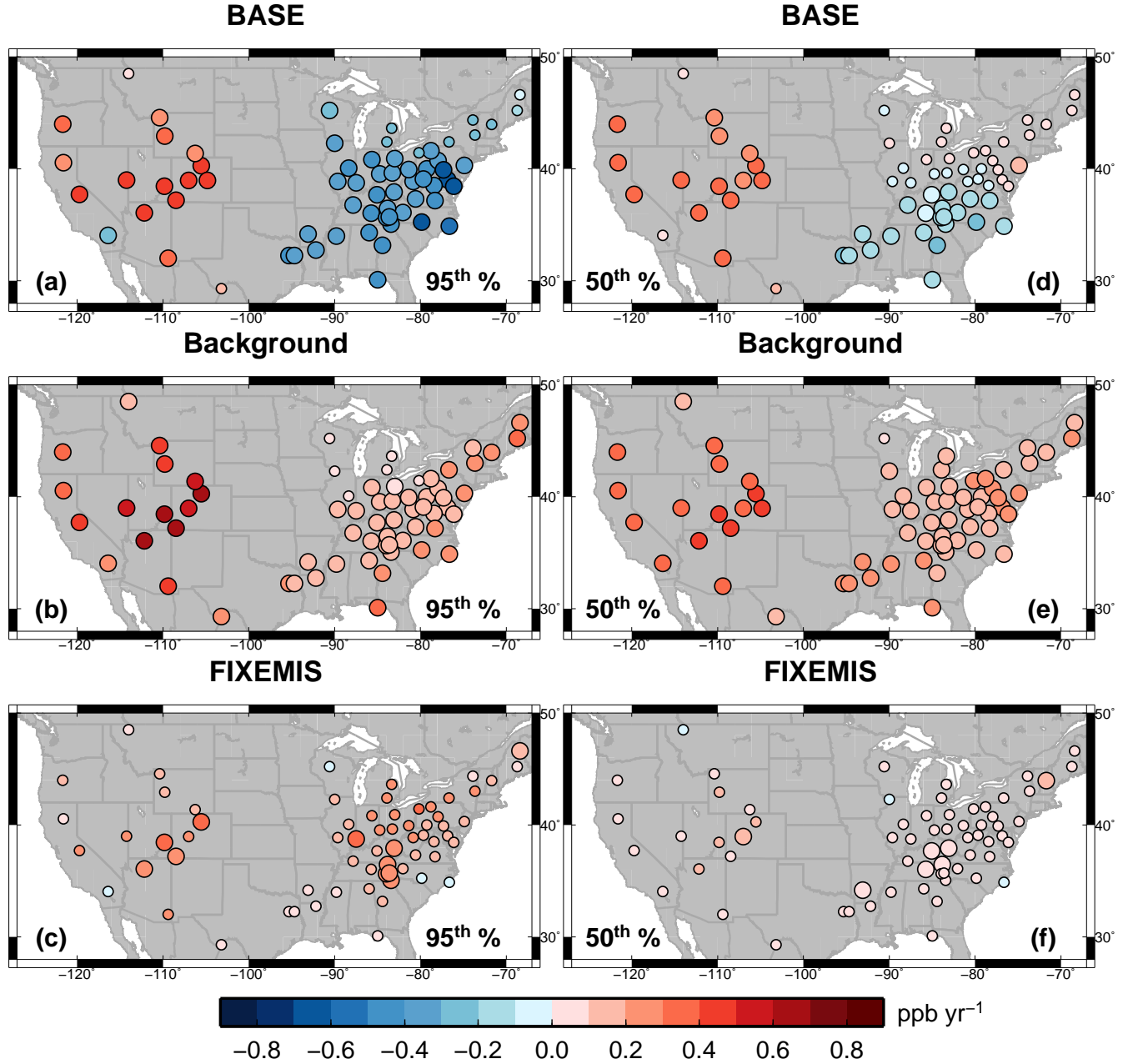


Figure 10. Linear trends in the 95th (left) and 50th (right) percentile springtime MDA8 O<sub>3</sub> over 1988-2014 at US rural sites from BASE (top), Background (middle) and FIXEMIS simulations (bottom). Larger circles indicate sites with statistically significant trends ( $p < 0.05$ ). Top panels are repeated from Fig. 7d,e. Note that the 95th (50th) percentile is sampled separately from the Background and FIXEMIS simulations without depending on the times when the BASE simulation is experiencing the 95th (50th) percentile days.

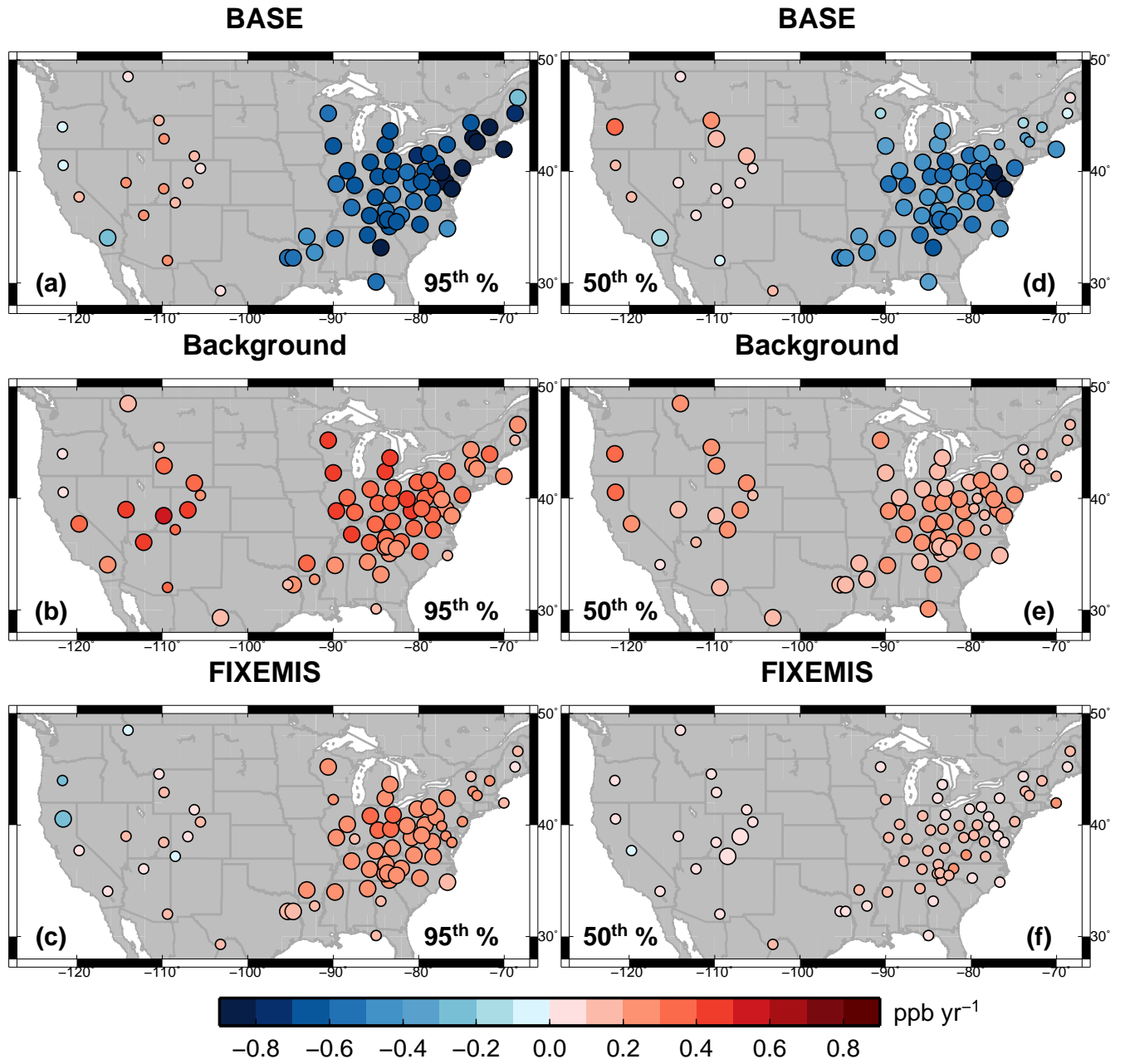


Figure 11. As in Figure 10, but for summer. Top panels are repeated from Fig. 8d,e.

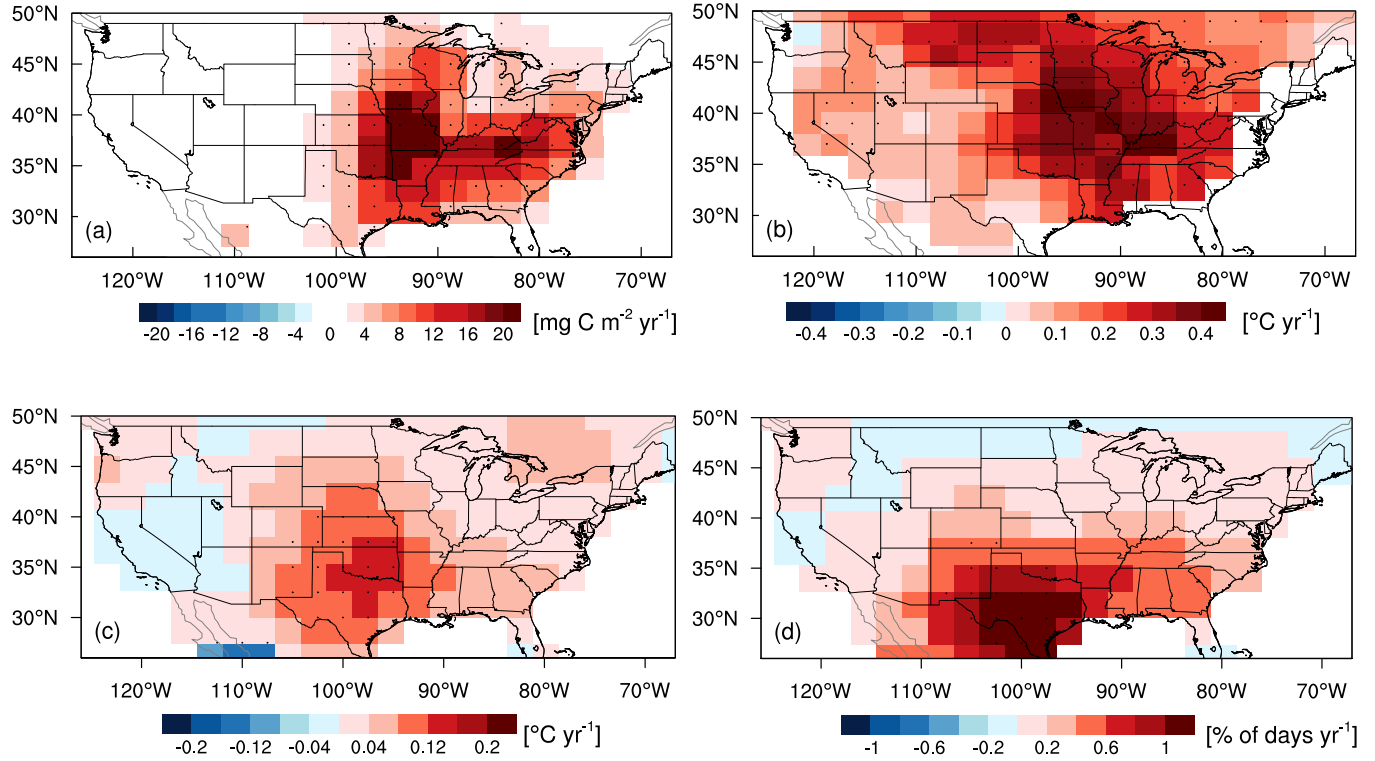


Figure 12. The 1990-2012 trends in: (a) model JJA total biogenic isoprene emissions; (b) model 90<sup>th</sup> percentile JJA daily maximum temperature; (c) the warmest daily maximum temperature and (d) the frequency of warm days (i.e., those above the 90<sup>th</sup> percentile for the base period 1961-90) for August obtained from GHCNDEX dataset (Donat et al., 2013; available at [http://www.climdex.org/view\\_download.html](http://www.climdex.org/view_download.html)). Stippling denotes areas where the change is statistically significant ( $p < 0.05$ ). Note that the trends are calculated for the 1990-2012 period, instead of 1988-2014, to avoid the influence from hot extremes in 1988 and cold conditions in 2014 (Sect. 6). When these years are included, the trends in (c) and (d) are swamped by the anomalies. The trends in (a) and (b) are similar between 1990-2012 and 1988-2014.

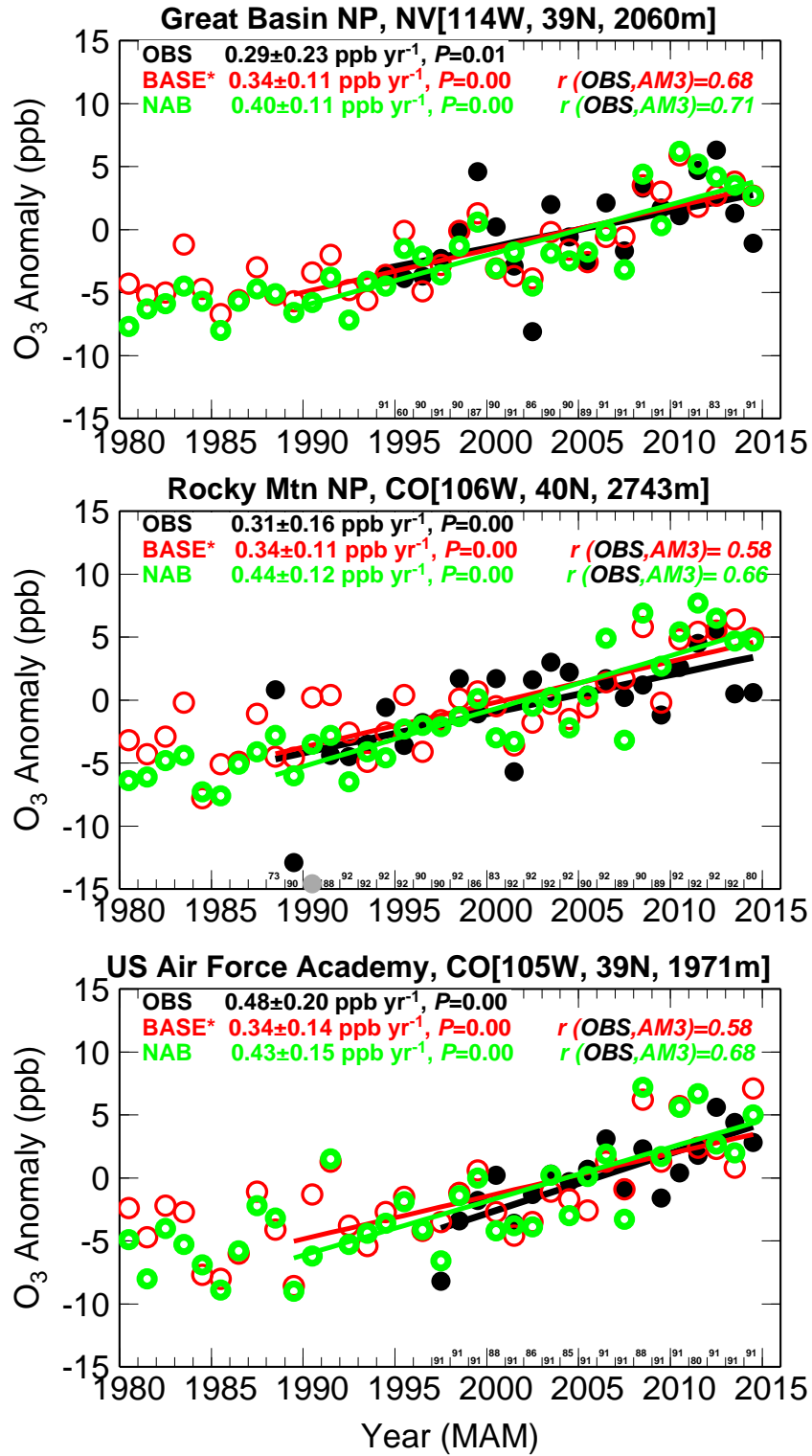


Figure 13a. Time series of median spring MDA8 O<sub>3</sub> anomalies (relative to the 1995-2014 mean) at Great Basin, Rocky Mountain, and US Air Force Academy as observed (black) and simulated in AM3 BASE filtered for baseline conditions (red, see Sect.2.4) and in Background with North American anthropogenic emissions zeroed out (NAB; green). Presented on the top of the graph are statistics from the linear fit and correlations between observations and simulations. Numbers on the bottom of the graph denote the sample size of observations for each year. Grey dots indicate uncertain observations that are removed from the linear fit (see Sect. 2.3).

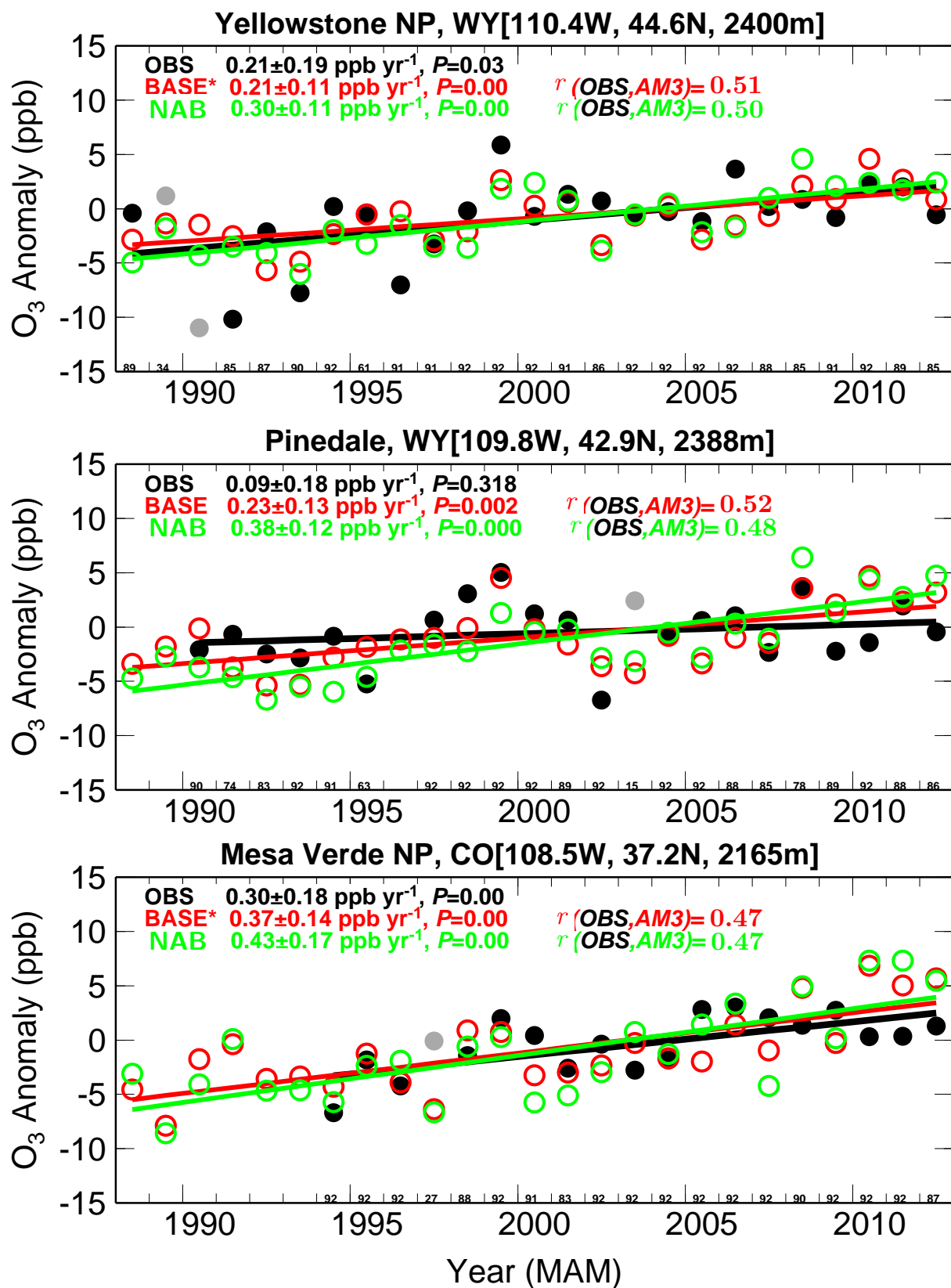


Figure 13b. Same as Figure 13a, but for Yellowstone, Pinedale, and Mesa Verde over the period 1988-2012.

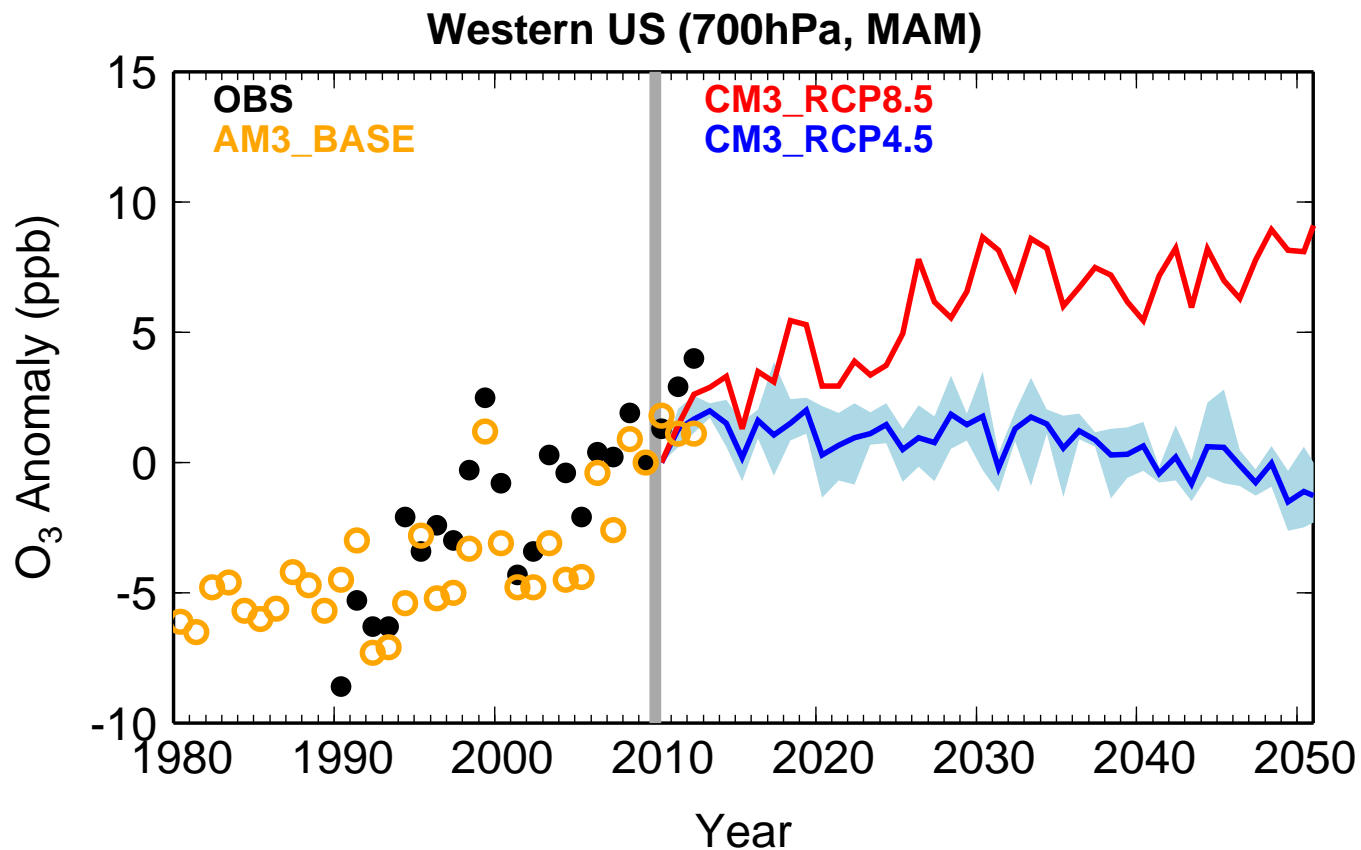


Figure 14. **Future projections.** Time series of median springtime O<sub>3</sub> changes relative to 2010 in GFDL AM3 hindcast (orange circles) and CM3 future simulations for RCP8.5 (red) versus RCP4.5 (blue; shading represents the range of three ensemble members), sampled at 700 hPa over the WUS (35–45N,120–105W). Black circles indicate observed changes averaged from Lassen, Great Basin, and Rocky Mountain National Parks.



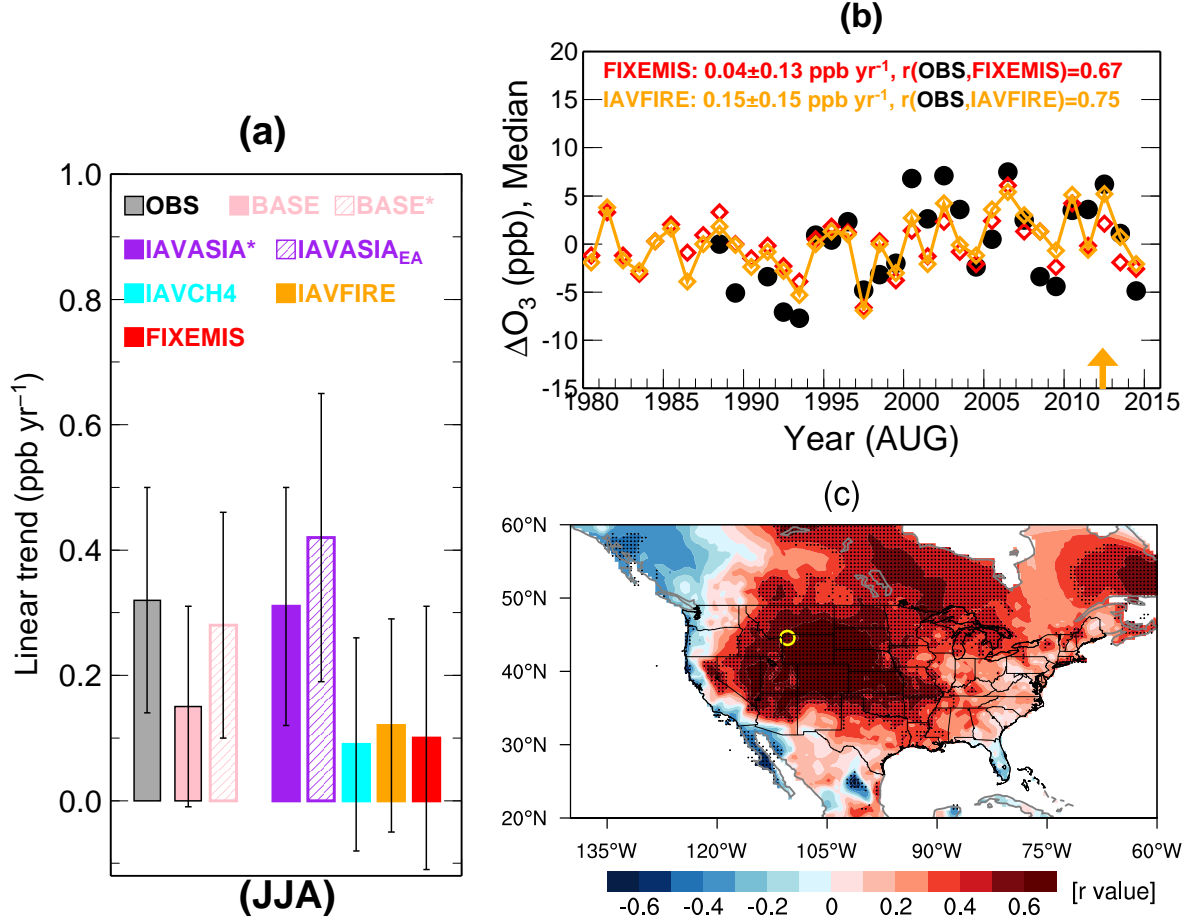


Figure 15. **Summertime O<sub>3</sub> in Yellowstone National Park.** (a) Median JJA MDA8 O<sub>3</sub> trends over 1988-2012 at Yellowstone from observations (black) and simulations sampled at 700 hPa for BASE without filtering (pink), BASE filtered for baseline conditions (hatched pink), IAVASIA (solid purple, baseline), IAVASIA filtered for Asian influence (EACOt<sub>≥</sub>67th, hatched purple), IAVCH<sub>4</sub> (cyan), IAVFIRE (orange) and FIXEMIS (red). (b) Time series of anomalies in August median MDA8 O<sub>3</sub> at Yellowstone as observed (black) and simulated by the model sampled at the surface, with constant (red) and time-varying wildfire emissions (orange). Trends over 1988-2014 are reported. (c) Interannual correlations of JJA mean MDA8 O<sub>3</sub> observed at Yellowstone with JJA mean daily maximum temperature from observations (Harris et al., 2014).

## IAVFIRE - FIXEMIS: Surface MDA8 O<sub>3</sub> Anomaly

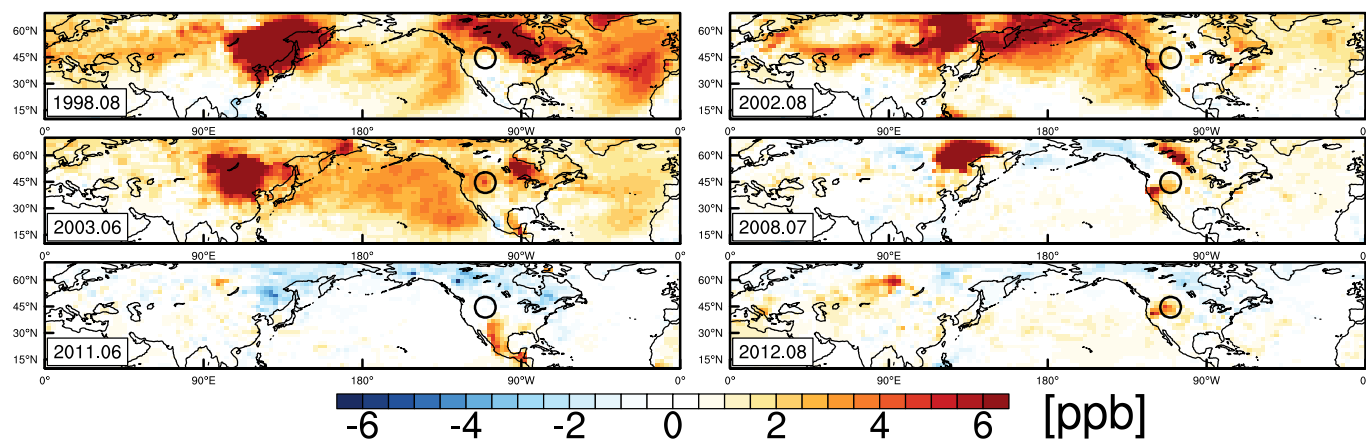


Figure 16. Surface MDA8 O<sub>3</sub> enhancements from wildfire emissions for individual months in the years with large biomass burning in boreal regions (1998, 2002, 2003) and over the WUS (2008, 2011, 2012), as diagnosed by the differences between IAVFIRE and FIXEMIS. The black circle denotes the location of Yellowstone National Park.

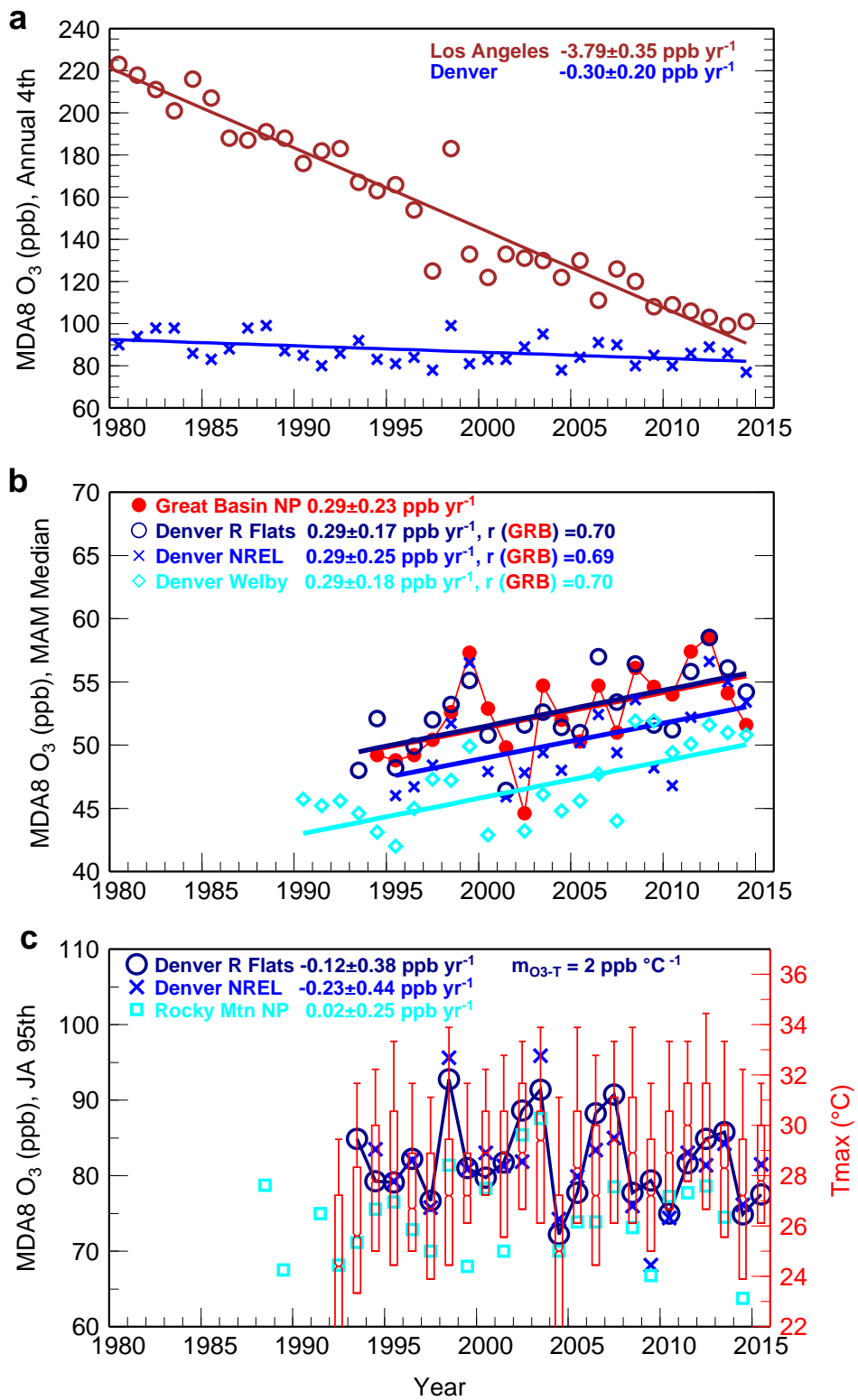


Figure 17. **Surface O<sub>3</sub> trends in Denver.** (a) Comparison of observed trends in annual 4<sup>th</sup> highest MDA8 O<sub>3</sub> at Crestline Los Angeles (brown) and in Denver (blue, computed from all monitors available in Denver non-attainment counties). (b) Time series of observed median MAM MDA8 O<sub>3</sub> at Great Basin National Park (red), in comparison with three monitors in Denver. (c) Time series of observed 95<sup>th</sup> percentile July-August MDA8 O<sub>3</sub> in Denver, together with statistics (25<sup>th</sup>, 50<sup>th</sup>, 75<sup>th</sup>, 95<sup>th</sup>) of observed July-August daily maximum temperature at Rocky Flats (red, right axis).

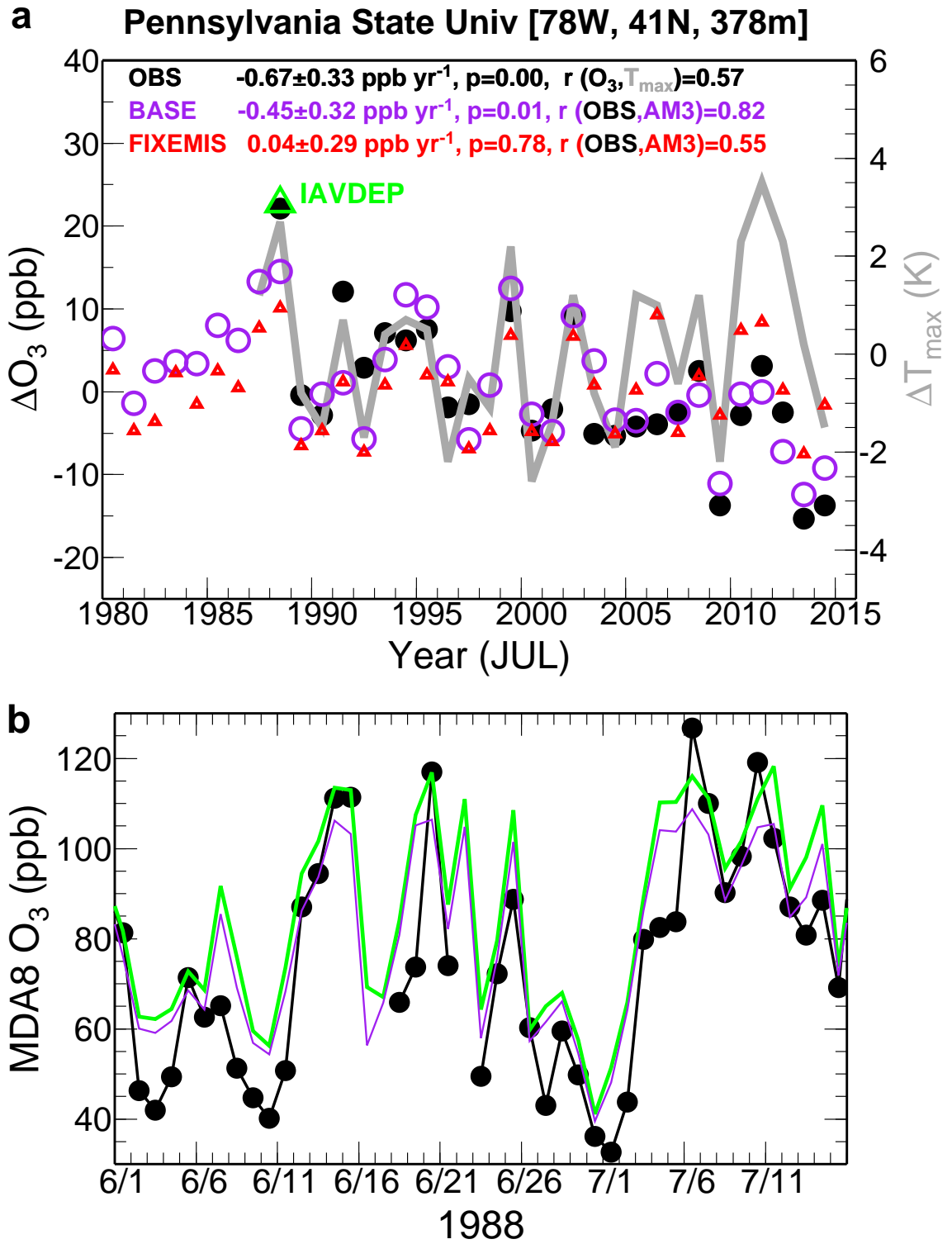


Figure 18. (a) Time series of July mean MDA8 O<sub>3</sub> anomalies (relative to 1988–2014) at the Pennsylvania State University (PSU) CASTNET site as observed (black) and simulated by the GFDL-AM3 model with time-varying (purple) and constant anthropogenic emissions (red), along with observed anomalies in July mean daily max temperature (gray lines; right axis). The green triangle denotes the 1988 O<sub>3</sub> anomaly from a sensitivity simulation using BASE emissions but with 35% decreases in  $V_{d,O_3}$ . (b) Time series of daily MDA8 O<sub>3</sub> at PSU from June 1 to July 16 in 1988 as observed (black) and simulated by the BASE model (purple) and the sensitivity simulation with 35% decreases in  $V_{d,O_3}$  (green).

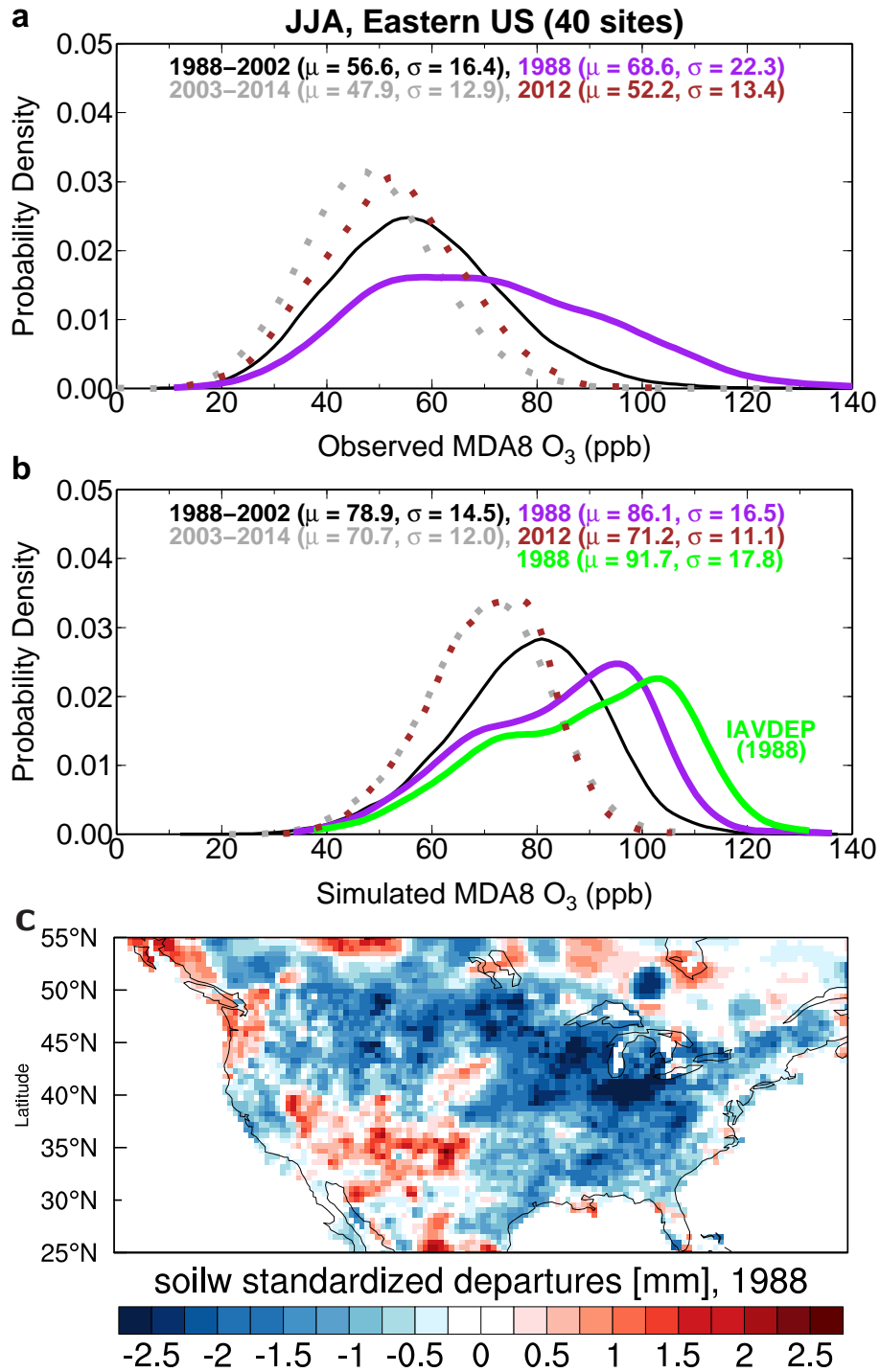


Figure 19. **(a)** Comparisons of probability distributions of summertime MDA8 O<sub>3</sub> from 40 EUS CASTNet sites for the pre-NO<sub>x</sub> SIP Call (1988–2002; solid black) versus post-NO<sub>x</sub> SIP Call (2003–2014; dashed gray) periods and during the extreme heat waves of 1988 (solid purple) versus 2012 (dashed brown). The median ( $\mu$ ) and standard deviation ( $\sigma$ ) are shown (ppb). **(b)** Same as **(a)** but from AM3 BASE. Also shown is the O<sub>3</sub> distribution in 1988 from a sensitivity simulation with 35% decreases in  $V_{d,O_3}$  in drought areas (green). **(c)** Standardized soil moisture departures for JJA 1988 (calculated by dividing anomalies by the 1979–2010 climatological standard deviation, using data from NOAA Climate Prediction Center).

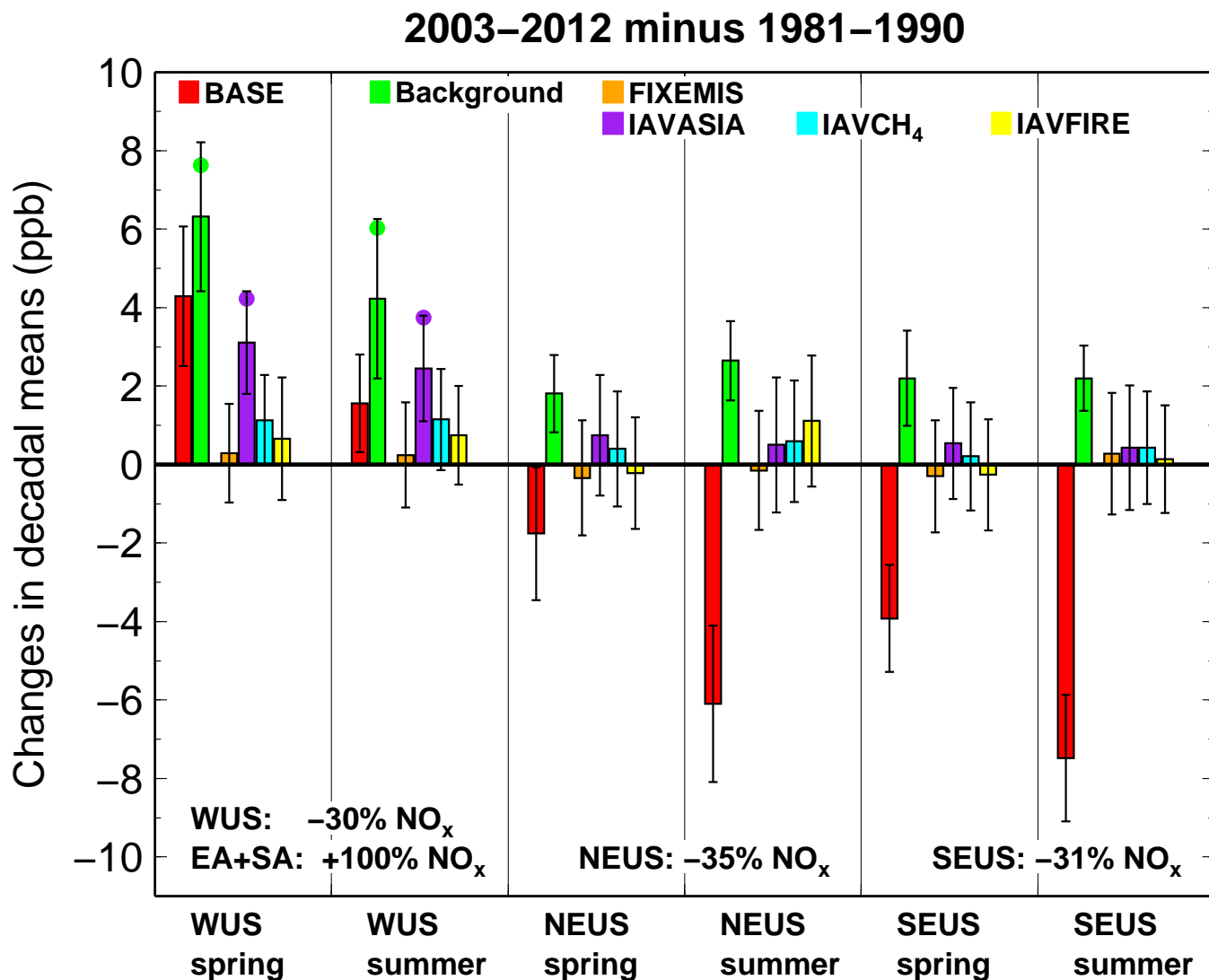


Figure 20. **Summary of US surface O<sub>3</sub> trends and drivers.** Changes in decadal mean MDA8 O<sub>3</sub> from 1981–1990 to 2003–2012 simulated in a suite of GFDL-AM3 experiments for spring and summer for the western (32N–46N and 123W–102W), Northeast (37N–45N and 90W–65W) and Southeast (30N–36N and 95W–77W) US domains. Observations are not shown because limited data are available during 1981–1990. Experiments are color-coded with the error bars indicating the range of the mean change at the 95% confidence level. Filled circles represent the changes under Background (green) and IAVASIA (purple) when filtered for Asian influence ( $EACOt \geq 67^{th}\%$ ), while other results are from the unfiltered models. The text near the bottom of the plot provides the change in NO<sub>x</sub> emissions over the same period for each region.